Fondul Social European
Investeste in oameni!
Programul Operational Sectorial pentru Dezvoltarea Resurselor Umane 2007-2013
Proiect POSDRU /159/1.5/S/132397 – Excelență în cercetare prin burse doctorale si postdoctorale – ExcelDOC

UNIVERSITATEA „DUNĂREA DE JOS" DIN GALAŢI

Școala doctorală de Inginerie Mecanică și Industrială

DOCTORAL THESIS

-ABSTRACT -

DEGRADATION PHENOMENA DURING THE MECHANICAL IMPACT OF SANDWICH COMPOSITE STRUCTURES

PhD:
Florentina ROTARU (PARASCHIV)

Scientific leader,
Prof. univ.dr.ing. Ionel CHIRICĂ

Seria I6: Mechanical engineering No. 42
Galati 2018

Fondul Social European
Investeste in oameni!
Programul Operational Sectorial pentru Dezvoltarea Resurselor Umane 2007-2013
Proiect POSDRU /159/1.5/S/132397 – Excelență în cercetare prin burse doctorale si postdoctorale – ExcelDOC

UNIVERSITATEA „DUNĂREA DE JOS" DIN GALAŢI

Școala doctorală de Inginerie Mecanică și Industrială

DOCTORAL THESIS

-ABSTRACT -

DEGRADATION PHENOMENA DURING THE MECHANICAL IMPACT OF SANDWICH COMPOSITE STRUCTURES

PhD:
Florentina ROTARU (PARASCHIV)

Scientific leader, **Prof.univ.dr.ing. Ionel CHIRICĂ**

Scientific References: **Prof.univ.dr.ing. Anton HADĂR**
Prof.univ.dr.ing. Dan-Mihai CONSTANTINESCU
Prof.univ.dr.ing. Leonard DOMNIȘORU

Seria I6: Mechanical engineering Nr.42
GALAȚI 2018

Seriile tezelor de doctorat sustinute public în UDJG începând cu 1 octombrie 2013 sunt:

Domeniul **ȘTIINȚE INGINEREȘTI**

- Seria I 1**: Biotehnologii**
- Seria I 2**: Calculatoare și tehnologia informației**
- Seria I 3**. Inginerie electrică**
- Seria I 4**: Inginerie industrială**
- Seria I 5: **Ingineria materialelor**
- Seria I 6**: Inginerie mecanică**
- Seria I 7**: Ingineria produselor alimentare**
- Seria I 8: **Ingineria sistemelor**

Domeniul **ȘTIINȚE ECONOMICE**

- Seria E 1: **Economie**
- Seria E 2: **Management**

Domeniul **ȘTIINȚE UMANISTE**

- Seria U 1: **Filologie- Engleză**
- Seria U 2: **Filologie- Română**
- Seria U 3**: Istorie**

Keywords:

Composite sandwich plates;

Polypropylene honeycomb cells: circular, hexagonal, square;

Static analysis;

Dynamic analysis;

Impact.

Content

Introduction

Wishing to accomplish things sustainable over time people have tried to replace the beginning wood, then iron with other materials that fully meet the needs and solve some inconveniences arising from cause use iron or wood such as weight reduction.
In the shipbuilding industry along the temps, the most used materials were and still are steel and wood. These two materials, in which a vessel is performed have come to be known in detail: from the point of view of advantages and disadvantages. Following the studies, engineers and researchers came up with a new proposal: to replace these materials with a new type of material that has similar characteristics, but whose properties can be molded as required: composite material. Developing research, it was introduced another revolutionary material with truly topical: composite sandwich. These structures are still studying, still doing research to find the best solution possible replacement of iron and wood, which is not easy given the quality of their particular which is not yet ignore. The steel industry has naval tradition is known in detail, it is working with technology perfected known standards then choose the types of steel etc. By choosing engineered composites or composite sandwich concept is changing almost all, from manufacturing technology up to and choice of composite and can even talk about personalization of the finished result. The transition from individual production to the large series is a big challenge in the future. Fiber composite materials for use in mass production and plastic for shipping indus still needed further developments in manufacturing, simulation-based calculation methods and processes of repair and recycling.
Considering the disadvantages of wood but particularly disadvantages iron, try a sandwich composites to fill the following minuses of iron:
-Corossion In contact with water;
-Weight-large;
-Noise and vibration in motion and impact;
The challenge facing the shipping industry as a whole at the moment, is to produce vessels of these materials economically in large quantities. But the problem arises especially local resistance and general construction of large ships. As in naval structures using increasingly advanced materials sandwich because they have multiple features required by the classification societies, the girl thesis I studied these special types of composites.
Classification societies require that materials used in naval shipbuilding to meet the following requirements:
- Tolerance to damage (after the panel is damaged, it should not lose its right for the performances);
- Shock good behavior;
- Good performance to adapt conventional technologies (in particular welding technologies);
- Acoustic and vibration characteristics, good;
- Corrosion resistance and fire resistance (especially anti-flame)
- no water absorption.
Almost all of these issues using the structures of ships gives the innovativeness of composite sandwich panels.
In the industry, various technologies have been developed for the manufacture of sandwich panels combining forms and to different types (materials) for coatings. Shipbuilding, material must meet the following properties: corrosion resistance, strength (impact, fatigue, compression and bending), adhesive properties, damage tolerance, weldability, toughness, formability and cost. A very important feature is that imposed by "fire retardant" which sets mandatory use of materials that conform to the code regarding: the propagation

characteristics of low flame, limiting the heat flow (taking into account the risk of ignition of furniture compartments) limited rate of heat release (on the risk of fire spread to adjacent compartments), gas and smoke must not exceed certain amounts that could be hazardous to personnel on board. The potential benefits of exploiting new composite sandwich panel can be used to start at small and medium vessels structures (bulkheads, decks and coatings) that do not support important requests.

The purpose and objectives of the work:

The main purpose of this paper is to analyze the impact of dynamic behavior for certain types of plates. The rationale is simple structures base thus analyzing the behavior of compressive static structure of three types of geometries cells (non-circular, hexagonal and square) where hearts cellular, then analyzes the plates sandwich composites with different geometries and configurations.

General objectives:

Theoretical and experimental development of methodologies for assessing degradation phenomena, arising from mechanical impact phenomena of composite sandwich.

Specific objectives:

- The analysis of general degradation phenomena to mechanical impact structures.
- Rules for design and construction of structures with high efficiency at the request of impact, combining metal with the characteristics of advanced materials.
- Design methodology for calculating the impact composite structures.
- Experimental tests to simulate the impact of simple and complex structures made of composite materials: to determine material characteristics and parameters of response to impact.
- Develop the concept of integrity of composite materials used in different structures.
- Evaluation of technical and economic performance of the materials used to build the structure by implementing a continuous improvement avant-garde solutions.

This book consists of six chapters divided as follows:

Chapter 1: Introduction to the Theory impact mechanical structures (Impact viewed as a transient dynamic action, also called shock).

Chapter 2: Current state of research in the production and use of composites sandwich.

Chapter 3: Numerical simulations on the impact of mechanical structures.

In this chapter, we were investigated behavior of sandwich plates on static and dynamic requests for a range of materials for core, in order to define the impact properties of sandwich structures. Initially, the compression properties of the honeycomb core were measured for each cell separately, and the entire sandwich panel. The next step was conducting a series of crash tests for sandwich structures with different geometries polypropylene core: circular, hexagonal, square and also unstructured square of bricks in a wall. Finally it was carried out crash tests for two foam materials with different densities, to use for the core.

Chapter 4: Static and dynamic sandwich plate analysis includes:

-determination of mechanical properties of composite materials using ANSYS software,
- numerical simulation using the finite element method for static and dynamic analysis of sandwich composite plates.

Chapter 5: Experimental simulations of the impact, include:

- Determination of mechanical properties of composite materials;
- Manufacture of composite sandwich plates;

Impact tests were conducted in the Laboratory of Advanced Strength of Materials Department of Mechanical Engineering of the University "Lower Danube" University of Galati, using two stands:

- Stand for impact test in which force is developed by a pneumatic system;

- Stand for type test to gravitational force which is developed by dropping a rigid balls to a certain height.

Dynamic test bench with pneumatic system consists of:

- The force development;
- System support composite plate;
- The measurement of test parameters.

The testing stand gravitational dynamic system consists of:

- The supportive;
- The development of gravity (ball + traverse support);
- The measurement of test parameters.

This is similar to the one above only ball falls freely. This system is designed and built entirely in the doctoral thesis by the author.

Chapter 6: Comparative Analysis of results: experiment to finite element analysis. This chapter presents comparison of experimental results with simulated in Ansys software.

Chapter 7 General conclusions, original contributions and perspectives. In this chapter we are presented general aspects but also the entire paper main conclusions on the results obtained in both experimental and modeling finite element. Proposals for future studies are done. The theme of this thesis is highly topical research in this area can be large and therefore can address other solution methods and experimental tests than those presented here.

CHAPTER 1 INTRODUCTION IN THE IMPACT OF THE MECHANICAL STRUCTURES

1.1 Basic Impact Theory

The first researchers of the impact were Galilei and Newton. Galileo was the one who studied the fall of the bodies, discovering that the phenomenon respected the law of uniformly accelerated movement, and Newton was the one who systematized the first correct Mechanics, that we call classical today.

Impact is the phenomenon of sudden contact of two or more bodies, accompanied by the instantaneous variation of their speeds. The contact runs in time $\Delta t \neq 0$, very short, when the speed suddenly changes its characteristics - the size, the direction and sometimes the meaning.

1.1.1 Impact seen as a mechanical phenomenon of collision

The study of collisions can be carried out under conditions of renouncing the hypothesis of rigidity of the bodies. This hypothesis is considered in mechanics, admitting that during impact bodies deform both elastically and plastically.

During impact, the bodies are subjected to the action of very large *forces*, called *striking forces.* All other forces (weight, friction, etc.) are negligible.

The percussion forces have very rapid variations in the interval $\Delta t=t'-t$, (*t* represents the moment when the colliding bodies come in contact and t' is the moment when they collapse). The Δt interval is very small, so it can be considered that there is no variation in the position of the bodies during the impact. The percussion is a vector size formed by the action of the percussion forces intervening in a collision, expressing itself as:

$$\bar{P} = \int_t^{t'} \bar{F} dt \tag{1.1}$$

$\bar{F}$- is the resultant of all percussion forces acting within the time interval (t'-t) as long as the collision phenomenon lasts.

The vector is collinear capital exclusively percussion the same meaning as the percuting force vector. The percussion module $|\bar{P}|$ is numerically equal to the area under the variation of the percussion force $|\bar{F}(t)|$.

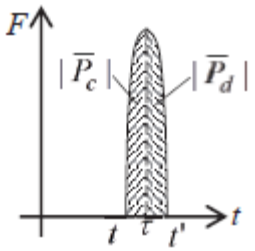

Figure 1.1 Percussion forces [1]

The phenomenon of the impact has two running phases: the compressing phase t-τ and the expansion phase t -t ' (τ is the time the percussion power reaches the maximum value). Accordingly, the percussion can also be divided into two phases:

$$\bar{P} = \int_t^{\tau} \bar{F}\, dt + \int_t^{t'} \bar{F}\, dt = \bar{P}_c + \bar{P}_d \tag{1.2}$$

The ratio between the impulse corresponding to the return phase (P_d) and the impulse corresponding to the compression phase (P_c) has the name of coefficient (k):

$$k = \frac{\vec{P}_d}{\vec{P}_c} = \frac{v_2 - v_1}{v_{10} - v_{20}} \tag{1.3}$$

called restitution coefficient or collision elasticity coefficient . For a given combination of materials this coefficient is considered constant.
The restitution coefficient is defined as the ratio between the relative velocity of body centres at the end of the impact phase and their relative velocity at the beginning of this phase. Theoretically, the value of the restitution coefficient is between 0 and 1, the value 0 corresponding to a perfect plastic impact in which the bodies maintain their common speed at the impulse point until the end of the impact, and the value 1 corresponds to the perfectly elastic impact in which transformed kinetic energy in compression energy in the compression phase is fully returned to the restitution phase.
Thus, given the speeds at the end of the impact, the kinetic energy consumed during collision in the form of deformation energy can be determined:

$$E_D = \frac{m_1 \cdot m_2}{2 \cdot (m_1 + m_2)} \cdot (1 - k^2) \cdot (v_{10} - v_{20})^2 \tag{1.4}$$

For *k=0*, the *ΔE* value is maximum, specific for non-elastic collision, while for *k=1*, the energy consumed during the collision is null (*ΔE=0*, perfect elastic collision).
The restitution coefficient is determined experimentally and has a positive subunit value. The following situations are different:
- the perfect elastic collision (k=1) in which the percussions in the two phases are equal; after collision, the bodies break away and deformation does not occur. Total kinetic energy conservation.
- perfect plastic crash (k=0) in which the percussion in the decomposition phase is null; after impact the bodies remain in contact;
- the elastoplastic or natural crash (0<k<1) where the percussion in the de-stressing phase is less than in the compression phase due to an energy loss to the deformation of the bodies. In this case, the bodies remain partially deformed by impact [2].
At the basis of the impact calculation is the principle of energy conservation, in which the mechanical work consumed by the two bodies turns into deformation energy. Elastic deformation propagates at a speed comparable to sound, and is consistent with each type of material. At impact, the speed of the hitting body drops to zero over a very short time frame, and the deformation does not spread throughout the body, but focuses only on the impact area.
After this phase, the deformation propagates throughout the body, resulting in random deformations. As initial data of the process, the following hypotheses, introduced by many authors, including Tong L. [3] and Jeronimidis G. [4]:
- the body that strikes is considered to be rigid;
- the link between dynamic forces and dynamic displacements is similar to that between forces and static deformations.
The difference from static stress is that in case of impact the static stresses will be multiplied by a coefficient ζ>1, which is considered identical throughout the body.
This theory is applied to isotropic materials.

1.1.2 The dynamic impact of two bodies

There are several approaches to the impact phenomenon because it is based on the complexity and the parameters involved in studying the phenomenon. Impact is also called

collision or collision. The dynamic crash is a remarkable physical phenomenon not only for changing the conditions for each point of contact between both bodies from the beginning to the end, but also for the progressive tensioning of the bodies. The main parameters that change as a result of this phenomenon are: the deformations and the displacements describing the theory of impact. It is natural for all theories to be organized according to the level of difficulty of the study, that is, the progress of the mathematical and physical constants being the main point of observation.

The deformation process during elastic impact was characterized by M. Szarvas, in [5], who studied the elastic impact pattern between a plate and a projectile. After the collision the projectile creates a temporary shock wave acting on the plate producing tensions that continue to the end of the plate. If a plate consists of more than one layer, then a small part of the wave will return, and much of it will continue to the plate. In the part where the shock wave propagates and does not return, in the case of bending it can cause the material to be destroyed. The cross-section shock wave has a shape close to a cone and lasts several milliseconds, then it turns into a bending wave and changes the support points at both ends (fig. 1 .2). After a few tens of milliseconds, we can see the plate's response to an impact load. The general deformation will be a combination of Hertzian contact and total deformation that causes high tensions, producing also plastic bending of the plate. During the deformation process there will always be a dominant part. If it is a structural response, then the destruction of the board will occur through three possibilities: waves, vibrations or hertz contacts.

A: The deformation is characterized by tension waves, if the time (impact) is short and the stress fails to reach the edge areas of the plate.

B: The Herzian contact is dominant when the plate is sufficiently strong or the impact energy is a relatively low deformation and can generally be neglected.

C: If the plate weight is small compared to the projectile, it can be considered static deformation instead of higher order vibrations.

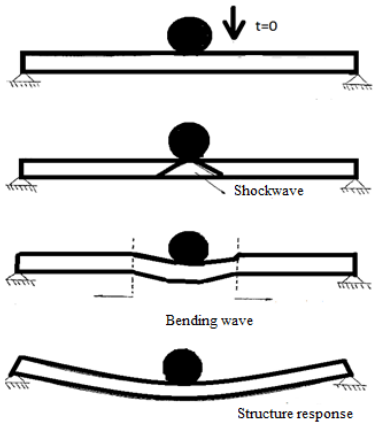

Figure 1.2 Propagation of shock waves [5]

Researchers tried to classify the types of impacts according to their speeds, but also their damage, [5, 6, 7, 8] so:

1) elastic impact (quasi-static);
2) plastic impact;
3) hydrodynamic impact (material hardness is neglected);
4) supersonic impact (vaporization, explosion) .

Kilchert has also delineated impact velocities as follows:

- Low-speed impact at ranged between (0-50 m/s),
- High speed impact (50-1000 m/s) and

- Impact with hyper- speed or (>1000 m/s).

In the last decade, low-speed impact for honeycomb sandwich structures has been investigated by various researchers [9, 10, 11, 12].

Serge Abrate [13] discussed in detail the plates impact Theory by combining the known theories of researchers: Reissner Mindlin (plates theory), Timoshenko (crossbeams and thin plates theory) and Bernouli-Euler (girders theory).

The first theory (First-order shear deformation theory, abbreviated FSDT) is also known as Mindlin or Plate Theory of Reissner Mindlin.

Timoshenko's theory, for thin plates, which takes into account the effect of shear deformation and rotational inertia, is reduced to the classical plate theory (CPT).

Bernoulli-Euler's theory is applicable to girders.

1.1.3 Impact seen as a contact problem of elastic bodies

Impact can also be seen as a short-lived contact issue. In the case of the reduced load velocity, the state of stresses and deformations occurring in the elastic body resolves with theories of elasticity, based on the static mechanical equilibrium. In mechanical impact conditions the speed of application of the load is very high. In this case, the dynamic phenomenon has important effects.

1.2 The drop shock theory

A mechanic shock occurs when the position, speed or acceleration of an object suddenly changes. Such a shock can be characterized by a rapid increase in acceleration followed by a rapid decrease over a very short period of time (Fig.1.3). In the figure 1.3, the acceleration variation during a collision is represented. Area A represents the change in speed during collision.

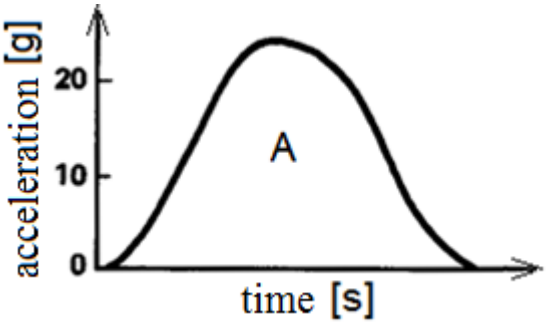

Figure 1.3 The variation of the curve of acceleration at impact [15]

A force applied to a system for a short time span produces a shock or impact. If this force is high, large accelerations can occur. Newton's second law shows that the acceleration of a body is related to the forces applied to the body.

Under normal conditions, the duration of a shock may be 20 milliseconds (0.020s) with a magnitude ("height") of 150g. Therefore, to characterize the shock phenomenon, it is necessary to know both the amplitude of the acceleration and the duration of the shock. Thus, the length of time is given by:

$$t = \sqrt{\frac{2h}{g}} \tag{1.20}$$

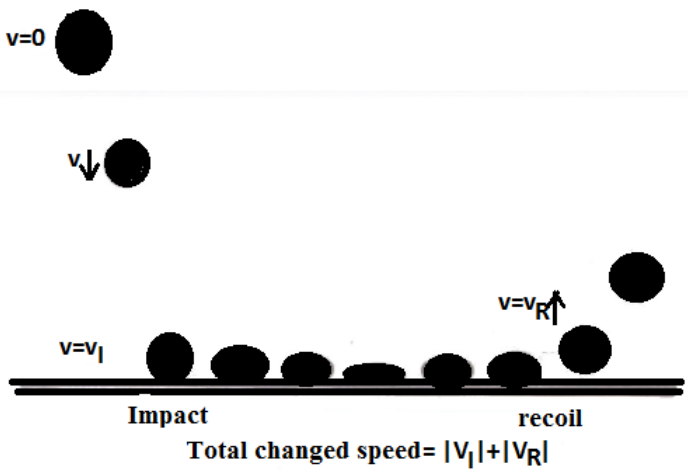

Figure 1.4 The fall of a ball on a flat surface [15]

In Figure 1.4 the stages of a collision are shown. Speed has a rebound that depends on the mass of the ball (if it was another object it would also depend on its shape) and the surface on which it falls. In the case of high speed shock phenomena, the measure unit for the acceleration relative to the gravitational acceleration *g* is used. The value has to be multiplied with the gravitational acceleration ($9.81 m/s^2$) for obtaining the measure unit of the acceleration in the international system. The restitution coefficient, *e*, describes the rate of return according to the impact velocity.

$$v_R = ev_I \tag{1.21}$$

Total changed speed:

$$\Delta v = v_i + v_r \tag{1.22}$$

$$\Delta v = (1+e)v_I = (1+e)\sqrt{2gh} \tag{1.23}$$

The impact speed is:

$$v = (v_0^2 + 2gs)^{\frac{1}{2}} \text{ or } v = \sqrt{v_0^2 + 2gs)} \tag{1.20}$$

Where:
v = impact velocity [m/s]
v_0 = initial speed [m/s]
g = gravitational acceleration ~9.81 [m/s^2]
s = drop distance [m]

When performing a large impact calculation involving sandwich structures, impact tests are required to extract all the parameters for the study. Before starting an impact test, the following questions should be asked:
What is the structure?
What information do you have about the structure to be analysed?
What parameters are known about the specimen or sample? Do they affect the shape? What is the weight of sandwich and the weight of impactor? What is the shape of the impactor?
What parameters do I know?
What output parameters is there an interest in?
What is the purpose of the test?

Typically, for an impact test for sandwich structures that is carried out with a test machine the output parameters are: the maximum force, the maximum force energy, the maximum force deformation, the penetration force (representing half of the maximum force), the penetration force energy, the deformation at the deformation force;

If the impact force and the deflection plate at the same time points during the impact test are known, then the released energy E_i until the moment of the specific time t_j is

calculated by determining the area of the force-deformation curve. Based on the data extracted from the data acquisition and processing system, the characteristics of the composite impact materials can be determined: the maximum contact force, the contact time, the maximum deformation, the permanent deformation, the impact energy, the energy absorbed by the sandwich plate Bunea [7, 16]. In the works from Heimbs and Apetre [17, 18], it is stated that the performance impact of a sandwich structure, meaning the damages and their ability to absorb energy, is strongly dependent of the material of the faces and their thickness. However, the core also influences significantly the impact behaviour. Other factors of influence for the sandwich structure are: the thickness, the boundary conditions, the impactor geometry and the stiffness.

1.3 Impact tests

Impact tests can be performed on equipment that differs from one another through the impact force development system, through the structure of the mainframe and through the measurement methods of the parameters of the phenomenon. An impact test machine may be the Drop-Weight type one.

1.4 A impact testing mechanism with compressed gas

Impact tests for layered or sandwich structures can also be done with the help of mechanisms based on the pneumatically driven cylinder-piston system. In this thesis, tests on such an impactor will be performed in Chapter 4. Figure 1.8 shows the compressed air test mechanism with its components. The compressed air gets into a battery at a pressure controlled by a pressure regulator. The pressure is released via a valve by breaking a thin diaphragm. The body then goes through a tube and passes through a speed recorder. Such a simple device consists of a light emitting diode (LED) and a photometric detector. The body, which has a known length, produces an interruption in the light radiation, and the duration of the interruption in the signal produced by the sensor is used to calculate its velocity [25].

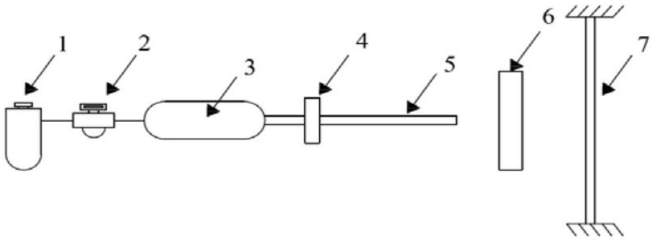

Figure 1.5 Impact test mechanism with compressed air [25]

The components are:
1 - air filter, 2 - pressure regulator, 3 - air accumulator, 4 – valve, 5 – tube, 6 - speed recorder 7 - specimen.

1.5 Charpy Impact Test Mechanism

Impact tests can be made with this system, but it would not be suitable for sandwich structures because this system uses the method of notchting for the specimens. If the sandwich type has 1mm thick faces, making the crest to initiate the crack, then that test may be considered invalid. By comparison, the Izod test is similar with the Charpy pendulum test except for the fact that the impact with the hammer is executed at the free end (Ellis, 1996).
Cantwell and Morton suggested that Chapy and Izod are appropriate test mechanisms for assessing the impact performance of materials and a step in determining the dynamic hardness of materials [27].

CHAPTER 2 ACTUAL STAGE OF RESEARCH IN THE FIELD OF PRODUCTION AND USE OF SANDWICH COMPOSITE MATERIALS

2.1 Applications of composites and composite sandwich

The use of composite materials and their structural components in shipbuilding [29], aircraft, cars, civilian or military construction is a great challenge as they significantly reduce the weight of the structures, leading (in the case of vehicles) to good fuel economy and overall to reduce operating costs. The application of sandwich polymer composites in the shipbuilding industry is constantly increasing, introducing new basic materials such as: fibers, resins, adhesives, curing accelerators, additives [30]. In order to decide on the selection of materials with good impact performance, it is indicated to study Table 2.1, where a brief assessment of the most used composite materials in the shipbuilding industry is made.

Table 2.1 Qualitative assessment of the properties of composite composite materials

Properties	Fibers			Resins					Cores					
	E-Glass	Kevlar	Carbon	Poliester	Vinil Ester	Epoxy	Phenolic	Termoplastic	Balsa	Cross Link PVC	Linear PVC	Nomex/Alum Honeycomb	Termoplastic Honeycomb	Sintactic Foam
Resistance to static traction	■	■	■	□	□	■	□	□	■	■	■	□	□	□
Rigidity to static stretching	□	■	■	□	□	□	□	□	■	□	□	■	□	□
Resistance to static compression	■	□	□	□	□	□	□	□	■	□	■	■	□	□
Static compressive rigidity	□	□	■	□	□	□	□	□	■	□	□	■	□	□
Fatigue performance	□	■	■	□	■	■	□	■	■	□	■	□	■	□
Impact performance	■	■	□	□	■	■	□	■	□	■	■	□	□	□
Resistance to water	■	□	□	□	■	■	□	■	□	■	■	□	□	□
Fire resistant	■	□	□	□	□	□	■	□	■	□	□	■	□	□
Workability	■	□	□	■	□	□	□	□	■	□	□	□	□	■
Cost	■	□	□	■	□	□	□	■	■	□	□	□	■	■
	■ **Good Performance** □ **Poor Performance**													

For the manufacture of sandwich plates, suitable materials should be selected for both sides and core. This would have been difficult without a rigorous study of the literature. Thus, Eric Green, in the book Marine Composites [31], has succeeded in structuring composite materials and has delimited them into fibers, resins and cores. The materials used in the studies are the following: glass fibers, epoxy resin, polypropylene honey, foam (extruded polystyrene). The finite element modeling was done for those listed as well as for PVC (vinyl polychloride) and SAN (styrene acrylonitriles). The first two materials (glass fiber and epoxy resin) were constituted to make the faces of the sandwich plates. The other three were the sandwich cores. The newly formed sandwich has been manufactured to withstand impact, good tensile and compressive strength, good tire and compression stiffness, good

water and fire performance, good workability and cost little. That is, the newly created sandwich must fulfill all the properties in the table.

2.2 Composite materials

Composite materials are mixtures of two or more components whose properties complement each other, resulting in a material with properties superior to those specific to each component. Thus, the deficiencies of some are complemented by the qualities of others, conferring to the whole ensemble properties that no single component can take [33]. Properties that can be improved include [34]: mechanical strength, stiffness, corrosion resistance, wear resistance, attractiveness, weight, fatigue strength, thermal insulation, thermal conductivity, acoustic insulation. The base material is called matrix. The other constituent is called reinforcement. The reinforcement can be in the form of fibers or particles and is added to the matrix to improve its qualities. In composite material we also find technological additions. Both the matrix and the reinforcement of a composite material can be obtained from different types of materials. Classification of composite materials can be done depending on the type of matrix material, reinforcement material, composite design, use, mechanical, physical or chemical properties etc. [35]. Composite materials can be viewed and analyzed at different levels and at different scales, depending on the particular characteristics and behavior involved:

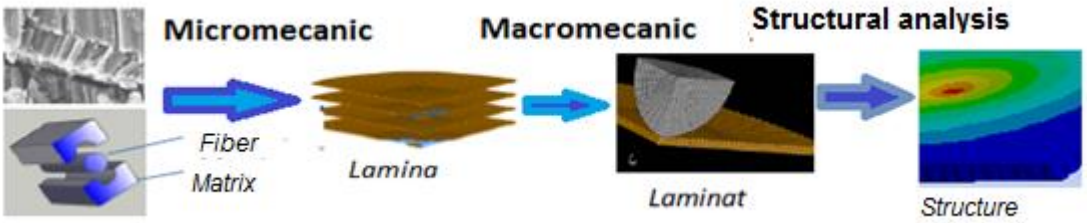

Figre 2.1 Observation level and assay types for composite materials [36]

2.3 Sandwich structures

A "sandwich" structure (Figure 2.2) consists of three main elements [47,48]:
A pair of thin, resilient, metallic or polymeric composite faces that take on axial and shear forces and convey normal tasks to their hearts. A thick core (also called "core", in English), with a low weight, separating the two faces, ensuring the effort is passed from one face to the other.Typically, this core may be honeycomb (aluminum, paper, plastic), foam (polyurethane, polystyrene) or profiles (metallic, plastic). A few years ago, sandwiches used in metal naval structures were metallic.
- A material with adhesive properties that transmits the axial or shear stresses from the envelopes to the core of the structure or vice versa. In the case of faces made of polymeric composite materials, the polymeric matrix may also have the role of adhesive.

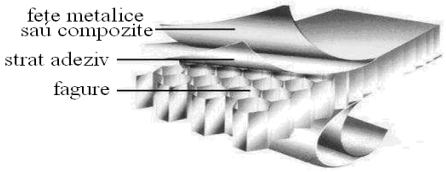

Figure 2.3 "Honeycomb core" sandwich structure [47, 48]

CHAPTER 3 NUMERICAL SIMULATIONS ON THE IMPACT OF MECHANICAL STRUCTURES

3.1 General presentation

Due to its special features, the structure of a honeycomb (honeycomb) material is widely used lately for making sandwich plates cores. This type of material is manufactured with a geometric structure of several shapes. In order to choose the most suitable structure for the proposed purpose, on the basis of commercially available materials, the first part of the chapter presents the resistance calculation of a unit volume of the plate comprising: a honeycomb cell and the additional coatings. Since during impact the cells are compressed, the calculation shown below is related to this type of request.

3.2 Modelare numerică pentru structuri celulare de tip sandwich

Numerical investigations were performed on a single cell belonging to a sandwich plate. The purpose of the analysis was to track the static behavior under the action of an F = 5N force. The analysis was performed for three geometric cell types: cylindrical, hexagonal and square.

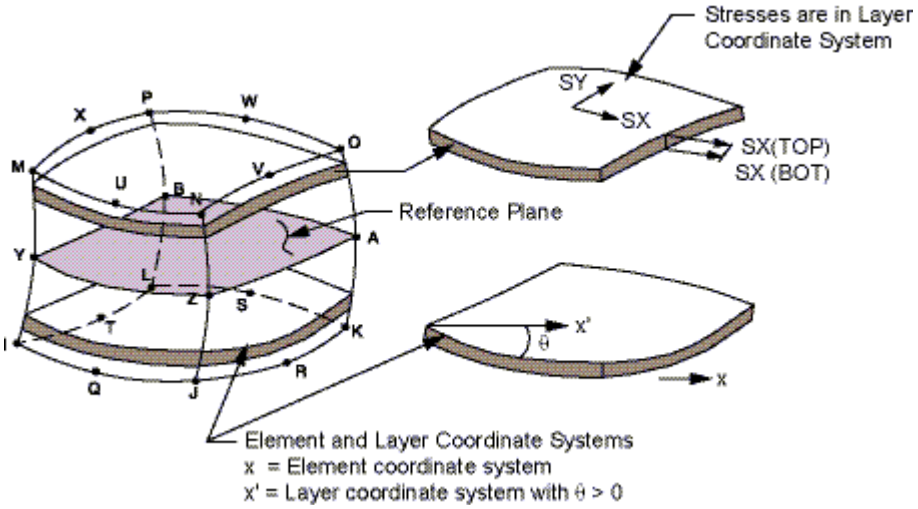

Figure 3.1 SOLID element geometry 186 [ANSYS Manual [58]]

The materials used in the analyzes are: two-sided fiberglass epoxy resin and polypropylene for core. The numerical calculation was done with the FEM ANSYS package. The type of element used is Solid186, as described in Figure 3.1. The element must not have a volume close to zero. Also, the element can not be twisted so that the element has two separate volumes (it can happen frequently if the element is not numbered properly). Elements can be numbered either as shown in Figure 3.1 or may have interchanged IJKL and MNOP. The element is specially chosen for composite materials or for nonlinear solution (if the element has a non-linear material) [58].

3.3 Determining the optimal shape of the cell in a honeycomb

To analyze the behavior of composite sandwich plates with honeycomb core, it is first necessary to study the behavior of the cells from which the entire plate is formed. A detailed analysis was done by Gibson and Ashby in [59] and Zhang [60], in which they set predictive methods to determine the properties in the plan. This reduces the complexity of honeycomb cells to the one-wall equivalent model and the determination of forces and moments so that planar properties can be calculated.

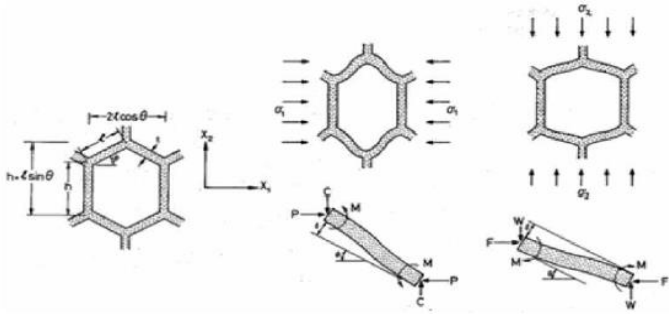

Figure 3.2 Elastic deformation in W and L directions [Gibson and L.J. Ashby M.F. [59]]

3.4. Properties of materials used for different types of cells

Materialul pentru miezul din fagure este polipropilena cu caracteristicile conforme cu cele din Zeleniakiene [62], prezentate în tabelul 3.1.

Table 3.1 Mechanical properties of polypropylene

Properties of polypropylene	Value	Measurement units
Density	900	Kg/m^3
Isotropic material		
Young's module	1750	MPa
Poisson's coefficient	0,42	
Yeld stress	24	MPa
Tangent modulus	4,4	MPa

Table 3.2 Values taken from the ANSYS Software Composite Materials Library

Properties Epoxy_E-Glass_UD	Value	Measurement units
Density	2000	Kg/m^3
Elastic ortotrope:		
Young's Modulus x direction	45000	MPa
Young's Modulus y direction	10000	MPa
Young's Modulus z direction	10000	MPa
Poisson's Ratio xy	0,3	
Poisson's Ratio yz	0,4	
Poisson's Ratio t xz	0,3	
Shear Modulus xy	5000	MPa
Shear Modulus yz	3846,2	MPa
Shear Modulus xz	5000	MPa
Orthotropic Stress Limits		
Tensile x direction	1100	MPa
Tensile y direction	35	MPa
Tensile z direction	35	MPa
Compressive x direction	-675	MPa
Compressive y direction	-120	MPa
Compressive z direction	-120	MPa
Shear xy	80	MPa
Shear yz	46,154	MPa
Shear xz	80	MPa

The material properties for the sandwich plate layers are shown in Table 3.2 of the one-sided fiberglass reinforced epoxy resin which has been taken from the ANSYS Library.

3.5 Static analysis of honeycomb core elements

The analysis was performed on the unit volume elements of the existing honeycomb structures (circular, hexagonal and square cells). The geometries for each cell are shown in figures 3.3, 3.4 and 3.5. Thus, the height of the core is H = 20mm for all three cases, the face thickness t = 1mm, the core wall thickness is g = 0.25.

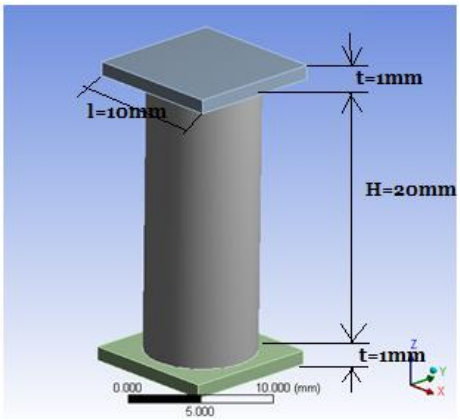

Figure 3.3 Circular cell geometry

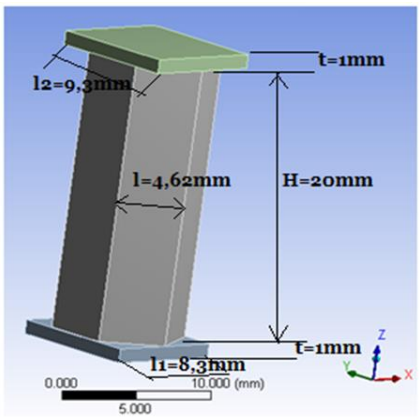

Figure 3.4 Hexagonal cell geometry

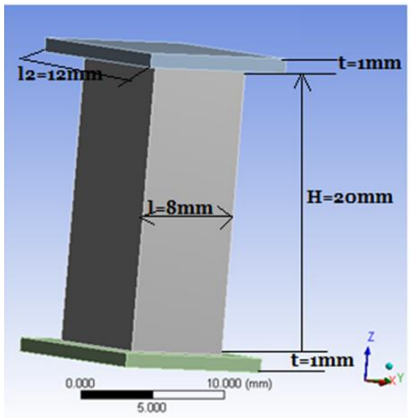

Figure 3.5 Square cell geometry

3.6. Results and conclusions for cell models with SOLID186 elements

The static analysis performed with the ANSYS software took into account the following output parameters: the total deformation for each cell, the Z-direction deformation (which represents the exact direction of force application F = 5N), the specific deformation (or linear equivalent) denoted by ε (is a dimensionless dimension), the equivalent tension (von Mises), the shear stress and the deformation energy. Each cell was embedded in the bottom surface of the face, as shown in Figure 3.15. Concentrated force F was applied to the center of the top face, just as in figure 3.16.

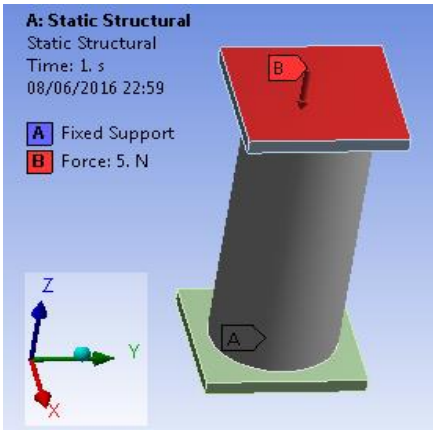

Figure 3.6 Application of force F = 5N

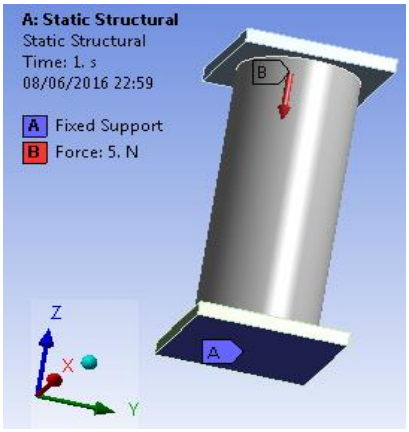

Figura 3.7 Fixed support

In order to make a viable comparison, the equality of volumes (or at least approximately equal) was considered as a criterion. For the three models this criterion is based on the values:

- The circular cell has the volume V = 321.74 mm³, the total mass M = 3.7974e-004 kg
- The hexagonal cell has the volume V = 286.65 mm³, the total mass M = 3.1558e-004 kg
- The square cell has the volume V = 443 mm³, the total mass M = 5.884e-004 kg.

3.7 Solving the contact problem

When two separate surfaces touch each other so that they become tangent they are considered to be in contact. Physically, the areas in contact have the following features:

- do not interfere;
- can transmit normal forces of compression and tangential friction;
- do not transmit normal stretching forces.

The rigidity of the system depends on the state of contact, whether the components are touching or being separated (ANSYS [63]).

The results obtained with the ANSYS software can vary depending on how the contact between the three simple bodies is made into a more complex structure, there are four types of contact:

1) Augmented Lagrange
2) Pure Penalty
3) MPC (Multi Point Constraint)
4) Normal Lagrange.

In ANSYS, the contact problem is solved differently depending on the wording used.

- The Penalty Pure and Augmented Lagrange formulations use integration of the detection point (Figure 3.17 (a)). This leads to more detection points.
- Normal Lagrange and MPC formulas use node detection (it goes in the "Target" direction) (Figure 3.17 (b)) This leads to fewer detection points.
- During contact detection, contact manipulation can be performed. Better discrepancy will alleviate this situation by choosing a point of integration with detection.

The MPC adds constraining equations to "tie" the displacements between the contact surfaces.

- This approach is based on Lagrange multipliers. It is a direct and efficient way for the areas of contact areas that are linked.
- For high deformations MPC is used based on bonded bonding.

-Better meshing of models can solve these inconveniences [64].

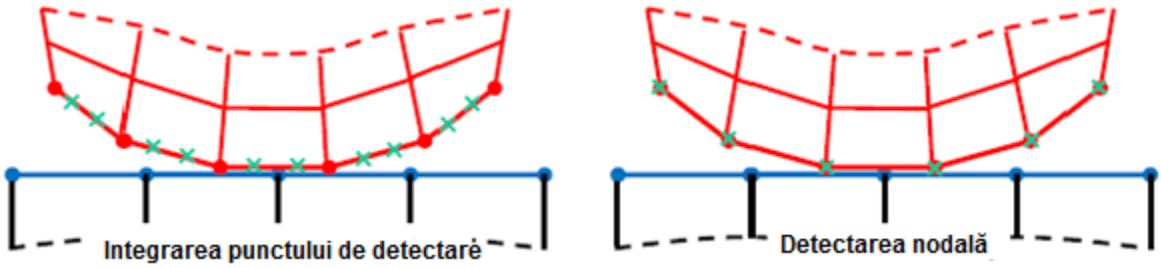

(a) (b)

Figure 3.9Identification of Gauss (a) or node (b) point contact [63]

Numerical analyzes were performed with the four types of contact formulations. Tables 3.3, 3.4 and 3.5 present the results obtained with the four types of contact formulations for the three types of cell geometries.

Table 3.3 Augmented Lagrange Method

No.	Output Parameters	Values for the model		
		Circular cell	Hexagonal cell	Square cell
1	Total deformation [mm]	0,00966	0,00906	0,00766
2	Displacement in the direction (z) [mm]	$8,1779*10^{-7}$	$1,9064*10^{-6}$	$9,1021*10^{-7}$
3	Specific deformation	0,000625	0,000669	0,000662
4	Equivalent stress von Mises [MPa]	1,0918	1,5236	1,1416
5	Shear stress [MPa]	0,6256	0,8734	0,6113
6	Total deformation energy U [mJ]	0,0234	0,0215	0,0187

Augmented Lagrange and Pure Penalty methods give identical results. That's why the table does not reproduce.

Table 3.4 MPC (Multi Point Constraint)

No.	Output Parameters	Values for the model		
		Circular cell	Hexagonal cell	Square cell
1	Total deformation[mm]	0,00957	0,00907	0,00752
2	Displacement in the direction (z) [mm]	$2,5569*10^{-7}$	$7,9725*10^{-7}$	$6,7689*10^{-7}$
3	Specific deformation	0,000903	0,000650	0,0007873
4	Equivalent stress von Mises [MPa]	1,5791	1,5373	1,3124
5	Shear stress [MPa]	0,9097	0,8826	0,7409
6	Total deformation energy U [mJ]	0,0244	0,0225	0,0217

Table 3.5 Normal Lagrange Method

No.	Output Parameters	Values for the model		
		Circular cell	Hexagonal cell	Square cell
1	Total deformation [mm]	0,00965	0,00906	0,00765
2	Displacement in the direction (z) [mm]	$1,1325*10^{-6}$	$2,0162*10^{-6}$	$9,1372*10^{-7}$
3	Specific deformation	0,000579	0,000692	0,000687
4	Equivalent stress von Mises [MPa]	1,0055	1,5236	1,1658
5	Shear stress [MPa]	0,57555	0,8734	0,6106
6	Total deformation energy U [mJ]	0,0294	0,0213	0,0197

As a result of this analysis it was found that for the cylindrical and hexagonal cell models, the values of the approximate total displacements and the 0.00965 [mm] circular cell, 0.00906 [mm] were obtained with the normal Lagrange method for the square cell, the total displacement being 0.00765 [mm]. For tensions resulting from force application, the best model is the circular cell because it obtained the lowest voltage, namely: 1.0055 [MPa], 1.5236 [MPa] the hexagonal cell and the square cell with a Von voltage Mises of 1.1658 [MPa].

Since the geometric shape of the 3 cells is different (and the volume is different), it is necessary to work with the specific energy (the ratio of energy to cell volume) in order to

compare the obtained values.The contour-specific deformation values being different, a mediated value (for static cell counting) was introduced.
The deformation energy of an element is:

$$U^{(e)} = \int_{v^{(e)}}^{1} \{T^{(e)T} y[\varepsilon^{(e)}] dv\}$$

Knowing that: $< V_1 \neq V_2 \neq V_3$,

$$U = \sum_{(e)} U^{(e)}$$

$$KU = \frac{U}{V}$$

U - represents the internal energy of total deformation
V- represents the volume of the entire circular, hexagonal or square cell type

$$KU = \frac{U_{circular}}{V_{circular}} = \frac{0.0234}{321.74} = 0.0000726 (mJ/mm^3)$$

$$KU = \frac{U_{hexagon}}{V_{hexagon}} = \frac{0.0215}{286.65} = 0.000075 (mJ/mm^3)$$

$$KU = \frac{U_{pătrat}}{V_{Square}} = \frac{0.0187}{443} = 0.0000423 (mJ/mm^3$$

Where KU is the intrinsically specific internal energy of the structural deformation
V- is the volume of the entire structure (hexagon, circular, square).
Conclusion
The hexagonal and circular cell structure have comparable characteristics based on the internal strain energy density criterion.
The square structure has lower characteristics than the density of the deformation energy density, requiring a significantly larger volume to absorb the same mechanically.
Between the hexagon structure and the circular structure, the maximum efficiency in taking over the mechanical work, ie the volume of the necessary material, is obtained in the case of hexagon, frequently encountered in the natural composite structures (wood, honey, etc.).

3.8 Analytical calculation for sandwich cell structures

Total displacement is the sum of sandwich's face and sand movements:

$$\delta_{total} = \delta_{miez} + 2\,\delta_{fața} \quad (3.1)$$

Using the Compressing Compressing Resistance Compressing Base Formulas, the values of cell core and cell movements are obtained:

$$\Delta_{core} = \varepsilon_{core} \times h_{core} \quad (3.2)$$

$$\delta_{core} = \frac{F \times h_{core}}{A \times E_{core}} \quad (3.3)$$

$$\delta_{face} = \varepsilon_{face} \times h_{face} \quad (3.4)$$

$$\delta_{face} = \frac{F \times h_{face}}{A \times E_{face}} \quad (3.5)$$

By replacing (3.3) and (3.5) in (3.1), the expression is applied for the applied force:

$$F = \frac{\delta_{total}}{\left(\frac{h_{core}}{A \times E_{core}} + 2\frac{face}{A \times E_{face}}\right)} \quad (3.6)$$

Considering that the applied force on the cell has the value F = 5N, the analytical and numerical calculation was performed.

Table 3.6 Comparison of results of forces calculated with AEF and theory

Cell geometry	Force (Ansys) [N]	Force (of theory) [N]	Difference[%]
Circular	5	5,2	4
Hexagon	5	5,5	10
Square	5	5.3	6

These studies were conducted to better understand the behavior of the cells forming a sandwich plate. A comparison was made between the results obtained with the Ansys software package and the results of the theory using equation (3.6) for the three cell geometries presented in Table 3.6. Some differences in results are noted in the comparative analysis. The large discrepancy between the results can be explained by the use of the solid-solid modeling of faces and honeycomb core walls, which can lead to errors during inter-laminar studies [65].

3.9 Finite Element Modeling of Sandwich Composite Plates Application

The static analysis of the sandwich plates with the honeycomb core determines the behavior of the plate under the action of a concentrated force applied to the center of the upper face. The purpose of the analysis is to determine:

- Total deformation [mm], deformation in direction (z) [mm], elastic equivalent displacement [mm / mm], Von Mises equivalent [MPa] tension, shear stress [MPa], deformation energy [mJ]. The materials used are the same as those used in previous modeling, respectively:
- For both sides, reinforced glass fiber epoxy resin with a thickness of 1 [mm];
- Heart (or core) of polypropylene with thickness t = 20 [mm];

The applied force for the three cases is F = 1000 [N];

The sandwich plates are square, L = 340 [mm].

Thickness of cell walls is tc = 0.25 [mm].

3.9.1 Circular cell sandwich plate

The above conditions are valid in all four cases, as this is particularly important when making a plate comparison. Dimensions and boundary conditions must be the same in all cases in order to compare the results obtained.

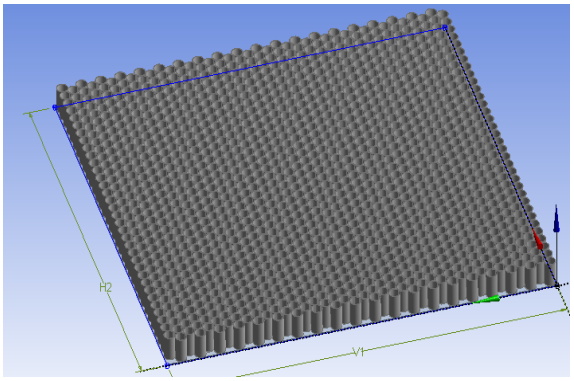

Figure 3.10 Detail for Plain Plates with Cells circular

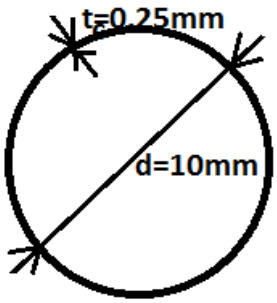

Figure 3.11 Dimensions of the cell circle

Figure 3.36 shows the core of the 340X340 mm polypropylene sandwich and in Figure 3.37 a circle with diameter d = 10 mm and thickness tc = 0.25 mm (the base of the circular cell). The sandwich plate was embedded on all lateral surfaces and the analysis mode was done with finite elements in ANSYS Mechanical, using the concept of volume elements, Volume - Volume - Volume (the concept Solid - Solid - Solid - Solid). A force of F = 1000 [N] was applied to the top surface of the sandwich panel, as can be seen in Figure 3.38 a).

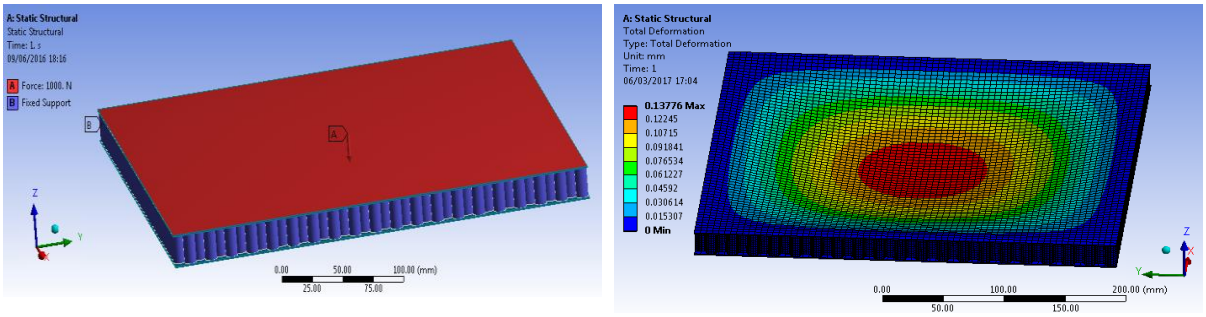

a) b)

Figure 3.12 Application of fixing conditions and force F = 1000N for circular cell sandwich plate a) Map of total deformations b)

The above conditions are valid in all four cases of cell geometries.
Figure 3.38 b) shows the map of the displacements on the top of the plate. The maximum total displacement is 0,13776 [mm]. The red color in the center of the panel is the most affected area. On the edges of the plate the shifts become smaller and the damage disappears in contour, or they are insignificant.

3.9.2 Hexagonal cell sandwich plate

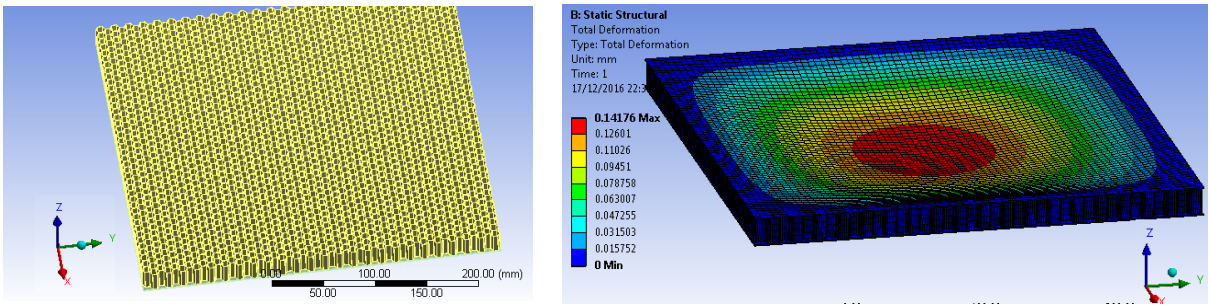

a) b)

Figure 3.13 Simple hexagonal plate geometry detail a), Map of total deformations b).

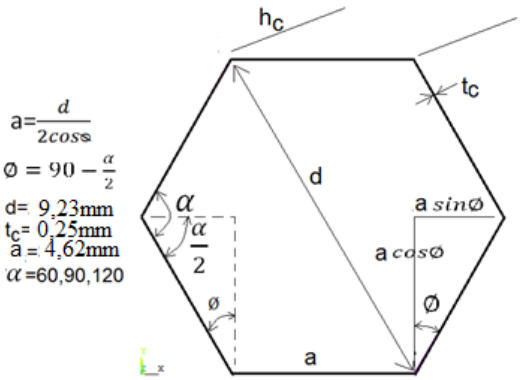

Figure 3.14 The size of the hexagonal cell

The cell dimensions, shown in Figure 3.41, have the following meanings: tc is the cell wall thickness, hc is the height of the cell "a" is the hexagon side "d" is the diagonal of the hexagon.

3.9.3 Square square sandwich plate

The square-cell sandwich plates are made such that inside the cell there is a filler that can be even polyurethane foam, different types of PVC, etc.

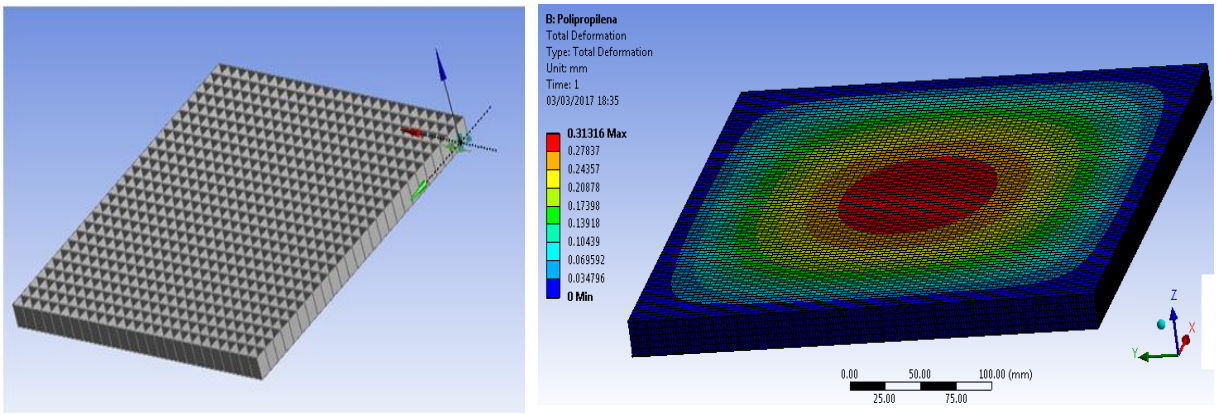

a) b)

Figure 3.15 Detail for square cell simple plate a), Map of total square plate sandwich deformations b).

3.9.4 Unstructured square cell sandwich plate

The following are the numerical tests performed at the bending of the unstructured square-shaped sandwich plate embedded in the contour.

Figure 3.45 shows a detail of the unstructured square cell plate and Figure 3.45 shows the map of the total deformations.

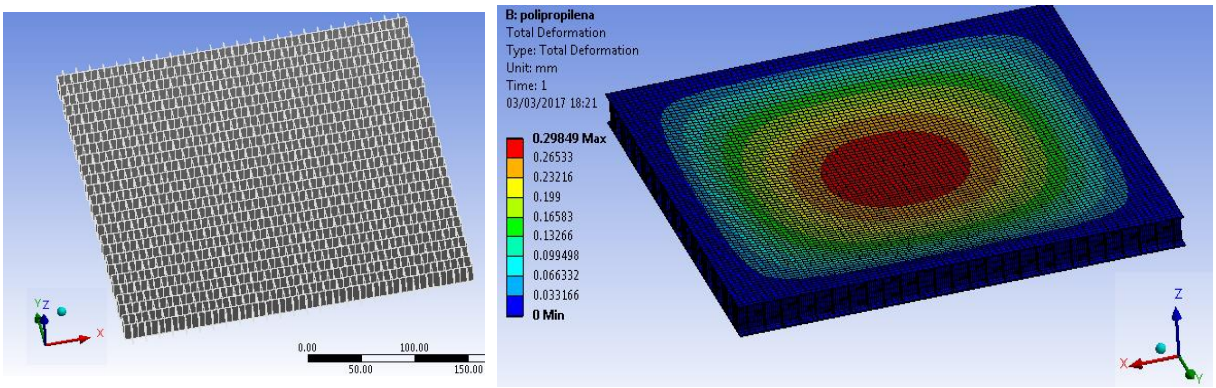

a) b)

Figure 3.16 Detail for Unstructured Square Single Plate Plate a), Map of the Unstructured Square Distributed Square Distortion Plans b)

The results of the numerical analysis for the bending of the embedded plate on the contour are presented in Table 3.7. As can be seen, circular and hexagonal honeycomb core plates are more rigid but have a higher strength. The deformation energy of these plates is lower than the other two types.

Table 3.7 Bending analysis resu

No.	Parameters (for maximum values)	Values for sandwich plate with:			
		Circular cells	Hexagonal cells	Square cells	Unstructured square cells
1	Total deformation [mm]	0,13776	0,14176	0,31316	0,29849
2	Displacement in the direction (z) [mm]	0,0003165	0,000246	0,000432	0.0010322
3	Specific deformation	0,001466	0,00162	0,002237	0,0055681

4	Equivalent stress von Mises [MPa]	5,5254	9,0081	18,32	15,476
5	Shear stress [MPa]	0,35019	0,59313	0,59552	1,11006
6	Deformation energy U [mJ]	0,0036708	0,0035717	0,010024	0,0065539

The complexity of sandwich structures with multi-layered geometric configurations makes modulation more difficult for an accurate analysis of the mechanical properties of honeycomb core panels. The general behavior of these structures depends on the properties of the materials, constituents (faces, cores, and adhesive if necessary), geometry, dimensions and type of loading. Moreover, experimental methods for composite materials are more complex than for isotropic materials and require significant changes [72, 73].

3.10 Impact calculation for sandwich plates with different cores

3.10.1 Presentation of analyzed cases

For finite element analysis, various FEM licensed packages can be used. The most used are: LS-Dyna, Abaqus, Ansys. In this study, the Ansys Workbanch geometry and Dynamic 3D software for impact modeling will be used. Four sandwich plates with different core geometry will be modeled as: circular, hexagonal, square, and unstructured squares. The impactor system - sandwich plate has been determined values, assumptions and calculation peculiarities as follows:

The steel ball with a radius R = 30 [mm] and the mass m = 5 [Kg]. Parameter calculation:

The sandwich plate is square with L = 340 [mm]

The material used for the faces of the sheet is glass fiber reinforced epoxy resin.

Core thickness: 20 [mm]. Material used: polypropylene honeycombs.

- the time passed by the ball to hit the board, "End Time", = 0.0025 [s]

ball velocity V = 4.81 [m / s].

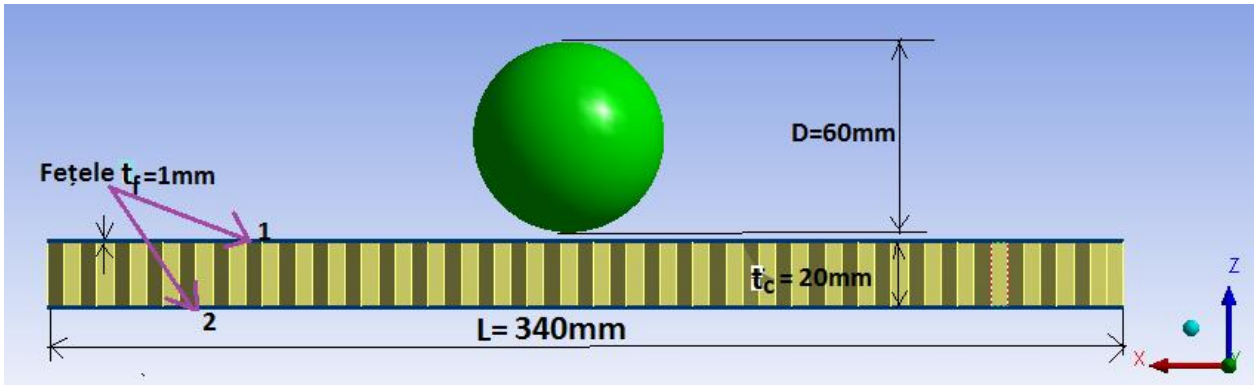

Figure 3.17 The impactor system geometry - sandwich plate

For geometry, the values below and shown in detail in Figure 3.53 were chosen:

Hypotheses and peculiarities:

- the gravitational acceleration is neglected as it influences very little (the value of the number from the eighth decimal is changed eg: If the movement without gravitational acceleration equals 0.00074842m, with a .g. is 0.00074845m);
- the material characteristics of the sandwich plate chosen in the Ansys software library [77, 58] have been established, respecting the particular conditions of Explicit Dynamics in Ansys Autodyn 3D;
- the initial velocity of the impact penetrator has been established and the plate has to be embedded on all side surfaces; According to the literature [77, 58] it has been established that the element that best adheres to the behavior of the sandwich plate in the studied cases is the SOLID 185 type specially chosen for sandwich composites (Figure 5.54).

- for the discretization of the physical system, it was appreciated that the finite element type is the hexadecimal one.

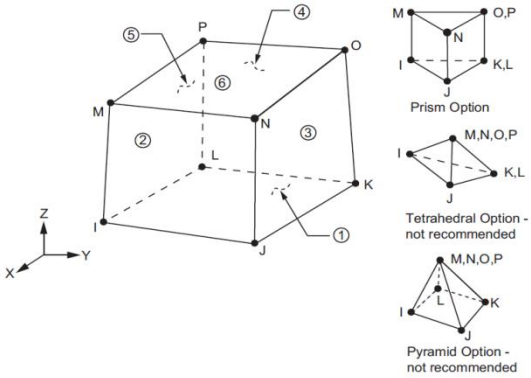

Figure 3.18 Element SOLID185 [58]

With this type of element, good plate results were obtained. Its particular forms (cube, rectangular parallelipiped, triangular prism, or pyramid) allow us to use it also for masking the impactor using the Solid 185 element [58].

3.10.2. Modeling the 4 cases analyzed with FEM in Ansys

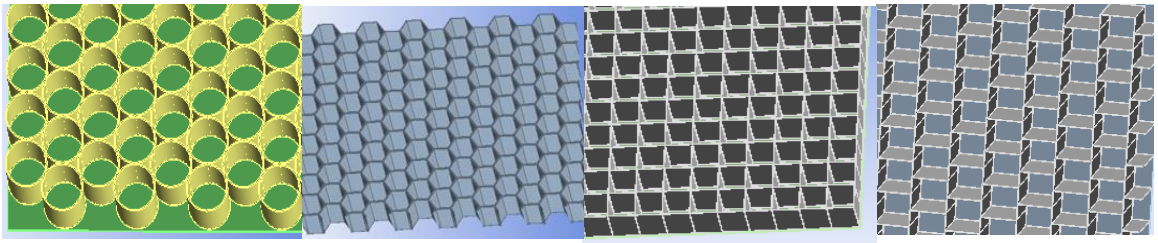

a) b) c) d)

Figure 3.19 Case 1: Cells: circular a), hexagonal b), square c), unstructured squares d)

During impact tests it is necessary to find kinetic energy - an essential component for the validation of the design criteria. The energy values must be obtained by performing the physical test so that these data can be calculated. Following the simple test, the impact force curve is plotted against the displacement and then the area under the curve is integrated, which represents the energy consumed. The problem is a specific application related to the Energy Conservation Law, which states that the potential energy (EP) must be equal to the kinetic energy (EC) (rel.3.8). Resolving the conservation problem from the energy equation above neglecting the resistance air, speed is calculated from Galileo's equation:

$$v = \sqrt{2gh} \tag{3.7}$$

According to potential energy and kinetic energy:

$mgh = mv^2/2$ (3.8)

$mgh = 5*4.81^2/2$

$5*10*h = 59J$ (3.9)

$50*h = 59 \Longrightarrow h = 1{,}18m$

The relationship between force and distance.

Using the principle of energy, the next step is to estimate, by testing, the expected force.

$W_{net} = mv^2_{final} / 2 - mv^2_{initial} / 2$ (3.10)

In a fall test application, $W_{net} = mv^2_{final} / 2$ because the initial speed ($v_{inițial}$) is equal to zero. Assuming the impact distance can easily be measured, the mean of the impact force F is calculated with the expression:

$$F = \frac{W_{net}}{d} \tag{3.11}$$

Where d is the distance traveled after impact.

Table 3.8 Dynamic impact results for the four cases of sandwich plates

No	Parameters (for maximum values)	Values for cell-based sandwich plate:			
		Circular cells	Hexagonal cells	Square cells	Square cells unstructured
1	Total deformation [mm]	4,7748	4,8838	6,821	7,6085
2	Displacement in the direction (z) [mm]	0,0016	0.9831	0,00694	0,01175
3	Specific deformation	0,5998	0,7915	1,9902	0,7565
4	Equivalent stress von Mises [MPa]	200,72	292,65	184,44	239,94
5	Shear stress [MPa]	28,941	34,501	27,963	30,683
6	Total ball velocity[m/s]	4,6334	4,4607	4,662	4,582

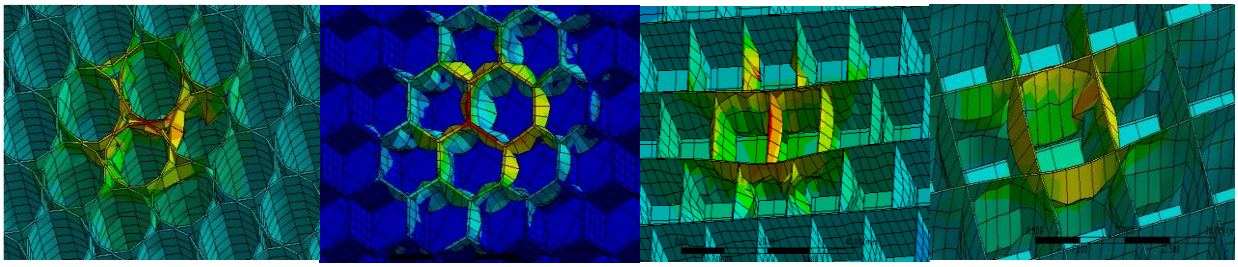

a) b) c) d)

Figure 3.20 Damage of circular cells a), hexagonal b), unstructured c) squares d)

In Figures 3.60 a), b), c), d), there are images of the damage occurring in the cells of the four types of plates obtained in the gravitational impact calculation.

The total deformation for the four analyzed cases is approximately equal for the first two cases and different for square and square unstructured squares. As can be seen in Figure 3.64, the deformation in relation to time is higher for

the unstructured square cell sandwich plate. Sandwich plates have approximately equal behavior (for circular and hexagonal cell sandwiches).

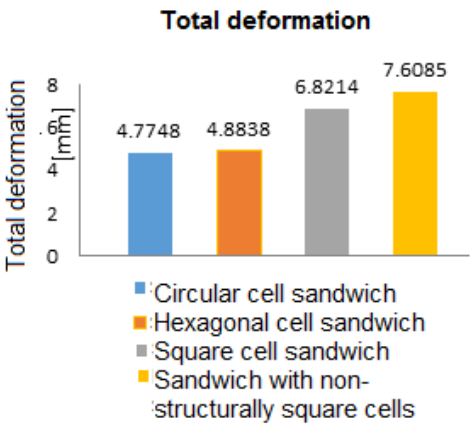

Figure 3.21 Total deformations for sandwich plates with different geometries

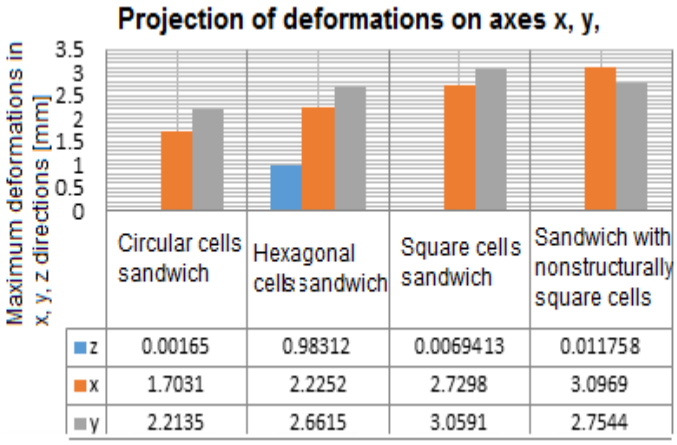

Figure 3.22 Deformation in the direction of the axis (z)

The deformation in the direction of the z-axis in relation to the time forms a significantly higher value curve for the intercalated sandwich plate. Good deformation behavior (good stiffness) is made by square and hexagonal square sandwich plates.

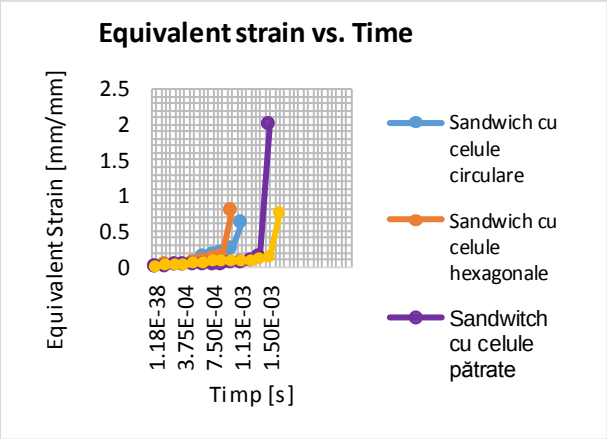

Figure 3.23 Equivalent Strain vs. raport cu time

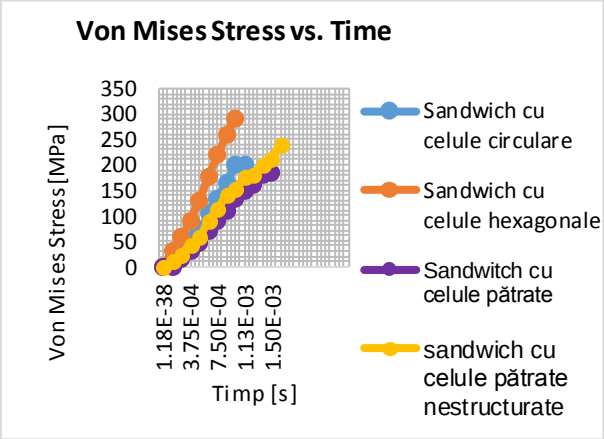

Figure 3.24 Stress von Mises în vs time

At the elastic equivalent deformation with respect to time, there is a significant increase in circular cell sandwich. It can be seen that it has a much higher value than the other three. A good behavior is seen in hexagonal and square cell sandwich plates.

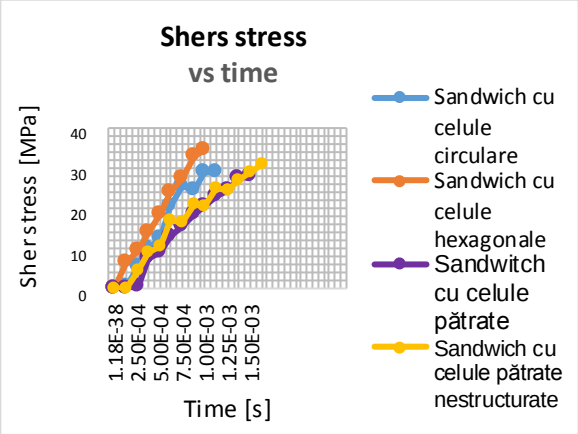

Figure 3.25 Shear stress vs. Time

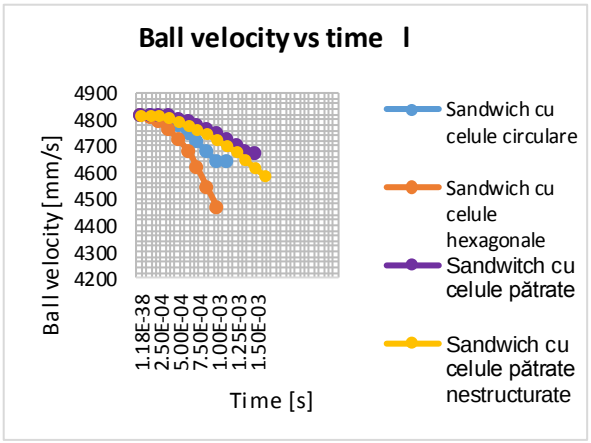

Figure 3.26 Velocity vs. Time

3.11 Sandwich plates with foam core (Foam)

Respecting the conditions of the calculation of sandwich plates with different geometries, four dynamic impact tests will be performed for sandwich plates with cores of different types of foams.

The properties of foam foam material are shown in the tables: 3.9, 3.10, 3.11, 3.12. These are: SAN Foam (SAN-styrene acrylonitriles) with a density of 81 and 103 kg / m^3 and PVC with density 60 andi 80kg/m^3.

Table 3.8 gives the results of the dynamic impact for the four cases of sandwich cell types. The input parameters for the calculation are:

- Ball velocity v = 4.81 [m / s];
- The time of the ball to hit the board, "End Time" = 0.0025 [s];
- 30 mm diameter steel balls impeller;
- sandwich plate with dimensions 340x340 mm;
- Ball weight m = 5kg.

Table 3.9 SANFoam Properties 81kg / m^3 (SAN-styrene acrylonitriles)

Properties SANFoam 81kg/m^3	Value	Measurement units
Density	81	kg/m^3
Elastic Isotropic		
Young's module	60	MPa
Poisson's coefficient	0,3	
Bulk module	50	MPa
shear modulus	23,077	MPa

Table 3.10 Properties of SAN Foam 103kg / m^3 (SAN-styrene acrylonitrile)

Properties SAN Foam 103kg/m^3	Value	Measurement units
Density	103	kg/m^3
Elastic Isotropic		
Young's module	85	MPa
Poisson's coefficient	0,3	
Bulk module	70,833	MPa
shear modulus	32,692	MPa

Table 3.11 Properties of PVC material Foam 60 kg / m^3

Properties PVC Foam 60kg/m^3	Value	Measurement units
Density	60	kg/m^3
Elastic Isotropic		
Young's module	70	MPa
Poisson's coefficient	0,3	
Bulk module	58,333	MPa
shear modulus	26,923	MPa

Table 3.12 Properties of PVC material Foam 80 kg / m^3

Properties PVC Foam 80kg/m^3	Value	Measurement units
Density	80	kg/m^3
Elastic Isotropic		
Young's module	102	MPa
Poisson's coefficient	0,3	
Bulk module	85	MPa
shear modulus	39,231	MPa

Table 3.13 Results obtained for Foam-type sandwich panels

No.	parameter (for maximum values) m	Values for the core sandwich plate from:			
		SanFoam 81kg/m^3	SanFoam 103kg/m^3	PVCFoam 60kg/m^3	PVCFoam 80kg/m^3
1	Total deformation [mm]	12,376	12,394	13,765	16,598
2	Displacement in the direction (z) [mm]	12,176	12,179	13,49	16,591
3	Elastic Strain	0,219	0,226	0,362	0,365
4	Equivalent stress Von Mises [MPa]	116,74	116,91	268,95	274,18
5	Shear stress [MPa]	7,6067	7,136	42,05	50,6
6	Total ball velocity [m/s]	4,725	4,721	4,132	3,896

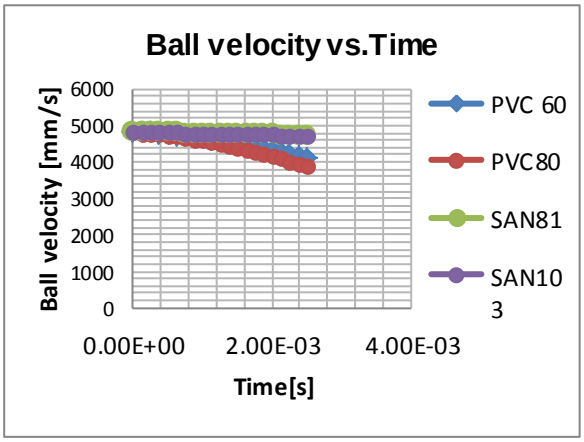

Figure 3.27 Total velocity vs Time

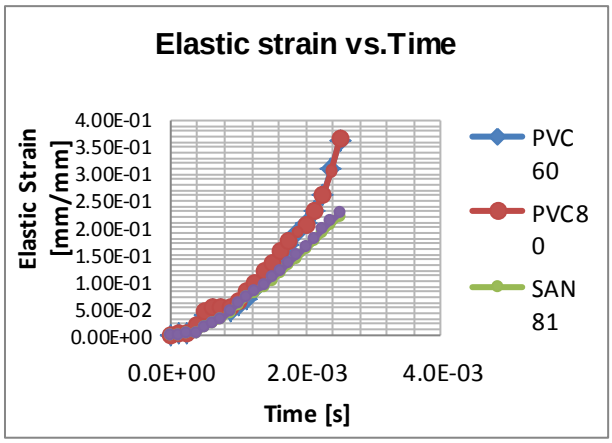

Figure 3.28 Elastic Strain vs.Time

The total speed of the ball is obtained during the actual bile-plate impact, on a case-by-case basis. Impact duration refers to the numerical calculation and not to the duration of the

experiment. Figure 3.72 shows that specific deformations keep variations around the same level in the graph, but higher values are recorded for PVC cases 60kg/m^3 and 80kg/m^3.

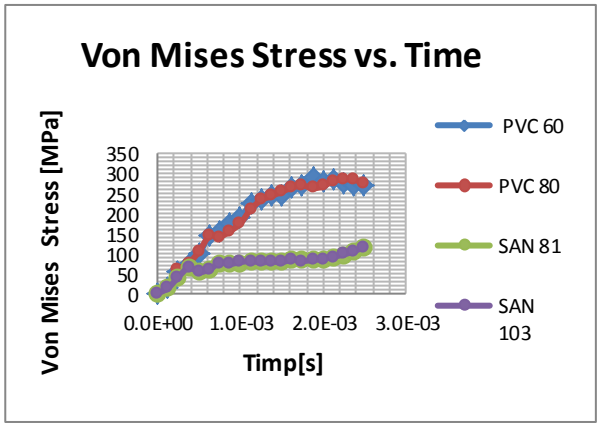

Figure 3.29 Equivalent stress vs. Time

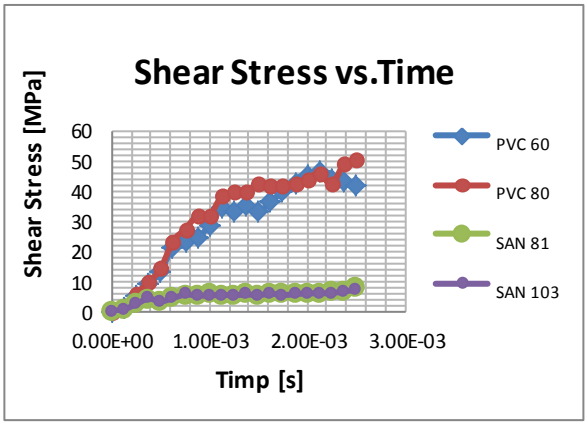

Figure 3.30 Shear Stress vs.Time

The tensions in this case are roughly equal to PVCFoam 60kg / m3, PVC Foam 80kg / m3, and SAN Foam 81kg / m^3 and SANFoam with a density of 103kg / m3 are much lower in the chart, with much lower values.

Figure 3.74 shows the variations in shear stresses, which have a different PVC behavior with densities of 60 kg / m^3 and 80 kg / m^3. Variations record a jump in the graph, which means a high shear stress on the top of the plate. This shows a weaker resistance for these cases. Lower voltages are recorded for SAN Foam with dens 81 kg/m^3 respectiv 103 kg/m^3.

3.12 Conclusions

1.The analysis of cells with hexagonal, circular and square geometries was performed to determine how they behave in applying a force. From the calculations it was found that for the hexagonal cell core the best results were obtained, observing that its volume was smaller than the other analyzed cells.

2. Static analysis was performed for the following types of sandwich plates: circular, hexagonal, square, and unstructured square sandwich plate. The results showed that the hexagonal core sandwich plate had a better behavior than the others.

3. For dynamic analysis of sandwich plates with different geometries, smaller displacements were obtained for hexagonal and circular core sandwich plates and larger displacements for unstructured square and square square sandwich plates.

4. For all parameters studied for PVC core sandwich plates with densities of 60 and 80 kg / m3, values significantly increased compared to SAN Foam 81 and 103 kg / m3 core sandwich panels, analyzed at dynamic impact.

5. Composite composite sandwich plates have a specific behavior different from conventional sandwich plates.

6. The rigidity of the composite sandwich plates is much higher than the rigidity of each component taken separately.

7. The overall strength of the composite sandwich plates is much higher than the strength of each component taken separately.

8. Designing advanced composite structures or components subjected to dynamic tests requires a profound understanding of the damage and degradation mechanisms that occur in the composite material. In this thesis, a numerical simulation with the Ansys finite element analysis package of low-impact impact for sandwich plates with glass fiber / laminated epoxy resin fiber webs with polypropylene honeycomb core and SAN Foam (SAN- styrene

acrylonitriles) with densities of 81 kg / m3 and 103 kg / m3 and PVC with densities of 60 kg / m3 and 80 kg / m3.
9. Good mechanical and thermal characteristics can also be added to the mechanical characteristics described above.
10. In numerical modeling, the calculation errors can occur due to: geometry of the model (non-observance of dimensions), contact problems (if surface contact is not done correctly, large differences in final results may occur), meshing problems (too fine refining of In some cases a fine refining of the model is possible, which can affect the final results. The so-called "mesh refinement" (fine meshing) if not done can result in final results which may differ from expectations).
11. The contact problem has been solved taking into account the following characteristics:
- the two surfaces in contact do not interpenetrate.
- the two surfaces can transmit normal compressive and tangential forces;
- the two surfaces do not transmit normal tensile forces.
12. Meshing problems. In some cases, the model is finely refined, which may affect the final results. The so-called "mesh refinement" (fine mesh) if it is not done can result in final results that may differ from expectations.
13. For the best results, the remarks listed above must be observed. On the other hand, the chosen parameters matter in obtaining correct results.
14. Choosing materials for sandwich boards requires special attention because the final result must distinguish between a simple (isotropic and homogeneous) material and the layered or sandwich taken together.
15. Fastening conditions. Appropriate links to the rest of the structure must be observed.
16. Impact analysis can also be performed for other (higher or lower) speeds to obtain other appropriate kinetic energies. This helps to observe the movements and tensions occurring in the sandwich plate, and also to observe the behavior of faces and cores.
17. The parameters computed in ANSYS are obtained for the impact duration of 2.5ms (one part of the duration of impact) for all plate specimens. Movement values are not significant for dynamic phenomena. The most important parameter is the energy absorbed by each plate, which is the purpose for which analyzes are made in this thesis.
18. The impact time may vary, which may also affect the strain and strain movement values in the plate. Also, the type of impact influences the deformation of the faces and the core. With low speed and short time, then displacements, deformations and tensions will be low.
19. The more a sandwich plate has more cells in a volume the more it can become more impact resistant than a sandwich plate

CHAPTER 4 AN STATIC AND DYNAMIC ANALYSIS OF SANDWICH PLATES

4.1 Introducere

Geometric modelling of the honeycomb structures requires a special attention in order to choose a good procedure for the calculation with finite elements.

Actually, there are two ways: the interaction between geometric modelling and the FEM modelling. The geometry imposes the FEM model but the FEM modelling requirements affect the geometric model. There are three methods of modelling a honeycomb structure sandwich type:

1. Full 3D modelling, these use volume elements (Solid)
2. Shell modelling (plate elements)
3. Mixed modelling (Shell and Solid)

4.1.1 Static calculation. Modelling by using Solid elements

10 sandwich plates with different core thicknesses and stressed with different forces were model by using solid elements, namely: 8.3, 14.95, 38.95, 53.55 [N]. These cases will be analysed also experimentally in chapter no 5.

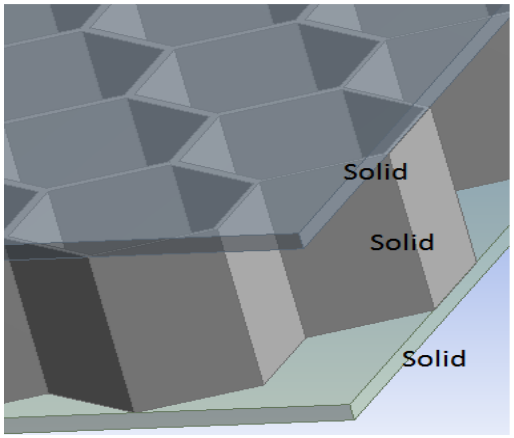

Figure 4.1Modelling the honeycomb core sandwich plates by means of solid elements.

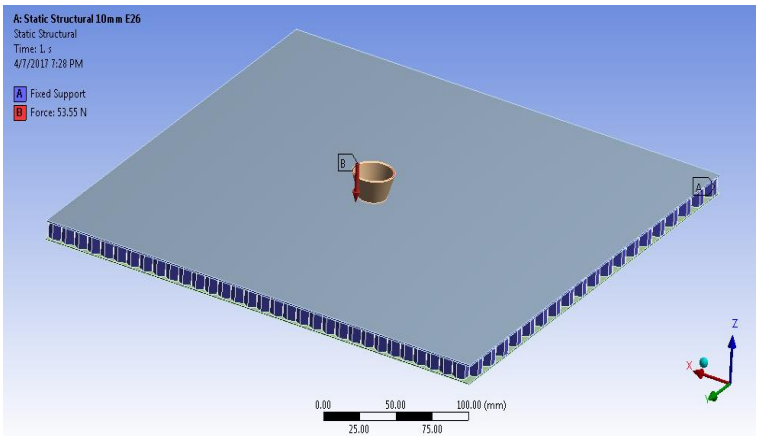

Figure 4.2 Applying the concentrated force and the connections embedded on the contour line of honeycomb-core composite sandwich plate

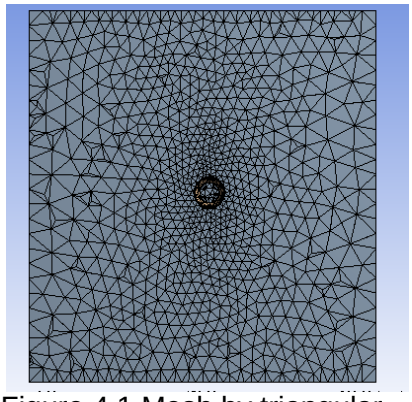

Figure 4.1 Mesh by triangular elements of the shell

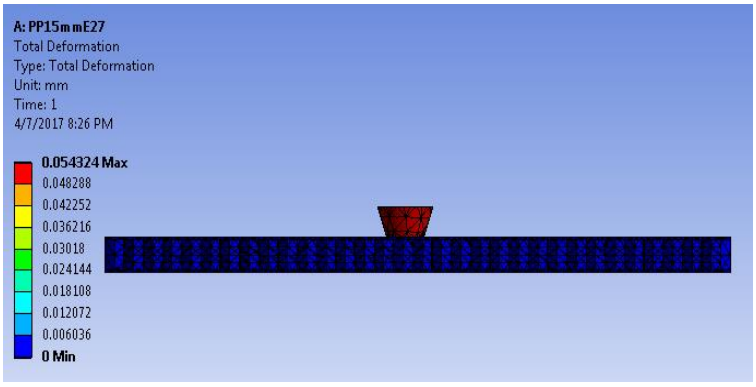

Figure 4.4 Map of the total strains for the core with thickness of 15 mm

The analysis with finite elements was done by using solid elements with shape of triangular prism as well as square.

Table 4.1 The results of sandwich plates static analyses with Solid elements

No.	Cases with Solid	U.M. For displacements	Forces			
			8.3N	14.95N	38.95N	53.55N
1	SP10/0.2x5	[mm]	0.01203	0.02168	0.05648	0.07765
2	SP10/0.33x3	[mm]	0.01215	0.02189	0.05703	0.07841
3	SP15/0.2x5	[mm]	0.00842	0.01516	0.03951	0.05432
4	SP15/0.33x3	[mm]	0.00848	0.01528	0.03982	0.05475
5	SP20/0.2x5	[mm]	0.00127	0.01152	0.03003	0.04128
6	SP20/0.33x3	[mm]	0.00643	0.01159	0.03021	0.04153
7	SP28/0.2x5	[mm]	0.00486	0.00876	0.02282	0.03137
8	SP28/0.33x3	[mm]	0.00488	0.00880	0.02292	0.03152
9	SF20/0.2x5	[mm]	0.00766	0.01380	0.03595	0.04942
10	SF20/0.33x3	[mm]	0.00770	0.01387	0.03615	0.04971

4.1.2 Static analysis. Mixed modelling Shell-Solid-Shell

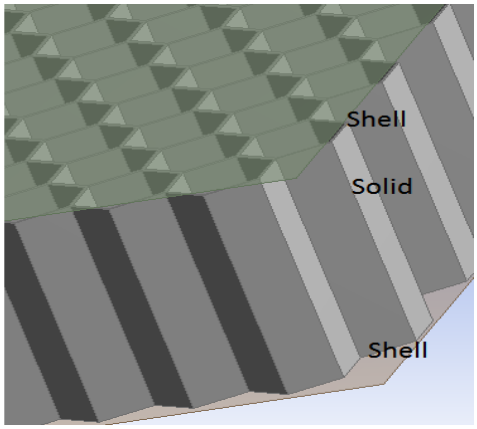

Figure 4.5 Modelling of composite sandwich plate with mixed elements mixte de tip Shell-Solid-Shell

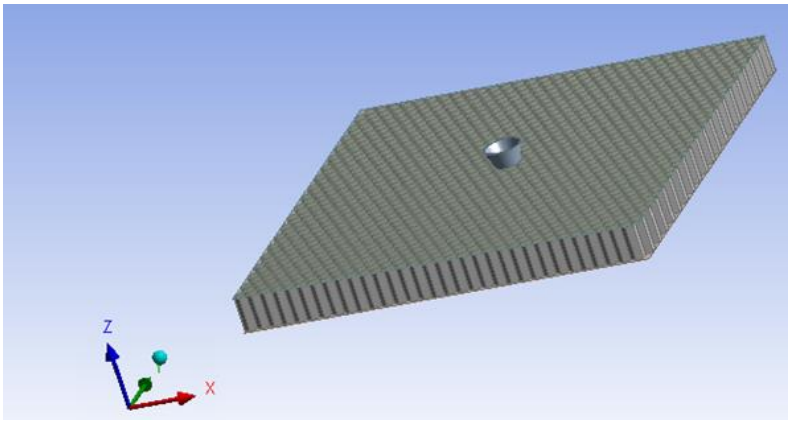

Figure 4.6 Geometria plăcii sandwich compozit

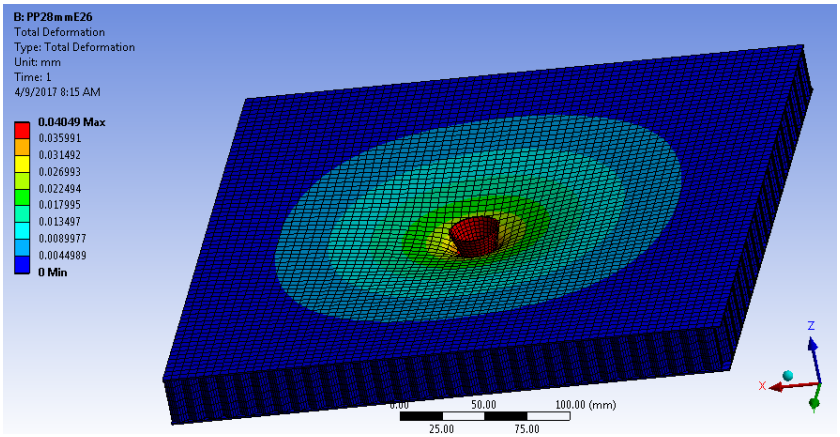

Figure 4.7 The map of the strains for sandwich plate with core thickness of 28 mm

Table 4.2 Analysis results of sandwich plates with Shell Solid Shell elements

No.	Cases with Solid	U.M. For displacement	Forțe			
			8.3N	14.95N	38.95N	53.55N
1	SP10/0.2x5	[mm]	0.014	0.02932	0.079	0.1206
2	SP10/0.33x3	[mm]	0.015	0.035	0.062	0.1217
3	SP15/0.2x5	[mm]	0.017	0.02106	0.0544	0.0750
4	SP15/0.33x3	[mm]	0.018	0.02108	0.0549	0.0755
5	SP20/0.2x5	[mm]	0.007	0.015	0.0339	0.0553
6	SP20/0.33x3	[mm]	0.008	0.013	0.0335	0.0556
7	SP28/0.2x5	[mm]	0.0069	0.019	0.0293	0.0403
8	SP28/0.33x3	[mm]	0.0068	0.013	0.0295	0.0405
9	SF20/0.2x5	[mm]	0.00915	0.01648	0.042934	0.0593
10	SF20/0.33x3	[mm]	0.00916	0.01649	0.04298	0.0591

4.2 Materials and geometrical properties of sandwich structures (honeycomb and foams)

The epoxy resins are part of a large materials family that contain a reactive functional group of these - the molecular structure. The epoxy resins have the best characteristics from all resins that are used in marine industry. Aerospace applications use, almost exclusively, the epoxy resins except the cases when the performance at high temperature is critical. The high cost of epoxy resins and the high demands have limited their use for big size marine structures. In this chapter, ten composite sandwich plates will be impact analysed. To decide the material properties for faces and well as for cores, some tests and calculations were performed but also some bibliographical special researches were considered for certain parameters which couldn't be determined by the test laboratory equipment because they require a more complex testing. Material properties from the table 4.3 were determined experimentally in chapter 5 but also calculated by the means of Ansys ACP soft. Thus the elastic modulus E_1,E_2 were determined experimentally and they were compared to the calculation from finite elements modelling and the results are very good. The other properties were taken from the special literature more specific from ANSYS library and Gama [78].

Tabelul 4.3 Materials properties for the composite faces

Properties, Units of measurement	**E-Glass/Epoxy (5 layers)**	**E-Glass/Epoxy (3 layers)**
Young's Modulus E1, MPa	27800	26800
Young's Modulus E2, MPa	27800	26800
Young's Modulus E3, MPa	11800	11800
Poisson's ratio, υ21	0.11	0.11
Poisson's ratio, υ31	0.18	0.18
Poisson's ratio, υ32	0.18	0.18
Sher modulus G12, MPa	5000	5000
Sher modulus G23, MPa	3557	3451
Sher modulus G31, MPa	3557	3451
Orthotropic Stress Limits		
Tensile strength in x direction, MPa	1100	1100
Tensile strength in y direction, MPa	1100	1100

Tensile strength in z direction, MPa	35	35
Compression strength in x direction, MPa	-675	-675
Compression strength in y direction , MPa	-675	-675
Compression strength in z direction, MPa	-120	-120
Shear strength in xy direction, MPa	46.154	46.154
Shear strength in yz direction, MPa	80	80
Shear strength in xz direction, MPa	80	80
Orthotropic strain limits		
Tensile strain in x direction, MPa	0.0244	0.0244
Tensile strain in y direction, MPa	0.0244	0.0244
Tensile strain in z direction, MPa	0.0035	0.0035
Compressive strain in x direction, MPa	-0.015	-0.015
Compressive strain in y direction, MPa	-0.015	-0.015
Compressive strain in z direction, MPa	-0.012	-0.012
Shear strain in xy direction, MPa	-0.016	-0.016
Shear strain in yz direction, MPa	-0.016	-0.016
Shear strain in xz direction, MPa	-0.012	-0.012
Tsai –Wu constants		
xy couple	-1	-1
yz couple	-1	-1
xz couple	-1	-1

4.3. Check-up the material properties based on the plate stiffness calculation

There were verified the results for E1 and E2 calculated by Ansys ACP software and afterwards they were compared to the experimental results.
For sample 1 with 0,33mm x 3 layers, where E=26,9 [GPa]
The following resulted:
Transversal elastic modulus = 5 [GPa]
Longitudinal elastic modulus E1 = 26.780 [GPa]
Longitudinal elastic modulus E2 = 26.780 [GPa]
Laminate stiffness to shearing stress G12 = 5 [GPa]
Laminate stiffness E1 = 26.780 [GPa]
Laminate stiffness E2 = 26.780 [GPa]
Shear outside the plane G23 = 3.451 [GPa]
Shear outside the plane G31 = 3.451 [GPa]
Shear correction factor k44 (G23) = 0.78
Shear correction factor k55 (G31) = 0.78

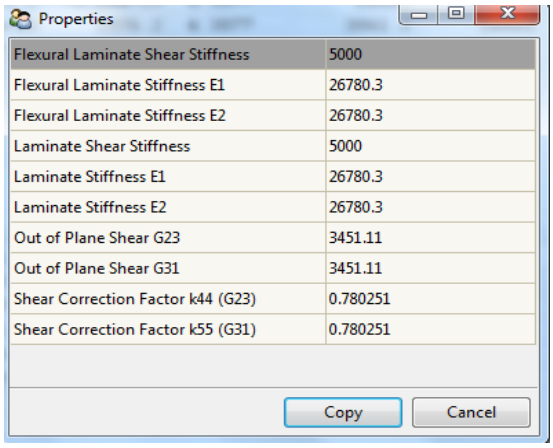

Figure 4.8 Check-up the material properties based on the plate stiffness calculation

Normalized Laminate Stiffness and Compliance Matrices

Stiffness Matrix:

i	0	1	2	3	4	5	6	7
0	28061	3061.2	−2.171...	−2976.2	−1.16e−13	4.3077...	0	0
1	3061.2	28061	2.1711...	−1.16e−13	2976.2	4.3077...	0	0
2	−2.171...	2.1711...	5000	4.3077...	4.3077...	1.16e−13	0	0
3	−2976.2	−1.16e−13	4.3077...	28061	3061.2	−2.171...	0	0
4	−1.16e−13	2976.2	4.3077...	3061.2	28061	2.1711...	0	0
5	4.3077...	4.3077...	1.16e−13	−2.171...	2.1711...	5000	0	0
6	0	0	0	0	0	0	4423.1	2.4265...
7	0	0	0	0	0	0	2.4265...	4423.1

Compliance Matrix:

i	0	1	2	3	4	5	6	7
0	3.7341...	−4.073...	1.6959...	1.1881...	−7.344...	−3.439...	0	0
1	−4.073...	3.7341...	−1.695...	−7.133...	−1.188...	−3.439...	0	0
2	1.6959...	−1.695...	0.0002	−3.439...	−3.439...	−1.391...	0	0
3	1.1881...	−5.818...	−3.439...	3.7341...	−4.073...	1.6959...	0	0
4	−3.634...	−1.188...	−3.439...	−4.073...	3.7341...	−1.695...	0	0
5	−3.439...	−3.439...	−1.391...	1.6959...	−1.695...	0.0002	0	0
6	0	0	0	0	0	0	0.0002...	−1.240...
7	0	0	0	0	0	0	−1.240...	0.0002...

Figure 4.9 Stiffness matrix and compliance matrix for three layers composite

In figure 4.9 , the stiffness matrixes and compliance matrix are drawn-up for the three layers composite with the 0,33 [mm] thickness and laminates direction to [0-90] degree. The orthotropic material is characterized by 9 constants, respectively E_1, E_2, E_3, υ_1, υ_2,υ_3, G_{12},G_{23}, G_{31}. The connection between the specific strains and stress is made by the compliance matrix.

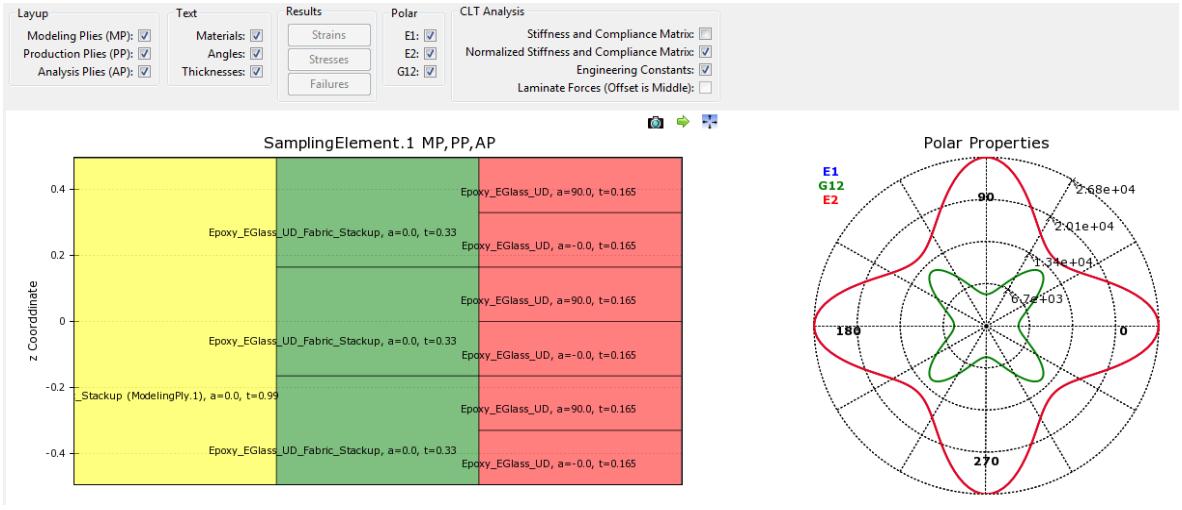

Figure 4.10 Display of the three layers properties of the composite material

Figure 4.10 exemplifies the elastic properties of the different layers within a polar diagram. Polar diagrams allow us to see the manner how the properties can change depending on the test angle. Comparing the material characteristics values resulted from experiments, from special literature and checking of the calculation with Ansys) it results a full accordance. The properties of texture with longitudinal and transversal direction (E1 and E2) are the same two properties only they are overlapped in the polar diagram from the figure. E1 can be understood as E (elastic modulus) in direction of the fibre (or in the direction of zero degree) and E2 as transversal towards the direction of fibre (direction to 90 degrees). G12 is the shear modulus in plane. The radius represents the values of the modulus, in MPa [79]. In

[80] and [81] there were published the comparative results of the numerical and experimental calculation for polystyrene and polypropylene core sandwich plates. In the study from [82] properties for composite faces were found. These are displayed below:

Table 4.4 mechanical properties of the composite faces from [82]

Elastic modulus	[MPa]	Transversal elastic modulus	[MPa]	Poisson's ratio	(-)
E_1	26000	G_{12}	3800	ν_{12}	0.1
E_2	26000	G_{23}	2800	ν_{13}	0.25
E_3	8000	G_{13}	2800	ν_{23}	0.25
Tensile strength	[MPa]	Compression strength	[MPa]	Shear strength	[MPa]
X_T	850 (414)	X_C	720 (458)	S_{12}	105
Y_T	850 (414)	Y_C	720 (458)	S_{13}	65
Z_T	120	Z_C	500	S_{23}	65
Inter-laminar normal breaking stress		[MPa]	Inter-laminar shear stress		[MPa]
NFLS		35	*SFLS*		65

Thus for sample 2 (5 layers with thickness of 0,2 [mm] each) where E=27,8 [GPa], the below properties were obtained:
Transversal elastic modulus = 5000.0 [MPa]
Longitudinal elastic modulus E1 = 27.386 [GPa]
Longitudinal elastic modulus E2 = 27.386 [GPa]
Shear elastic modulus G12 = 5 [GPa]
Shear outside the plane G23 = 3.557 [GPa]
Shear outside the plane G31 = 3.557 [GPa]
Shear correction factor k44 (G23) = 0.8041
Shear correction factor k55 (G31) = 0.8041

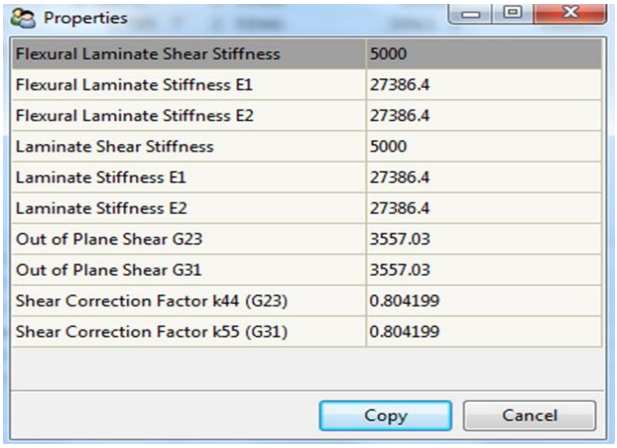

Figure 4.11 Material properties from Ansys ACP soft for the 5 layers composite material

Stiffness Matrix:

i	0	1	2	3	4	5	6	7
0	28061	3061.2	−2.171...	−1785.7	4.5475...	2.5846...	0	0
1	3061.2	28061	2.1711...	4.5475...	1785.7	2.5846...	0	0
2	−2.171...	2.1711...	5000	2.5846...	2.5846...	3.4106...	0	0
3	−1785.7	4.5475...	2.5846...	28061	3061.2	−2.171...	0	0
4	4.5475...	1785.7	2.5846...	3061.2	28061	2.1711...	0	0
5	2.5846...	2.5846...	3.4106...	−2.171...	2.1711...	5000	0	0
6	0	0	0	0	0	0	4423.1	2.4265...
7	0	0	0	0	0	0	2.4265...	4423.1

Compliance Matrix:

i	0	1	2	3	4	5	6	7
0	3.6515...	−3.983...	1.7225...	6.971e−06	3.5855...	−2.017...	0	0
1	−3.983...	3.6515...	−1.722...	3.5211...	−6.971...	−2.017...	0	0
2	1.7225...	−1.722...	0.0002	−2.017...	−2.017...	−4.092...	0	0
3	6.971e−06	3.5676...	−2.017...	3.6515...	−3.983...	1.7225...	0	0
4	3.5329...	−6.971...	−2.017...	−3.983...	3.6515...	−1.722...	0	0
5	−2.017...	−2.017...	−4.092...	1.7225...	−1.722...	0.0002	0	0
6	0	0	0	0	0	0	0.0002...	−1.240...
7	0	0	0	0	0	0	−1.240...	0.0002...

Figure 4.12 Stiffness matrix and compliance matrix for the 5 layers composite material

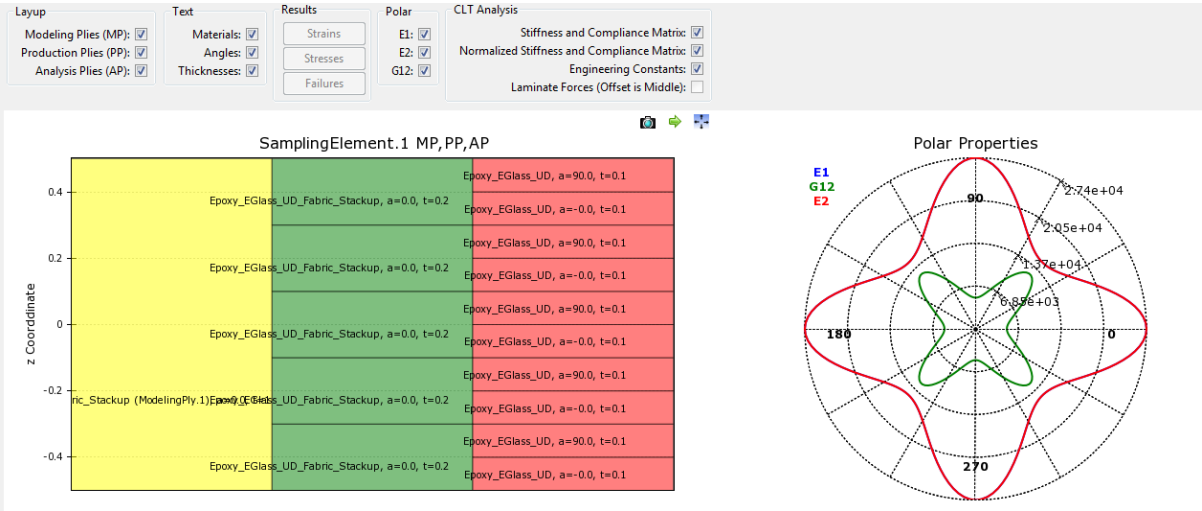

Figure 4.13 Properties display of the 5 layers composite material

Tabelul 4.5 Proprietățile mecanice ale bilei din oțel

Properties	Steel ball
Density [kg/m^3]	1750
isotropic -elastic properties	
Young's modulus [MPa]	2x10^5
Poisson's ratio	0,3

4.4 Impact modelling of sandwich plates

10 sandwich plates were modelled with different core geometry. The cores are type honeycomb with polypropylene hexagonal cells and thicknesses of 10, 15, 20 and 28 mm. Other two plates have the core made of extruded polystyrene with 20 mm thickness. The faces are made of epoxy resin reinforced with glass fibre of 1mm total thickness. These are of two types: with 3 layers (the thickness of fibre layer is 0.33mm) and with 5 layers (thickness of 0.2mm). The inlet parameters for calculation at impact are:

- The drop distance of the ball is 1180 [mm]
- The steel ball velocity in all cases is v=4.85 [m/s]

- The weight of the ball is m=5 [kg]
- The ball diameter is 106 [mm].
- The side of the square sandwich plate is 340 [mm].
- The characteristics of the polypropylene used at these simulations are presented in the below table 3.1.

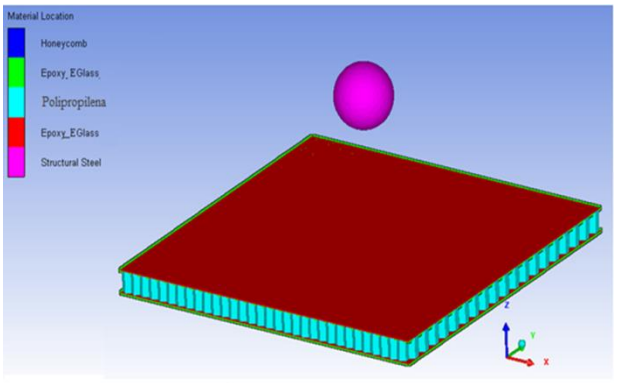

Figure 4.14 Composite sandwich plate geometry for impact modelling

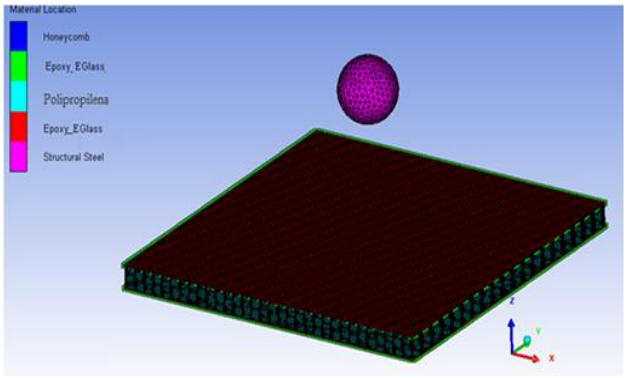

Figure 4.15 Digitization network of model: plate - ball

4.5 Impact modelling results for all the 10 sandwich plates analysed

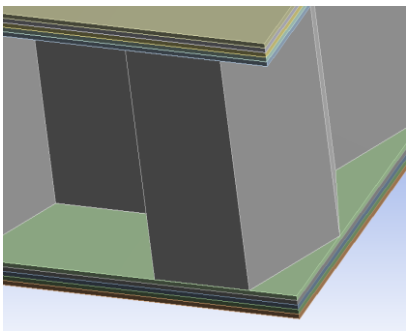

Figure 4.2 Plate with faces with 5 layers

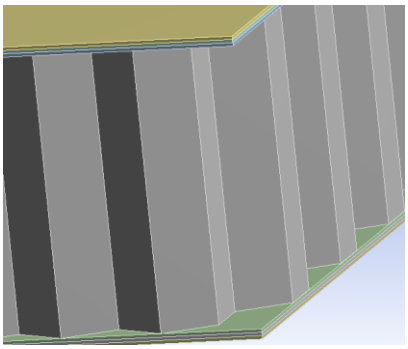

Figure 4.17 Plate with faces with 3 layers

In the table 4.6 there are presented the parameters calculated in ANSYS, obtained for the impact time period of 2.5ms (a part of impact time period), for those 10 specimens of plate. In the figures 4.18 and 4.19 there are presented the maximum travelling variations obtained for those 10 analysed cases. The same values are found in the columns 3 (for the top face) and 4 (for the bottom face) from table 4.6. The values of the travelling are not significant to the dynamic phenomena. The most important parameter is the energy absorbed of each plate that represents the purpose of the analysis performed in this thesis. Due to technical reasons the calculation couldn't be finalised, until the total consumption of the impact, the energy absorbed at the impact la impact couldn't be calculated for the entire time duration of the phenomenon, the total value being determined within the experiments.

Table *4.6 Parameters calculated in ANSYS*

No.	Specimens	Total displacement measured on the top face [mm][mm]	Total displacement measured on the bottom face [mm]	Strain equivalent [mm/mm]	von Mises stress [MPa]	Shear stress [MPa]	Ball velocity [mm/s]
1	SP10/0.2x5	11.243	8.9857	0.034	395.97	88.296	3681.4
2	SP10/0.33x3	11.253	9.0028	0.034	388.15	87.447	3694
3	SP15/0.2x5	10.984	8.0926	0.065	430.62	93.687	3417.5
4	SP15/0.33x3	10.995	8.0868	0.065	421.95	92.744	3430
5	SP20/0.2x5	7.4766	4.4298	0.669	363.5	83.126	4225.3
6	SP20/0.33x3	7.5688	4.4983	0.651	359.69	82.922	4211.5
7	SP28/0.2x5	6.3542	2.5234	0.274	343.66	84.015	4403.4
8	SP28/0.33x3	6.2925	2.5150	0.282	337.62	83.265	4407.5
9	SF20/0.2x5	12.667	7.5634	0.014	410.03	69.448	3545.2
10	SF20/0.33x3	11.758	8.304	0.009	257.15	34.554	4320.2

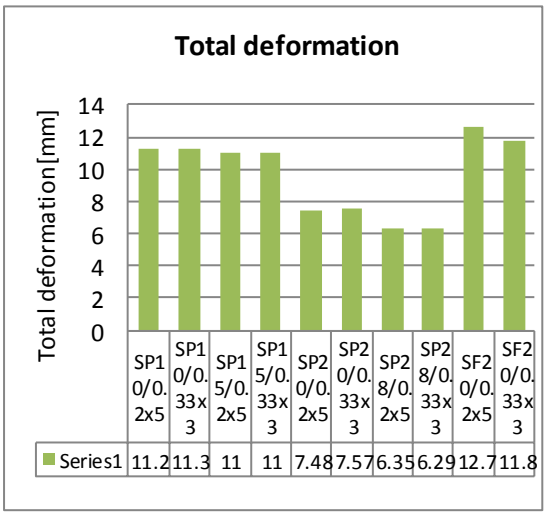

Figure 4.3 Total deformations for Those 10 analysed cases

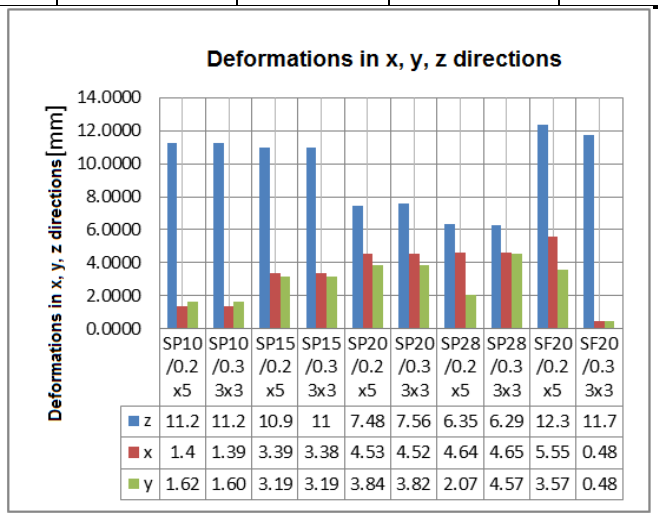

Figure 4.19 Deformations in ”z” direction of the ball drop

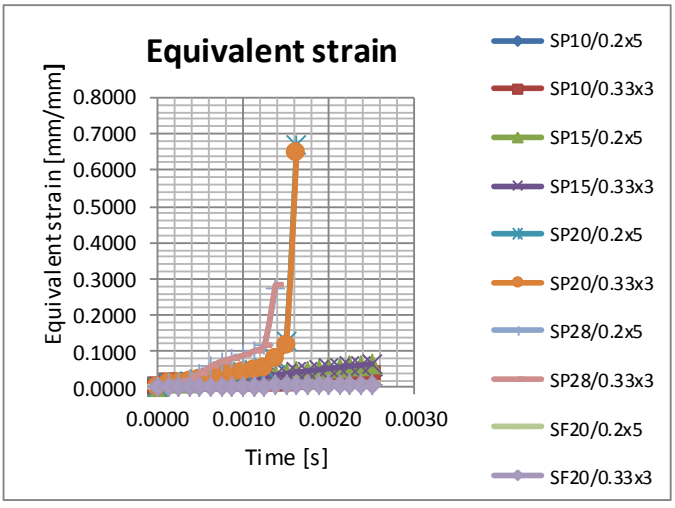

Figure 4.20 Equivalent strain those 10 analysed cases

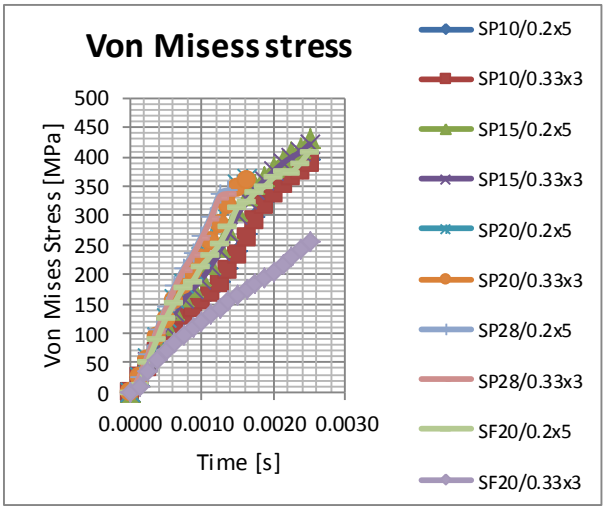

Figure 4.21 Von Mises stress for those 10 analysed cases

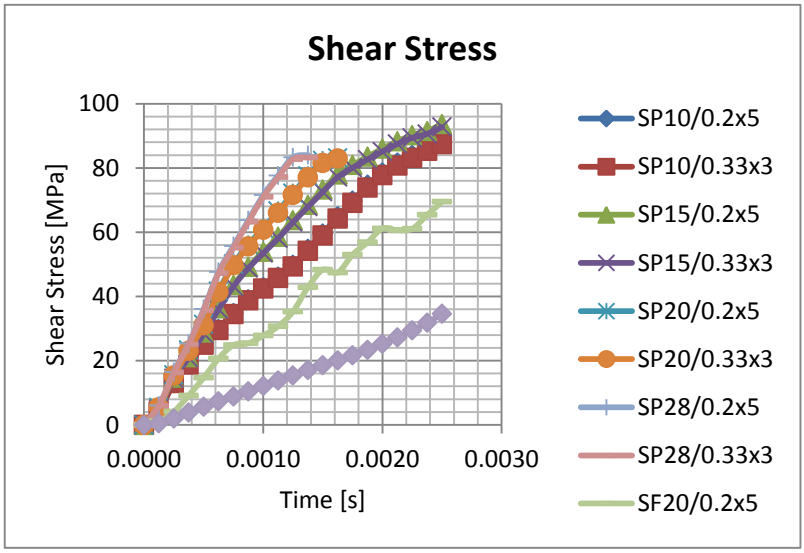

Figure 4.22 Shear stress for those 10 sandwich plates

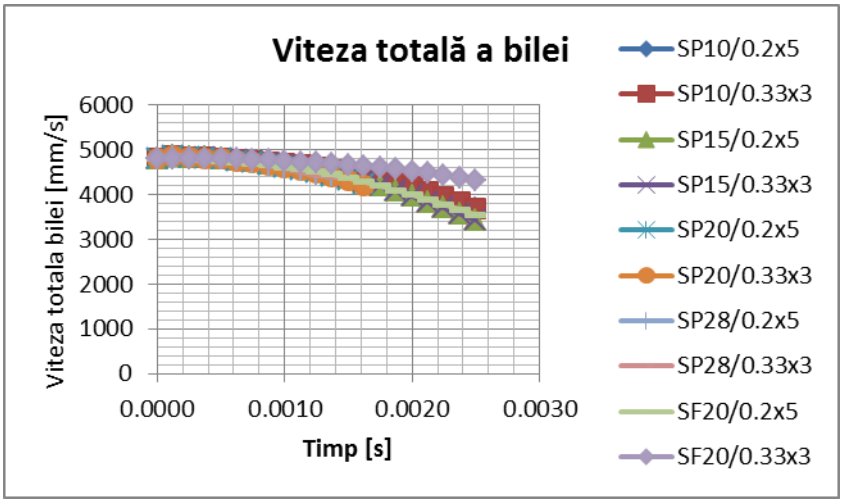

Figura 4.23 Total velocity of the ball

Total velocity = the velocity of the ball during displacement through sandwich

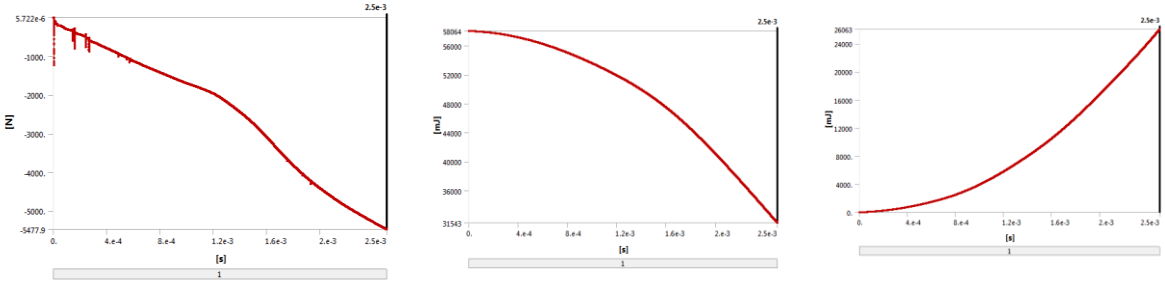

a) b) c)

Figure 4.4 Force contact graph a), kinetic energy graph b), Internal Energy graph c), for sandwich plate SP10/0.33x3

Table 4.6 The parameters obtained through modelling by finite elements

No	The plate specimen	Contact force [N]	Kinetic energy [mJ]	Internal energy [mJ]
1	SP10/0.2x5	5538.2	58064	26324
2	SP10/0.33x3	5477.9	58064	26063
3	SP15/0.2x5	6277	58064	31754
4	SP15/0.33x3	6202.3	58064	31514
5	SP20/0.2x5	4924.1	58064	20569
6	SP20/0.33x3	4951.4	58064	20839
7	SP28/0.2x5	4016.3	58064	16746
8	SP28/0.33x3	3971.9	58064	16689
9	SF20/0.2x5	4990	58064	26386
10	SF20/0.33x3	2343.2	58064	20865

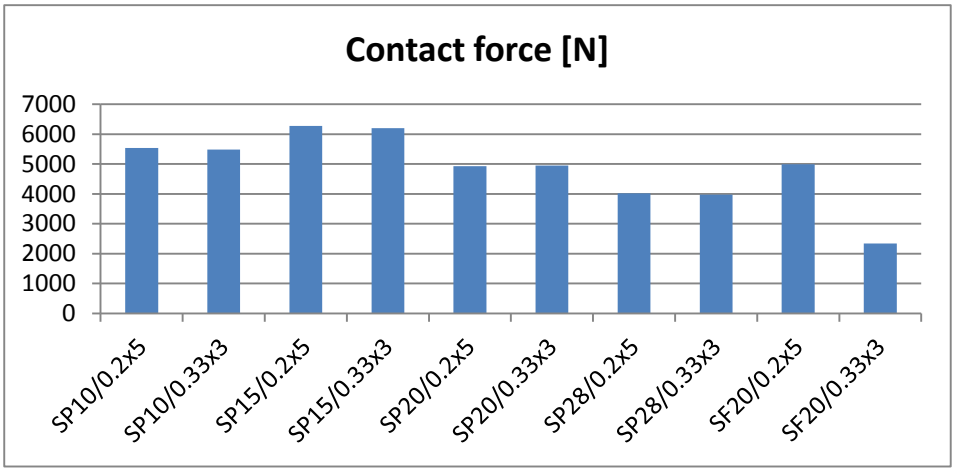

Figure 4.5 Graficul forțelor de contact pentru fiecare tip de placă

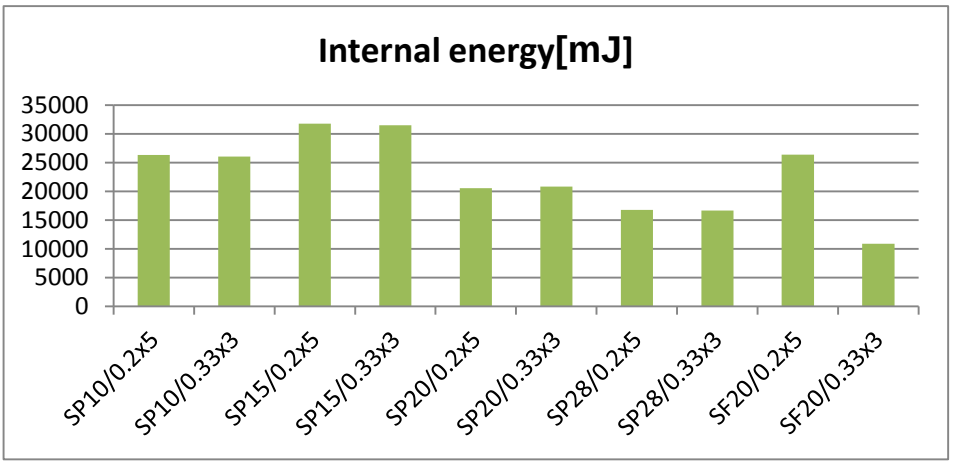

Figure 4.6 Graph of internal energies for each type of plate

4.6 Conclusions

There were studied 10 types of plates with solid elements, namely Solid-Solid-Solid, mixed with Shell-Solid-Shell elements;

The material characteristics were determined for the composite faces made of epoxy resin and glass fibre;

Dynamic impact modelling for the sandwich plates with Solid elements to determine the most important parameters as: total strain, strains projection in all the three directions x, y, z, von Mises stress equivalent, specific strains, shear stress, ball total velocities, maximum contact forces, internal energies, kinetic energy.
Calculations were made during a time period of 2.5ms.

The calculations purpose was to determine the behaviour of each type of material used for sandwich plates so that to determine the best configuration and the most appropriate type of material for impact stress. Due to technical reasons the phenomenon analysis was made in 2.5ms (a part from the total duration of the phenomenon). From the graphs analysis can be noticed the trend of each configuration, so that to be anticipated the behaviour of sandwich plate specimen, in order to make a decision at the end from this viewpoint. The results obtained in this calculation were compared to those resulted from experiments getting a good accordance for the sample of2.5ms. Based on this comparison can be concluded that the anticipation of plates behaviour until the end of impact phenomenon on numeric calculation is justified.

The used method can be applied also in engineering and calculation time can be saved during the stage of choosing the material and configuration of sandwich plate.
In figure 4.18 there are displayed the total travelling appeared after the ball impact, obtaining better predictable values for the sandwich plates with the cores thickness of 28 mm, for instance the specimens SP28/0.2x5 and SP28/0.33x3.
The travelling in the three directions x, y, z are presented in figure 4.19, where z direction is the ball drop direction.
The best specific strains were obtained for polystyrene foams respectively the specimens SF20/0.33x3 and SF20/0.2x5 figure 4.20. A good strength was got for the specimens SF20/0.33x3 with a stress value of 257.15 MPa, SP28/0.2x5 343.66 MPa and SP28/0.33x3 with 337.62 MPa from figure 4.21.

The issue of searing in a marine structure is very important because the same structure may react differently when is submitted to inclined burdens towards normal plate. The loading angle wasn't studied in here but it was considered only the normal force on the sandwich plate surface. In figure 4.22 can be noticed that the shear stress are higher on the sandwich plated with 15 mm thickness polypropylene core afterwards coming the 10 mm and better values are obtained for the sandwich plates with polystyrene foam core.

4.7 Plate SP10/0,2x5 impact calculation

In this subchapter the plate SP10/0,2x5 was impact analysed in a different manner using a HP computer workstation (workframe) XW6200, with the following properties:
- Intel (R) Xeon (TM) processor, CPU 2,8 GH (2 processors).
- RAM 8 GB memory
- running system: 64 bits.
- physical time for calculating this modelling was 277 hours using this type of computer.

This modelling had the same parameters as the previous modelling from this chapter changing only the contact time from 0,002 seconds to 0,02 seconds as it can be noticed in the figure 4.27.

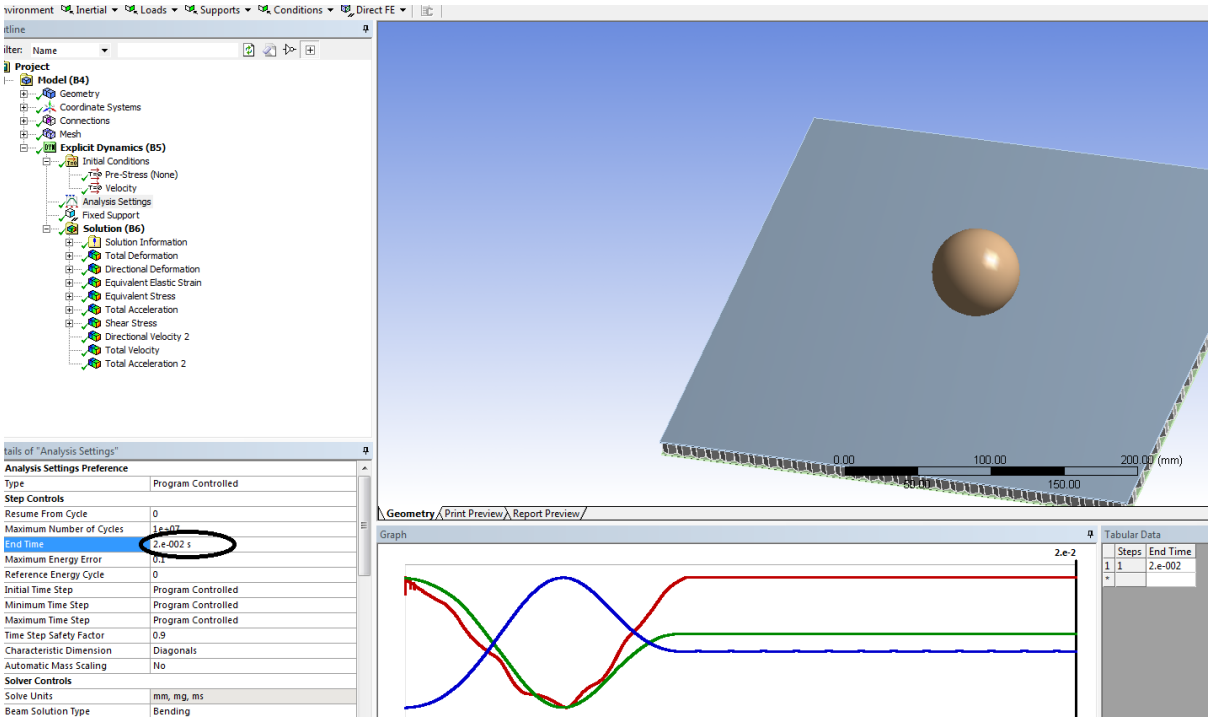

Figura 4.27 Contact time for the sandwich plate SP10/0,2x5 is 0,02s

4.7.1 Results

Internal energy is shown in Figure 4.28:

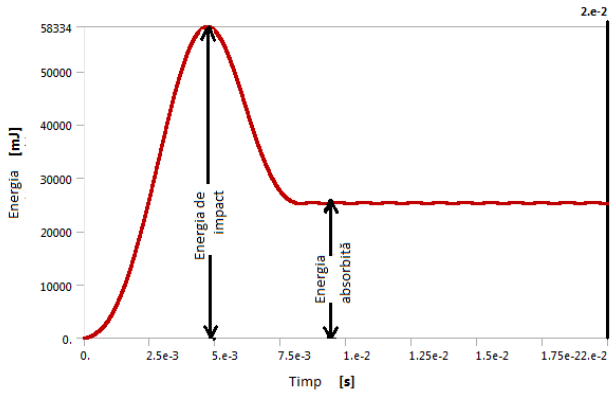

Figure 4.28 Energy – time impact curve impact for composite sandwich plate SP10/0,2X5.

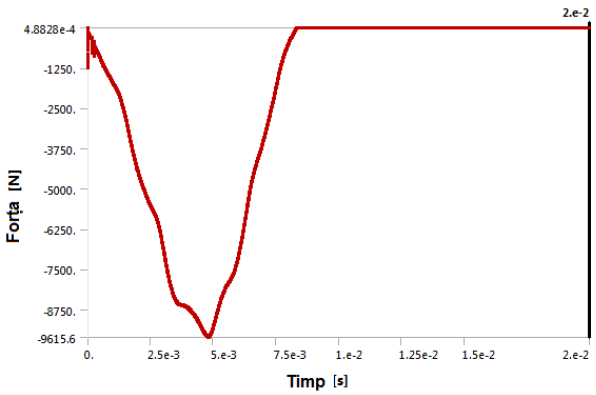

Figure 4.29 Force curve – impact time for the composite sandwich plate SP10/0,2x5.

As it can be noticed the impact energy (named also internal energy) is in this case 58334 mJ. Absorbed energy is 25255 mJ.

Contact maximum force is on the top of the curve with the value of 9,6156kN as it can be seen in figure 4.29.

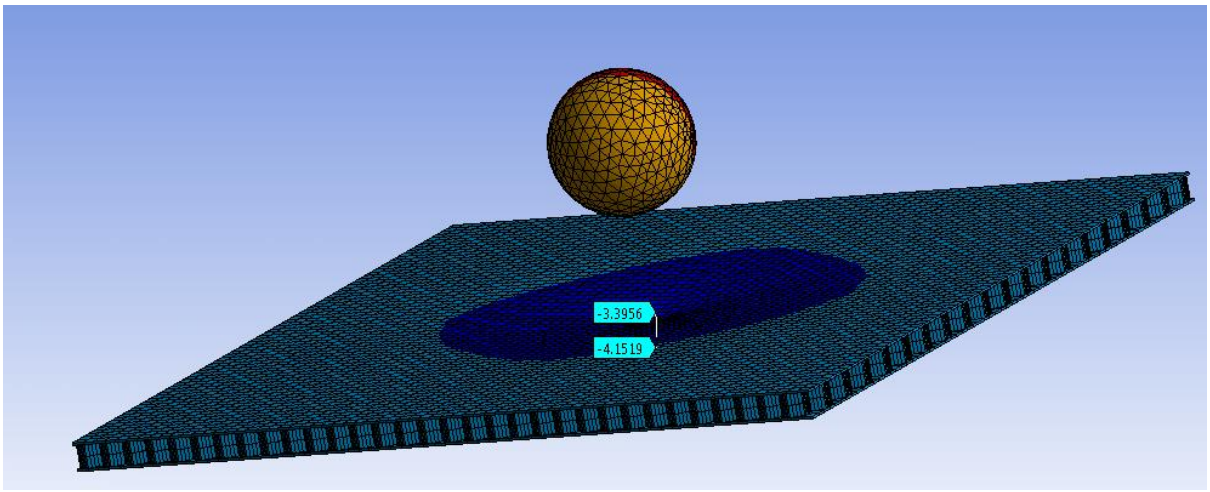

Figure 4.30 maximum deformation for the composite sandwich plate SP10/0.2x5

The maximum deformation for composite sandwich plate SP10/0.2x5 is -4,1519mm. The strain in the direction of the ball drop was measured under the plate fig 4.30.

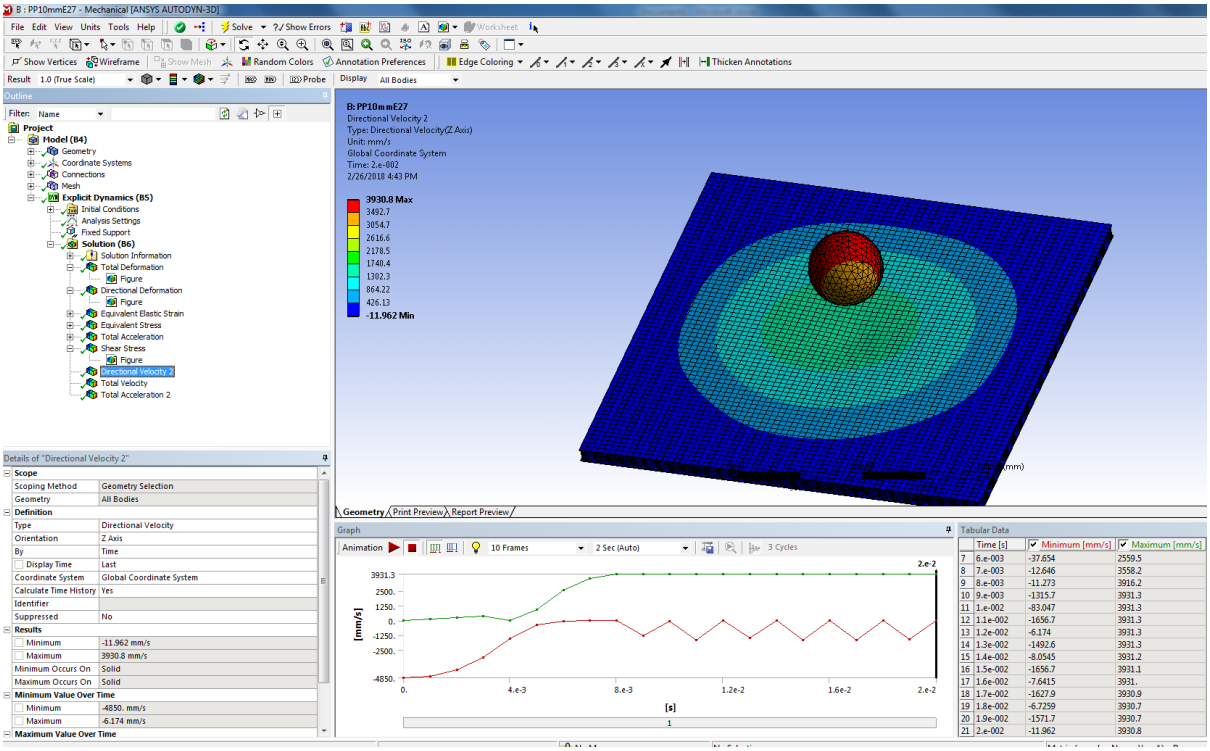

Figure 4.31 The ball return velocity is 3,93m/s.

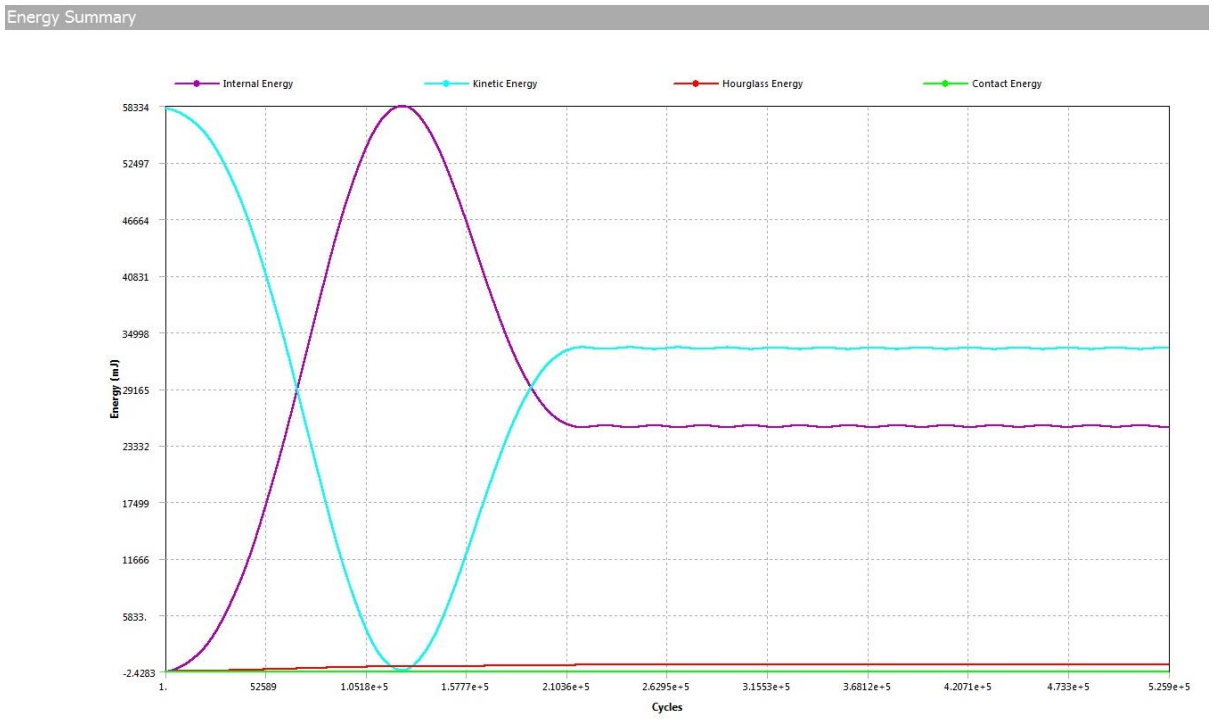

Figure 4.32 Graph of combined energies

Conclusions:

We performed the calculation of composite sandwich plate SP10 / 0.2x5 that consists of 5 epoxy resin layers reinforced with glass fibre texture T160, subjected to a material 5 kg ball impact.

This modelling is a convergent one (running time was 277 hours). In Figure 4.32 there are indicated the variations during the impact of internal energy and kinetic energy (with green).

The velocity calculated when the ball is falling was 4.85m / s and the return velocity of ball was 3.93m / s.

It was obtained the maximum strain of the composite sandwich plate of 4.1519 mm (the value from experiment being 2.8535 mm; the difference between the calculation and the experiment is 1.3055 mm).

The maximum contact force for this composite sandwich plate is 9.6156kN.

CHAPTER 5 EXPERIMENTAL SIMULATIONS REGARDING IMPACT

5.1. Overview

Three stands were designed and built-up for impact experimental simulations. The purpose was each stand to allow the determination of plates' impact parameters, especially the composite sandwich plates.
Basically, the stands consist of a system that develop an impact force (gravitational or pneumatic), a plate fastening system and a third system composed of instruments to monitor the impact parameters (impact force value, maximum travelling value, impact velocity value).
Measurement of plate elastic strains was done by means of electric resistance tensometry.
At the composite materials impact, the developed energies are lower than in metal cases. The composites have lower impact energies because they have low transversal shear strength and low interlaminar strength, these materials couldn't get plastic strain. .
Unlike metals, which after plastic strain they still maintain , to a certain extent, their structural integrity, the composite materials do not suffer plastic strain and once they achieve a certain stress level, they suffer permanent damage. This can lead to local or structural lifting power loss.
In a laminated composite structure (the case of sandwich plates coating), five types of damage may occur after elastic strain:
- Fiber breakage or cracking;
- Micro cracks or even large cracks that appear in the resin;
- Fibers and matrixes displacement;
- Adjacent laminae delamination;
- Remove fibers from the matrix.

When the composites are static stressed, the destruction by delamination rarely appears.
But, when these are subjected to impact loads, the delamination is the most frequent way of destruction.

5.2 Characteristics of dynamic tests

Structures' designing is generally based on the characteristics offered by the materials producers, which usually have the shape of specific stress-strain diagrams.

These diagrams are got on static models, the material properties being obtained during quasi-static tests, meaning that the strains stress of the specimen are very slow. Generally, the standards with regard to the determination of material characteristics are related to velocity tests (strain) on the materials of approximately 0,001 mm/s or less (Table 5.1).

The materials characteristics are usually determined from the stress-strain curve specific to the material; the curve is drawn-up based on the test with a testing machine in quasi-static conditions, more specific, with low strain rate. Nevertheless, the material behaviour may be significantly different under stress with dynamic loads. Depending on the dynamic character of the loads that appears within a structure, the designing engineer has to be aware of materials dynamic properties. Normally, a conventional material testing machine is not in condition to apply the high strain rate required by the dynamic stress.

Over the years, the structures behaviour at impact became interesting to many engineers for designing purposes well as for developing constructive models of tested materials. However, the mechanical characteristic of the materials were determined over the

years under conditions of static stress, so that their strength to be determined only for this type of stress to which structures are subjected.

The purpose of dynamic tests is to determine the material characteristics under conditions of high strain rates, as it is the case of some phenomena that occur in practice, as would be impact, sock, ballistic phenomena etc.)(Table 5.1).

The differences among the curves specific to the materials obtained with different velocities are presented in figure 5.1 ([83] Carlo Albertini, Ezio Cadoni, George Solomos, Advances in the Hopkinson bar testing of irradiated/non-irradiated nuclear materials and large specimens, Phil. Trans. R. Soc, 2014). In figure it can be noticed, depending on the material testing velocity, the results obtained for the maximum stress value, for the same specific strain value can be different from 10% until 30%.

However, there were few studies about the effect of loading rate on the material properties. Starting on 1950 and 1960 there was a maximum interest with regard to mechanical behaviour study at high loading rates. These studies were especially imposed along with the increase of the interest in military research filed that was involved in ballistic applications. Another interest was the one of aerospace industry that was focused on the meteorite impact on the satellites and the airplanes crash due to birds.

Table 5.1 Test conditions used based the strain rate $\dot{\varepsilon}$

Strain rate [s^{-1}]	$\dot{\varepsilon}$ **<10^{-5}**	**10^{-5}<** $\dot{\varepsilon}$ **<10^{-1}**	**10^{-1}<** $\dot{\varepsilon}$ **<10^{2}**	**10^{2}<** $\dot{\varepsilon}$ **<10^{4}**	**10^{4}<** $\dot{\varepsilon}$
Physical phenomenon	Creep	quasi-static	intermediate	High velocity	Impact
Inertia forces	Insignificant		Important		
Test type	Isothermal		Adiabatic		
Equipment used	Conventional test machines (hydraulic or electro-mechanic)		Special systems with servo-hydraulic drive	Hopkinson bar systems	Impact Taylor systems, blowing rings etc.

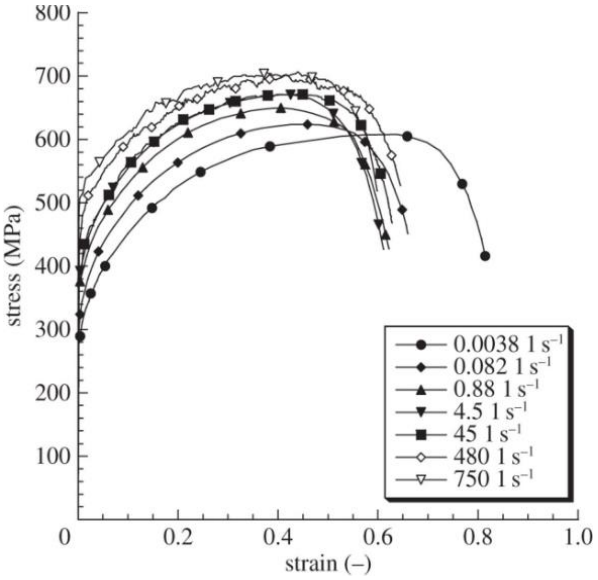

Figure 5.1 Curves specific to the materials for different test velocities [83]

Composite materials (as polymeric composite, polymeric foams, metallic foams) are considered soft materials, materials to which strength and stiffness have low values. however, the soft engineering materials have good impact properties being at the same time also good vibrations insulators, lately being used within a large amount of applications in fields as aerospace, automotive, navy with military and civil destinations.

Within these applications, the most of the “soft” materials are requested at assignments as impact, explosions, high speed collisions.

For numeric modelling of these, it is very important to use the material curves (stress-specific strain) to offer as realistic as possible their behaviour during stress. Reliable experiments, on study materials have the purpose of determining the stress – specific strain curves, in order to offer the most accurate values for obtaining structures real answers. Being compared to the quasi-static experiments cu, the materials dynamic characterization , especially the “soft” once at high strain rates is still under studies and acquire high importance along with the increase of impact phenomena number.

5.3 Mechanical characteristics determination of extruded polystyrene

Mechanical characteristics of extruded polystyrene were determined by standardized methods ISO 844 and from Galați.

Mechanical characteristics determination of extruded polystyrene was made through compression tests on this type of material. There were performed two compression tests on 2 samples.

a)

b)

Figure 5.2 a) compression test for determining mechanical properties of extruded polystirene b) sample with dimensions of 100X100 [mm] from extruded polystyrene

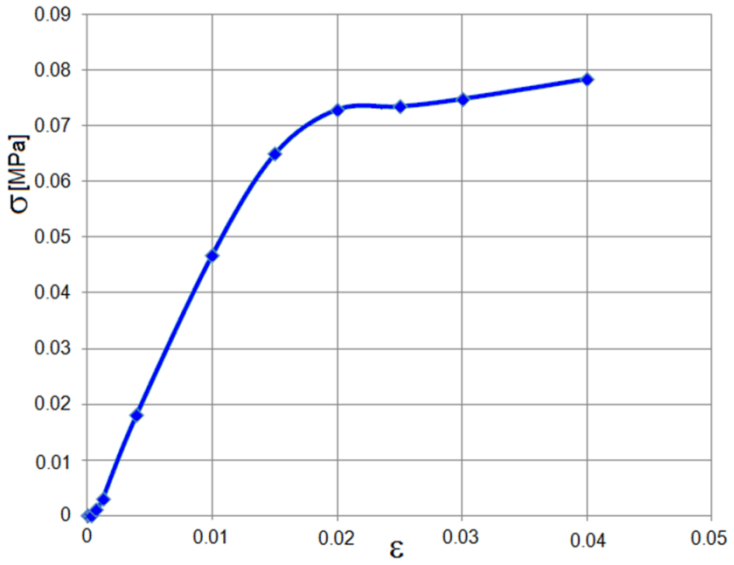

Figure 5.3 Polyurethane foam specific diagram (extruded polystyrene) in elastic area

The measured results for Young modulus E_c = 3.81 [MPa], and Poisson's rate ν_c = 0.08. transversal elastic modulus G = 1.76 [MPa] calculated with the equation 5.1:

$$G_c = \frac{E_c}{2(1+\nu_c)} \tag{5.1}$$

The results are suitable to those from [84] obtained by the researcher Pokharel in 2003. More details about this material can be found also in the paper work of Elragi from [85] "Selected Engineering Properties and Applications of EPS Geofoam".

5.4 Mechanical characteristics determination of polymeric composite made of slass fibre and epoxy matrix.

Mechanical characteristics determination of polymeric composite made of glass fibre and epoxy matrix used for the coating was made based on the American standard regulations ASTM 3039 [86].
Tensile strength assessment form polymeric composite sample is presented in figure 5.4.

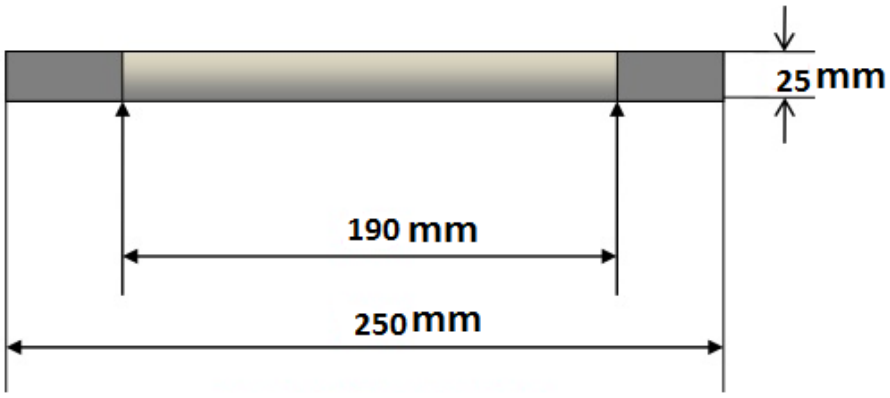

Figure 5.4 Sample of glass fibre and epoxy matrix

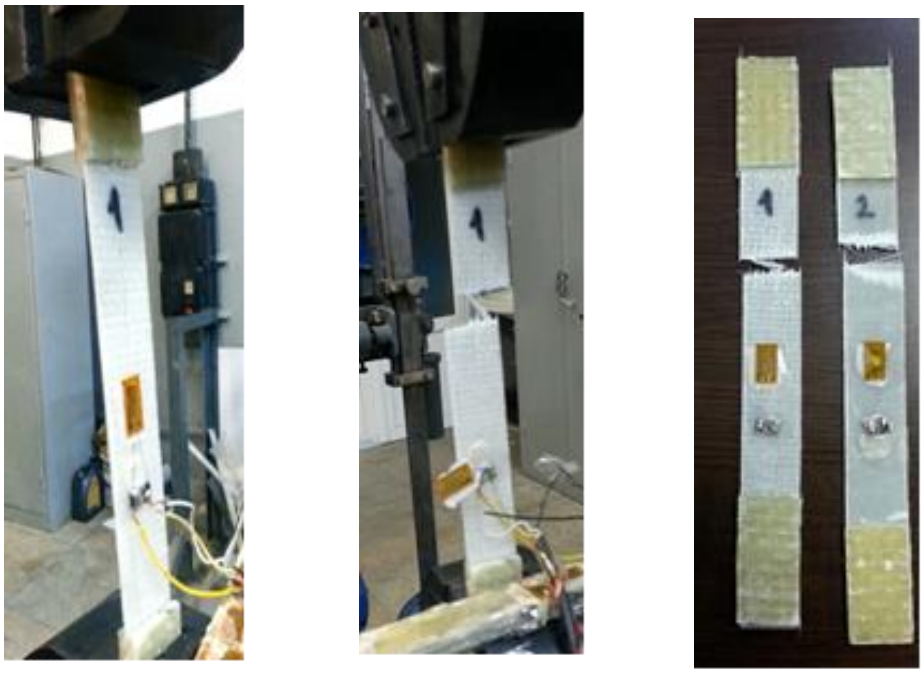

a) *b)* *c)*

Figure 5.5 Tensile test for determining the mechanical characteristics of polymeric composite

In figure 5.5 there are presented the samples 1 and 2 which were tensile tested. In the picture it can be seen that tensometric stamps were stick on the samples to determine the equivalent strains. In the pictures *a* and *b* there are presented the samples before and after breakage.

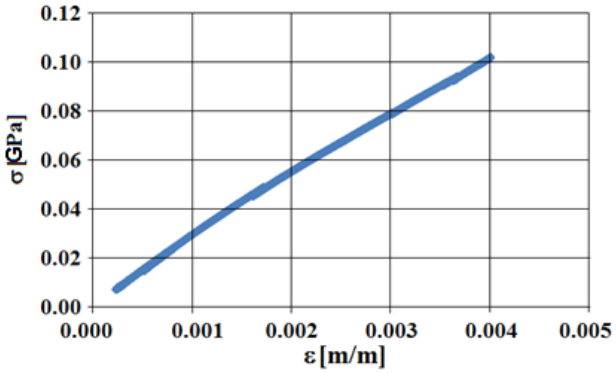

Figure 5.6 Polymeric composite specific diagram in elastic area

The dimensions of the sample made of polymeric composite were: L=250 [mm], b=25 [mm], t=1.2 [mm]. From the tensile stress diagram of sample (Figure 5.6) .

5.5 Fabrication program of tested composite sandwich structures

The composite materials are invented by the human being and are composed of two or more different materials having separating interfaces manufactured to obtain top performances comparing to those of constituent materials. the structure of the new composite material represents a continuous phase (the matrix) in which are included different interrupted phases (reinforcement).

For manufacturing the coating of composite sandwich plates, the matrix is made of heat rigidity polymers (epoxy resins) and glass fibre reinforcement. For manufacturing the composite materials, there are used technologies processes different from those of

conventional materials. During these processes, through copolymerization (poly-condensation) by means of a monomer, unsaturated polyester resins are passing from liquid state to solid state. To activate the polymerization reaction, a chemical agent is used (which is named also “intensifier"). To decide a certain fabrication technology depends on different factors: geometric shape and the parts dimension, the designed mechanical characteristics, final structure of the composite material, dimension accuracy and parts quality etc.
The purpose of the work is to find the optimum combination for making a complex composite structural plates type “sandwich" with extruded polystyrene cores and polypropylene honeycomb with imposed thicknesses. The sandwich faces are made of composite based on the glass fibre texture and unsaturated epoxy resins.
For the fabrication process of the composite sandwich structures, there were needed more preparation stages as follows:
- coating manufacturing:
    - textures preparation (fig. 5.8);
    - textures cutting (fig.5.9);
    - prepare the casting support (a plate glass - fig.5.10 a).);
    - epoxy resin casting operation, to make the coating (fig.5.10 c);
- cores manufacturing:
    - cutting of honeycomb plates / extruded polystyrene, for the core;
    - bind the layers for forming the sandwiches.

5.5.1 Shells manufacturing

The work method for manufacturing the laminated plates for coatings is called ”Hand Lay up technique” [87, 88, 89, 90, 91] by drying the plates at environment temperature of 22℃ for 1-2 days. The texture is prepared to be cut on a plane surface (knowing that by cutting the fibre “slips”). To lay on the epoxy resin, a metallic roller was used For hardening the epoxy resin it was used a hardening accelerator solution. The ration for this mixture is: 100 parts resin to 17 parts intensifier during a work time of 50 minutes. It is very important to resect this ratio otherwise the resin won’t get hard and will stay soft or hardening coms very quickly and the mixture cannot be used anymore. Also not respecting the ration will lead to thermal and mechanical properties decrease. The chemical reaction to the resin mixture with accelerator is exothermic meaning that after those 50 work minutes the heat spreading occurs which means that those two solutions have reacted and the hardening is taking place

a) b) c)

Figure 5.7 Prepare the support glass for casting the epoxy resin a), weighing the solutions and spreading the epoxy resin b), casting c).

In figures 5.8 and 5.9 are presented the types of textures from glass fibre which was used for the sandwich faces. The first one has a thickness of 0,2mm and the other one has a thickness of 0,33mm. the final thickness of the sandwich surfaces was 1mm, made of five

layers respectively three layers. So, for the thickness of 0,2 there were used five layers and for 0,33 there were used three texture layers. When the epoxy resin was added, the thickness suffered no modification (there is no important increase of volume) because this one was totally embedded in the glass fibre through the chemical reaction. In table 5.2 there are presented the characteristics of the used textures .

Figure 5.8 Twill texture, 0,2mm thickness

Figure 5.9 Texture with 0,33mm thickness

5.5.2 Cores manufacturing

The sandwich cores were manufactured by cutting the plates (honeycomb and extruded polystyrene) (figure 5.10 and 5.11).

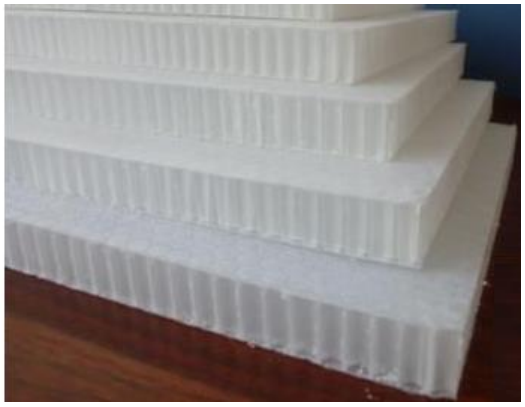

Figure 5.10 Honeycomb cutting

Figure 5.11 cutting of wafer extruded polystyrene

Extruded polystyrene has 20mm thickness, the wafer type having the following characteristics:

XPan 20 mm: XPS-EN 13164–T3–DLT(1)5-CS(10/Y)250-WL(T)0.7-WD(V)3-MU150–FT2, according to the table 5.2. The closed cellular structure, the control of process parameters, the quality of admixtures lead to obtaining the long-lasting top technical characteristics. This material has the next properties [92]:

- top mechanical strength;
- frost-defrost cycles resistance;
- good elasticity;
- higher adherence;
- reduced thermal conductivity;

- lack of capillarity ;
- homogeneous cellular structure, easy control;
- moisture high resistance;
- cutting (shaping) with common tools;
- vapours dispersion resistance;
- clean, inodorousness and skin non-irritating.

Polypropylene honeycomb plate may be made with or without non-woven polyester veil for a better laminating. Also it can have a film barrier under the polyester veil to limit the consumption of resin quantity. In this study there were used the polypropylene plates with polyester veil, for a better lamination.

The general characteristics of the polypropylene honeycomb are:

- high strength in relation to weight, good resistance to corrosion, mushroom, rot, chemical and moisture resistance, suppress sound and vibration, absorb energy, thermo-formable
- use the 85°C temperature, Recyclable.

Table 5.2 technical properties for extruded polystyrene [92]

Characteristic	Code SR EN 13164	Plate thickness [mm]	Unit of measurement	Value
Thermal conductivity	λ_D	15-60	W/m^{o}K	0,033
		80-120		0,034
Heat resistance	R_D	15	m^2KW	0,45
		20		0,61
		30		0,91
		40		1,21
		50		1,52
		60		1,82
		80		2,35
		100		2,94
		120		3,53
Compression strength to strain10%	CS(10/Y)	15-20	KPa	<250
		30-120		≥300
Shear strength	**ζ**	15-120	KPa	190
Water vapours transmission	MU	15-120	-	150
Long lasting water absorption by total immersion	WL(T)0,7	15-120	%	≤ 0,7
Water absorption by dispersion	WD(V)	15-120	%	≤3
Reaction class to fire	-	15-20	Euro -clasa	F
		30-120		E
capillarity	-	15-120	-	0
Frost – defrost resistance	FT2	15-120	%	1
Limit temperatures		15-120	^{o}C	-50 ÷ +170

Polypropylene mechanical properties are presented in table 3.1.

5.5.3 The composite sandwich plates typo dimension

S-au confectionat 10 plăci compozite de tip sandwich, având caracteristicile date în tabelul 5.3. Plăcile sunt de forma pătrat, cu dimensiunile brute de 380X380 [mm]. Datorită sistemului de fixare cu cadru de lățime de 20[mm], dimensiunea netă a plăcilor, măsurată între marginile interioare ale cadrului este de 340[mm]. Grosimile plăcilor sandwich variază de la

22[mm], până la 30[mm], în funcție de grosimea miezurilor, așa cum este arătat în tabelul 5.3.

Tabelul 5.3 Tipuri de placi compozite sandwich testate dinamic

No.	Plate type	Faces (shells)			Core		Interface adhesive face-core
		Type	Material	Gros. [mm]	Material	Gros. [mm]	
1	SP10/0.2x5	Layered composite 0.2x5	(fibră de sticlă-E) și rășină epoxidică	1	polypropylene	10	Epoxy resin
2	SP10/0.33x3	Layered composite 0.33x3	(fibră de sticlă-E) și rășină epoxidică	1	polypropylene	10	Epoxy resin
3	SP15/0.2x5	Layered composite 0.2x5	(fibră de sticlă-E) și rășină epoxidică	1	polypropylene	15	Epoxy resin
4	SP15/0.33x3	Layered composite 0.33x3	(fibră de sticlă-E) și rășină epoxidică	1	polypropylene	15	Epoxy resin
5	SP20/0.2x5	Layered composite 0.2x5	(fibră de sticlă-E) și rășină epoxidică	1	polypropylene	20	Epoxy resin
6	SP20/0.33x3	Layered composite 0.33x3	(fibră de sticlă-E) și rășină epoxidică	1	polypropylene	20	Epoxy resin
7	SP28/0.2x5	Layered composite 0.2x5	(fibră de sticlă-E) și rășină epoxidică	1	polypropylene	28	Epoxy resin
8	SP28/0.33x3	Layered composite 0.33x3	(fibră de sticlă-E) și rășină epoxidică	1	polypropylene	28	Epoxy resin
9	SF20/0.2x5	Layered composite 0.2x5	(fibră de sticlă-E) și rășină epoxidică	1	Extruded Polystyrene	20	polyurethane foam
10	SF20/0.33x3	Layered composite 0.33x3	(fibră de sticlă-E) și rășină epoxidică	1	Extruded Polystyrene	20	polyurethane foam

In figure 5.16 are presented the final products of sandwich plates, organised based on core thicknesses order.

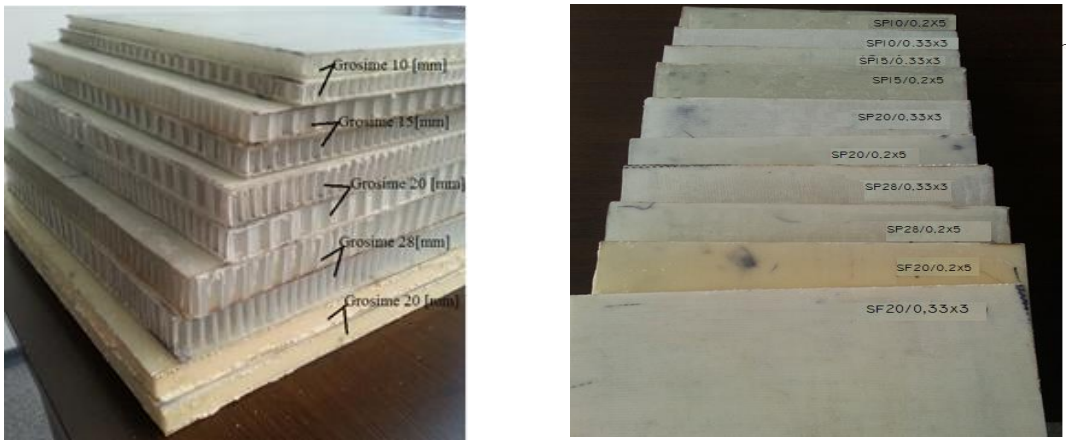

a) b)

Figure 5.12 a) sandwich structures manufactured (core thicknesses)
b) sandwich structures manufactured and organised based on the case number

5.5.4 Conclusions

- the polymers used for manufacturing the coatings have general emphasized viscoelastic properties.
- reinforcement fibres have a general elastic linear behaviour to stress high values.
- the test results are strongly influenced by the test velocity which has to be chosen to provide impact conditions.
- the test results depend on reinforcement element ratio.
- the temperature of obtaining the polymers mix samples affects the breaking strength and breaking elongation. Based on the experimental tests, to determine the mechanical properties, it was noticed there are differences between the values resulted from each sample.

5.6 Functioning conditions of experimental stands

For optimum and reproducible functioning of experimental stands there were made several tests for finding and removing the possible problems, many of them being anticipated, but other issues I faced only during practical use of the stand, the adopted solutions requesting time and a very big number of practice experiments .

The experimental stand calibration for measuring the impact force was made using a force cell. For a real functioning, there are needed two experiments performed in the same conditions to obtain similar results.

5.7 Experimental simulations regarding static stress

The static tests offer the possibility of finding the more stressed areas that have to be mandatory investigated at dynamic tests.

These tests are also performed to determine some material characteristics when the tests are made on strainer samples or compression, to standardized test machines. The difference between static tests and the dynamic/ cyclical ones consists of loading time (loading rate or strain rate). if to apply the force takes more than 0.1 seconds then the test is „static". Deflection, shear and torsion tests can be performed by means of additional devices. Static tests are most used mechanical tests when during the test, force increases slowly lasting several minutes at environment temperature. The test of the used parts in special conditions (high or low temperatures, impact loading or vibrations, radiations etc.), must be made under the similar conditions found in exploitation [12].

5.7.1 Experimental work procedure

To perform the static tests, there were used weights which were weighed with electronic scale. The weights 1,2,3,4 and 5 (fastening support) have the mass values: 1) m = 5.355kg; 2) m = 2.4kg; 3) m = 0.830kg; 4) m = 0.665kg; 5) m = 0.005kg.

Figure 5.13 Weights used at static test

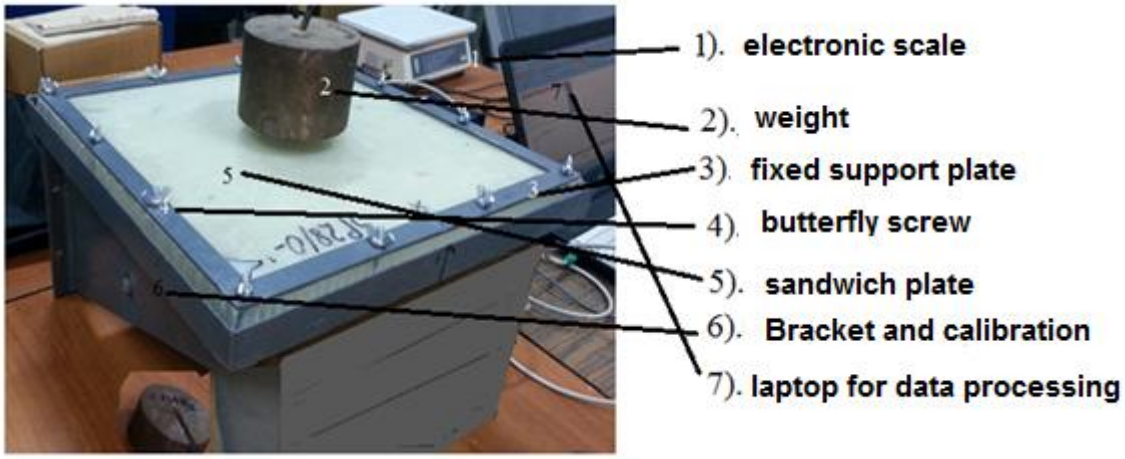

Figure 5.14 Components used at static tests

a) b)

Figure 5.15 a) detail for one of the static tests b)positioning of travelling transducer (LVDT) on the back of sandwich plate

For static tests each plate was fasten within a metallic frame with screws. After fastening and calibration, the weights were positioned one by one in the middle of plate. For each weight (stress) maximum travelling was measured (in the middle of the plate) using a travelling transducer.(Fig. 5.15 b)).

5.8 Static tests results and conclusions

In table 5.4 can be found the results of experimental static tests. The 10 sandwich plates were analysed during bending stress, registering maximum travelling (obtained in the middle of the face opposite to loading) for each applied weight.

Table 5.4 maximum travel obtained after static bending stress

Nr.crt	Studied case	**maximum deformation δ [mm] when applying a weight with the mass in [kg]**			
		0,830[kg]	1,495[kg]	3,895[kg]	5,355[kg]
1	SP10/0,2x5	0.0111	0.0201	0.0523	0.0719
2	SP10/0,33x3	0.0114	0.0205	0.0533	0.0733
3	SP15/0,2x5	0.0078	0.0141	0.0368	0.0505
4	SP15/0,33x3	0.0080	0.0145	0.0377	0.0519
5	SP20/0,2x5	0.0012	0.0110	0.0287	0.0394
6	SP20/0,33x3	0.0062	0.0113	0.0294	0.0404
7	SP28/0,2x5	0.0047	0.0085	0.0220	0.0303

8	SP28/0,33x3	0.0048	0.0086	0.0224	0.0308
9	SF20/0,2x5	0.0076	0.0136	0.0355	0.0488
10	SF20/0,33x3	0.0075	0.0136	0.0354	0.0487

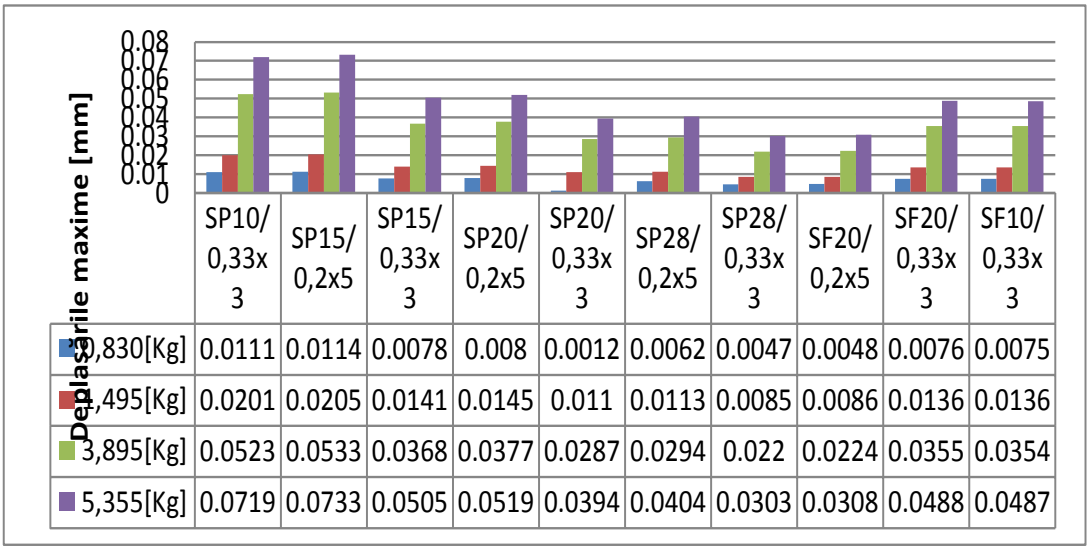

Figure 5.16 Maximum deformation of the plates when forces are applied concentrated in the middle of plates

5.9 Impact experimental tests

Composite materials especially those with shape of sandwich structures, with reduced weight and high energy absorption capacity are very attractive to the applications which require light structures, as naval industry, transports etc. especially due to impact remarkable behaviour.

Aside from visual analysis of damage after impact, it can also be made a 3D tomographic analysis to see the damages appeared in fibres as well as in core as it was done in Crupi's and colab paper work from [94], where it was analysed the behaviour during impact of some composite sandwich plates with different cores and faces. After impact the plates were subjected to a scanner, which can edit 3D images and was possible to see the damages appeared in figures as well as in core. This experimental study investigates the impact behaviour of different composite typologies, comparing their impact answer with regard to energy absorption and damage mode. In [94] impact tests were made with low velocity on composite serial types: laminated composites, sandwiches with PVC foam core, alumina foam and honeycomb. The tests results confirmed that the layers reinforced with Kevlar fibres had, as expected, a good impact performance and PVC foam sandwiches, with higher thickness, need a higher quantity of energy to produce the total collapse. A non-destructive advanced technique, as X ray tomography, was used to investigate the breakdown manner and the damages of composites subjected to loading through impact by analysing transversal sections views. In [95], the impact was made with low velocity using a pneumatic impactor Instron-Dynatup 8250 type Drop-weight. Impactor had 5.1kg and his shape was hemisphere with 16 mm diameter. There were analysed the composite sandwich plates with faces from hybrid material woven S2-glass-IM7, graphite fibre/epoxy resin (treated at 177ºC), to different energies afterwards were subjected to ultrasounds analysis at UltraPAC machine using UTW software. Some results and conclusions from this study are similar to the results

from the present thesis because we used an impactor with mass of 5 kg in both situations. The conclusions from (Brown and colab.) which are variable also to the thesis are:
- most of the composites get delaminated after the low impact;
- delamination appear sometimes inside the composite and it cannot be seen with naked eye;
- the shape of damages appeared on the plate is alike the plus sign"+";
- when the breakage occurs at a certain energy level, usually it exists a smaller delamination than when wouldn't exist any breakage. This thing happens because in case of a small breakage, the energy is absorbed and delivered to the specimen.

5.9.1 Experimental tests of free drop gravitational impact

For this experimental part it was used the stand with five main components of the system: the guiding frame of the impactor, the impactor, the support for sandwich plate, LVDT(travelling transducer), high velocity camera.
Stand parameters:
- the impactor is a ball of 5[kg] mass and 106 [mm] diameter.
- the impactor drop distance: H=1180[mm]
- impact maximum force was measured with the force transducer obtaining the value: F=0,8668kN.

In fig. 5.18 it is presented the gravitational impact stand, with free drop.
The stand consists of:
- frame of welded steel bars;
- a square shaped support equipped with 12 screws for fastening the plate;
- horizontal support, equipped with clamping and fastening screw in order to support the travelling transducer;
- the steel impactor has a screw which role is to lift the ball (fig 5.17).

Sandwich plates dimension are of 380X380 mm and the thicknesses varied from 22 to 30 mm. The plates are clamped within a support frame by 12 screws. The screws provide the required clamping force for achieving the connections type embedding on contour line. The hitting element is composed of a steel ball with a welded screw and a bolt nut, required for fastening in the system. The bolt nut has a hole through which a "safety bolt" can pass to be retracted. When the hex-key is pulled out from the support, the ball is released and fall perpendicularly on the plate (fig 5.17. the ball diameter is 106 [mm] and the mass is 5 [kg]. the falling height is of 1180 mm (with differences within 22 and 30 mm, based on plates thicknesses).
The tests were performed according to ASTM D 3029 standard.
In the Vineela's paper work [93] it was studied the impact of some composite plates from epoxy resin reinforced with glass fibres type E differently directed (0/90; 30/60; 45/90). They were studied experimentally and analytically using ABAQUS software and as standard was used the same type for "drop-weight".

Figure 5.17 Impactor with 5 [kg] mass

Figure 5.18 Gravitational impact stand with free drop

Figura 5.19 High velocity camera

Figura 5.20 Gravitational impact stand. Frame with square support

Drop velocity is determined by means of high velocity camera recordings.
The tests calibration is made using the application AOS Imaging Studio (Fig. 5.21-5.24). the calibration is made with this application after extracting the films made with high velocity camera.

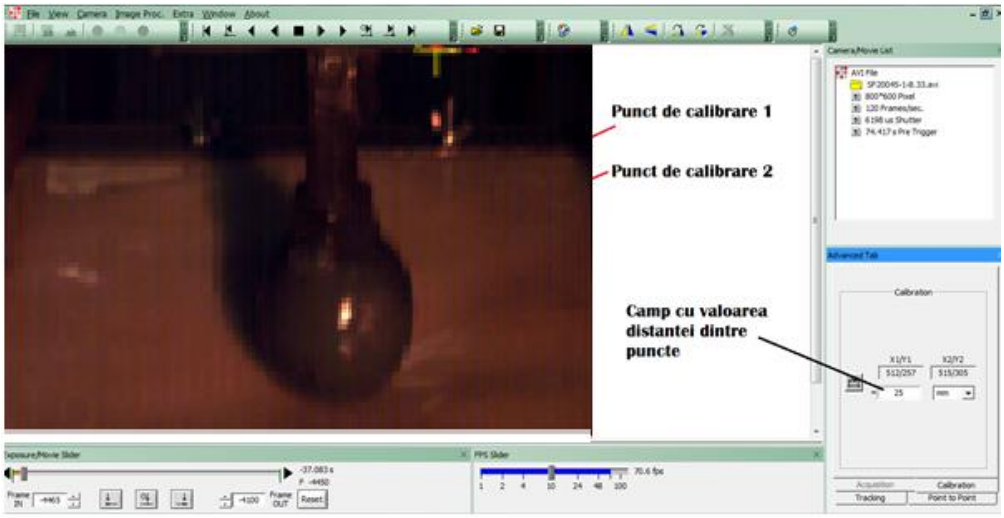

Figure 5.21 system calibration by the means of AOS Imaging Studio

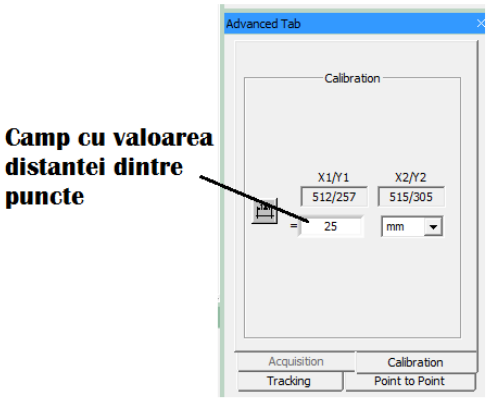

Figure 5.22 Field from AOS Imaging Studio, with the value of the distance between the points

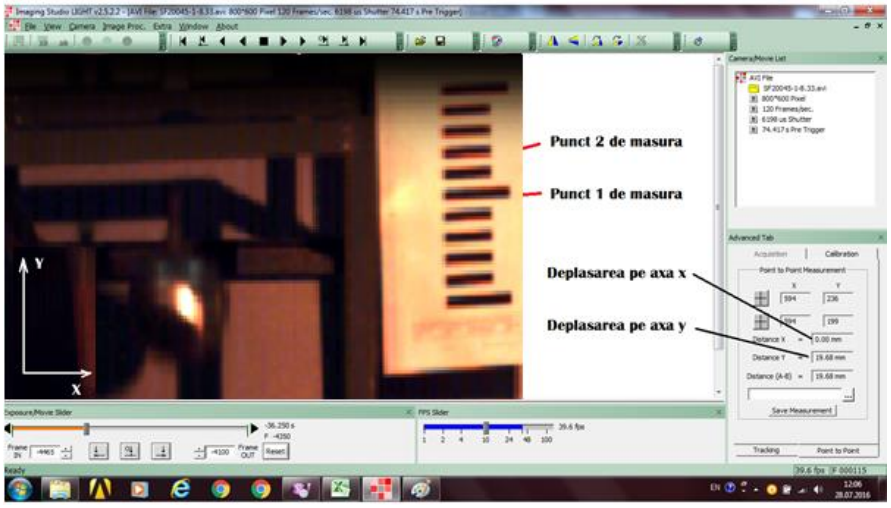

Figure 5.23 choosing the method of calculation the velocity between points (Point to point)

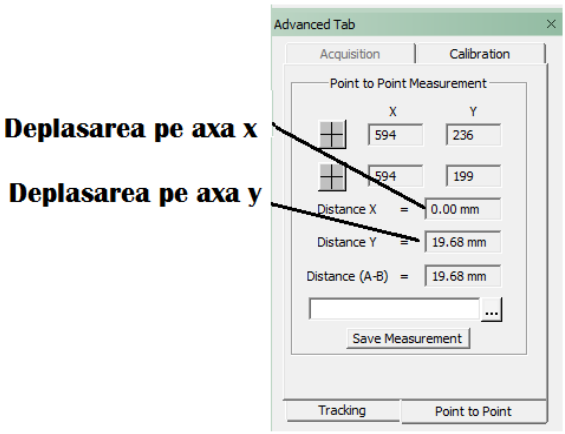

Figura 5.24 Projections on x and y axis of the impactor

5.9.2 Determination of the energy absorbed by the plate at the impact moment

The assembly behaviour is characterised by the 4 phases of the test:

1. *System preparation* – is the phase when the plate is installed within the clamping system, and the impactor is positioned at maximum height land ready for impact. In this phase the total energy of impactor is equal to his potential energy when he is at maximum height;

2. *Impactor drop* – in this phase the impactor is released for free drop. As the impactor accelerates, the potential energy is transformed into kinetic energy. When the impactor touches the plate, it has maximum kinetic energy at velocity of V_{impact}, relation (5.2);

3. *The plate deformation* – in this phase the kinetic energy of impactor is given to the plate, which get deformed elastically as well as plastic. Plastic deformations are shown as damages in plate structure (cracks, delamination, fibres breakages). Plastic deformation produces the energy irreversible, which cannot be returned to the impactor;

4. *Recovery after impact* – in this phase, the elastic deformation energy stored by plate, is transferred back to the impactor as kinetic energy. At the separating moment from test plate, the impactor has kinetic energy with velocity $V_{recovery}$, (relation 5.3).

The energy absorbed by the test plate represents the difference between kinetic energy held by impactor before impact and kinetic energy after impact, according to the relation (5.4).

Energia absorbită de placa de test, reprezintă diferența dintre energia cinetică pe care o are impactorul înainte și energia cinetică după impact, conform relației (5.4).

$$V_{impact} = \frac{D_{impact}}{dt} + \frac{1}{2} \cdot g \cdot dt \quad (5.2)$$

$$V_{recovery} = \frac{Drecovery}{dt} + \frac{1}{2} \cdot g \cdot dt \quad (5.3)$$

$$E_{abs} = \frac{1}{2} m (V_{impact}^2 - V_{revenire}^2) \quad (5.4)$$

V_{impact} is the impactor velocity before impact

D_{impact} – impactor between two frames measured on the image before impact

$V_{recovery}$– – impactor velocity after recovery

$D_{recovery}$ – impactor between two frames, measured on the image after recovery

$dt = \frac{n}{fps}$ – time difference between those two frames on which are measured the impactor , where fps is the number of frames per second set-up on the high velocity camera and n the number decided by the frames for measuring (1,2 or 4 frames).

E_{abs} – energy absorbed by the plate

m – impactor mass.

5.9.3 Measuring procedure of impactor travelling

Impactor travelling was recorded by a camera, the recording being processed in AOS Imaging Studio application. The procedure for travelling determination consists of the following stages:

1. The video file is loaded in AOS Imaging Studio application;
2. The calibration is made by marking on the image the two calibration points 1 and 2 (the distance between points was measured before the experiments start up, for instance: the plate thickness, head of sensors etc.) and the distance value is set up between the points in the adequate field from application (Fig 5.21);
3. The movie is unwound up to the moment when touches the plate, afterwards the first measure point is marked on a reference frame from the image (Figure 5.23);
4. A certain numbers of *n* frames are shown frame by frame and the second measure point is marked on an image reference frame.(Figure 5.23);
5. The travelling value is mentioned in the direction of x or y axis (Figure 5.24);
6. The values are filled up in Excel file.

At the same time the maximum traveling was measured with the travelling transducer LVDT. The results are presented in the table 5.8.

5.9.4 Results and conclusions

Table 5.5 Experimental tests results obtained by means of high velocity camera. The first contact with the sandwich plate

Method	Specimen	dt	$D_{impact}1$	$V_{impact}1$	$D_{ecovery}1$	$V_{recovery}1$	$E_{abs}1$
		[ms]	[mm]	[m/s]	[mm]	[m/s]	[J]
Gravitational impactor	SP10/0,2x5	8.33	40.4	4.85	34.57	4.15	31.52
Gravitational impactor	SP10/0,33x3	8.33	40.4	4.85	33.65	4.04	36.02
Gravitational impactor	SP15/0,2x5	8.33	40.4	4.85	33.63	4.04	36.13
Gravitational impactor	SP15/0,33x3	8.33	40.4	4.85	33.25	3.99	37.94
Gravitational impactor	SP20/0,2x5	8.33	40.4	4.85	34.03	4.09	34.16
Gravitational impactor	SP20/0,33x3	8.33	40.4	4.85	33.42	4.01	37.11
Gravitational impactor	SP28/0,2x5	8.33	40.4	4.85	35.03	4.21	32.19
Gravitational impactor	SP28/0,33x5	8.33	40.4	4.85	33.08	3.97	33.78
Gravitational impactor	SF20/0,2x5	8.33	40.4	4.85	34.08	4.09	33.93
Gravitational impactor	SF20/0,33x3	8.33	40.4	4.85	33.46	4.02	38.85

Table 5.6 Experimental tests results obtained by means of high velocity camera. The second contact with the sandwich plate

Method	Specimen	dt	$D_{impact}2$	$V_{impact}2$	$D_{recovery}2$	$V_{recovery}2$	$E_{abs}2$
		[ms]	[mm]	[m/s]	[mm]	[m/s]	[J]
Gravitational impactor	SP10/0,2x5	8.33	17.32	2.07	13.89	1.67	3.73
Gravitational impactor	SP10/0,33x3	8.33	19.05	2.29	9.52	1.14	9.81
Gravitational impactor	SP15/0,2x5	8.33	25.73	3.45	20.07	2.41	4.29
Gravitational impactor	SP15/0,33x3	8.33	26.04	2.66	12.17	1.46	6.32
Gravitational impactor	SP20/0,2x5	8.33	30.05	3.73	24.25	2.91	13.55
Gravitational impactor	SP20/0,33x3	8.33	29.37	2.61	8.14	0.98	15.61
Gravitational impactor	SP28/0,2x5	8.33	28.11	3.37	25.16	3.02	13.66
Gravitational impactor	SP28/0,33x3	8.33	26.12	2.94	11.87	1.42	16.29
Gravitational impactor	SF20/0,2x5	8.33	19.68	2.36	15.42	1.85	5.39
Gravitational impactor	SF20/0,33x3	8.33	23.09	2.67	6.75	0.81	16.31

Table 5.7 Experimental tests results obtained by means of high velocity camera. The third contact with the sandwich plate

Method	Specimen	dt	$D_{impact}3$	$V_{impact}3$	$D_{recovery}3$	$V_{recovery}3$	$E_{abs}3$
		[ms]	[mm]	[m/s]	[mm]	[m/s]	[J]
Gravitational impactor	SP10/0,2x5	8.33	12.77	1.53	9.46	1.14	2.65
Gravitational impactor	SP10/0,33x3	8.33	4.21	0.51	2.38	0.29	0.43
Gravitational impactor	SP15/0,2x5	8.33	19.55	2.35	11.93	1.43	8.64
Gravitational impactor	SP15/0,33x3	8.33	11.63	1.40	6.11	0.73	3.53
Gravitational impactor	SP20/0,2x5	8.33	23.98	2.88	18.25	2.19	8.72
Gravitational impactor	SP20/0,33x3	8.33	7.58	0.91	0	0.00	2.07
Gravitational impactor	SP28/0,2x5	8.33	24.96	3.00	18.27	2.19	10.42
Gravitational impactor	SP28/0,33x3	8.33	10	1.20	5.55	0.67	2.49
Gravitational impactor	SF20/0,2x5	8.33	14.9	1.79	11.7	1.40	3.07
Gravitational impactor	SF20/0,33x3	8.33	6.35	0.76	1.7	0.20	1.35

Table 5.8 Total energy consumed by impactor

Method	Specimen	$E_{abs}1$	$E_{abs}2$	$E_{abs}3$	E_{tot}
		[J]	[J]	[J]	[J]
Gravitational impactor	SP10/0,2x5	31.52	3.73	2.65	37.9
Gravitational impactor	SP10/0,33x3	36.02	9.81	0.43	46.26
Gravitational impactor	SP15/0,2x5	36.13	4.29	8.64	49.06
Gravitational impactor	SP15/0,33x3	37.94	6.32	3.53	47.79
Gravitational impactor	SP20/0,2x5	34.16	13.55	8.72	56.43
Gravitational impactor	SP20/0,33x3	37.11	15.61	2.07	54.79
Gravitational impactor	SP28/0,2x5	32.19	13.66	10.42	56.27
Gravitational impactor	SP28/0,33x5	33.78	16.29	2.49	52.56
Gravitational impactor	SF20/0,2x5	33.93	5.39	3.07	42.39
Gravitational impactor	SF20/0,33x3	38.85	16.31	1.35	56.51

5.9.5 Remarks and conclusions

Experimental tests are necessary to determine the type of damage and the energy absorbed by the sandwich plate. In every plate a delamination has occurred, for this being asorebed a certain quantity of energy. If the damage is a minor one, almost the entire kinetic energy is stored in elastic energy of the plate. In tables 5.5, 4.6 and 5.7 are given all the parameters values : D_{impact} (impactor travelling between two frames, measured on the image before impact), V_{impact}(impactor velocity before impact) $D_{revenire}$ (impactor travelling after recovery, measured between two image frames), $V_{recovery}$ (impactor recovery after impact), E_{abs} (energy absorbed by the plate).

During the impact, the energy absorbed by the plate has to correspond to a certain material damage.

The potential energy of impactor at the beginning of vertical travelling is being entirely tarnsformed into a plate deformation neglecting only the air friction.

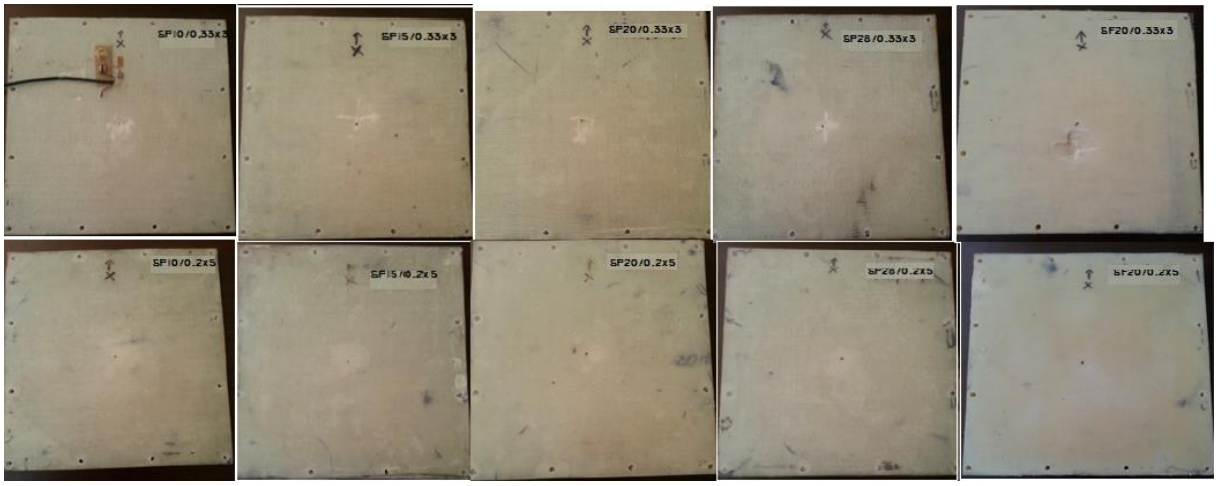

Figure 5.25 images with sandwich plates deterioration resulted from free drop gravitational

Table 5.9 Parameters of plates damaged areas

Plate specimen	Remanent deflection [mm]	Dimension in x direction of the damaged area [mm]	Dimension in y direction of the damaged area [mm]	Damaged state of the plate face
SP10/0,2x5	0	55	56	unstick
SP10/0,33x3	0.5	100	73	fissure
SP15/0,2x5	0	71	64	unstick
SP15/0,33x3	2.3	62	76	fissure
SP20/0,2x5	0	55	51	unstick
SP20/0,33x3	1.2	43	49	fissure
SP28/0,2x5	0	46	59	unstick
SP28/0,33x3	0.1	69	71	fissure
SF20/0,2x5	0	60	65	unstick
SF20/0,33x3	5.1	96	0	fissure

In the images from fig. 5.25 there are shown the sandwich plates damages after impact, in the cases where the coatings have 5 layers on each face, the texture thickness is 0,2mm. it can be noticed that damage in these cases is delamination type without breakage. Plates delamination from fig. 5.25 have values within 43 and 100mm. the biggest damage appear in case SP10/0,2x5. The smallest damage from this set was registered for SP20/0,2x5, horisontally (x axis) as well as vertically (y axis).

5.9.6 The results of travelling variations for free drop gravitational stand

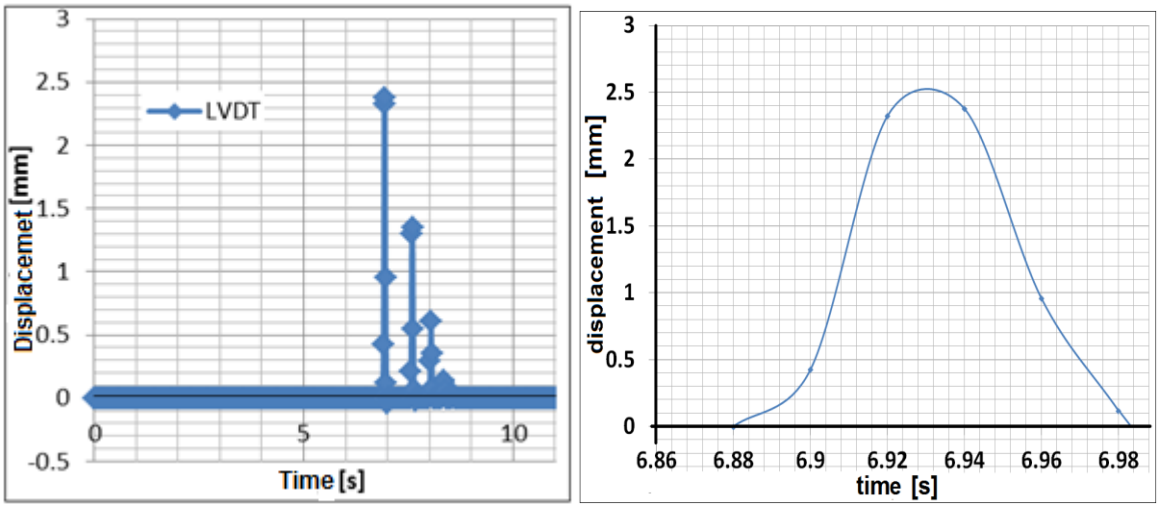

(a) (b)

Figure 5.26 Displacement variation in time for the case SP15/0,2x5

Displacement variations in time show that in figure 5.26 (a), is resented only the case of the plate SP15/0,2x5. In the figure 5.26 (b) is presented in detail, the displacement variation in area of the first contact (period from 6.88s to 6.98s).
In the table 5.10 the maximum displacement values obtained for the 10 plates, gravitational impact stressed.

Table 5.2 maximum tdisplacement values

Nr.crt	Sandwich plate	Maxim displacement [mm]
1	SP10/0,2x5	2.8535
2	SP10/0,33x3	2.3495
3	SP15/0,2x5	2.391
4	SP15/0,33x3	2.221
5	SP20/0,2x5	2.254
6	SP20/0,33x3	2.0755
7	SP28/0,2x5	1.2525
8	SP28/0,33x3	0.8987
9	SF20/0,2x5	2.5435
10	SF20/0,33x3	2.1785

In the table 5.10 and Fig. 5.27 there are presented the maximum traveling variation obtained for the 10 analysed plates (bottom face). The travelling values are tot significant to the dynamic phenomena. The most important parameter is the energy absorbed by each plate , this being the purpose of the analysis form this thesis

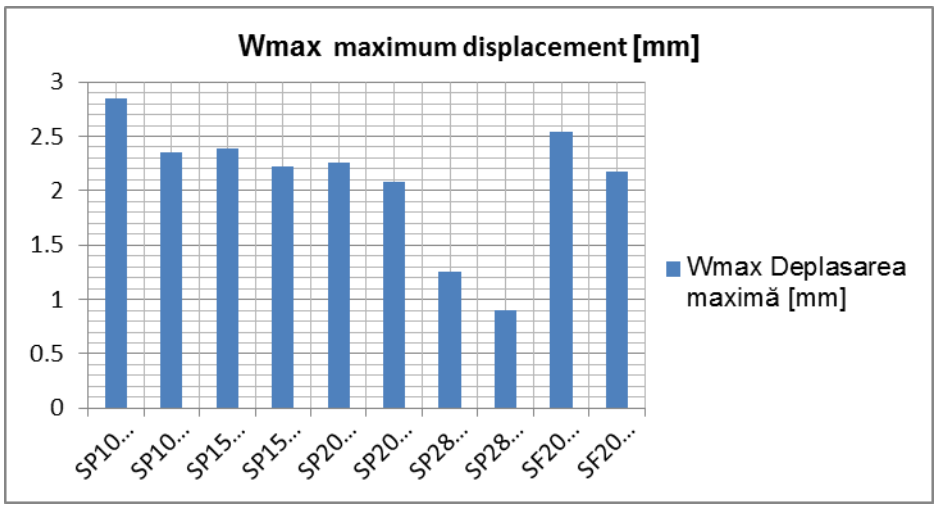

Figure 5.27 Maximum displacement results obtained with free drop gravitational system

In the graph from figure 5.27, it can be noticed that the trend of maximum displacement variation curve depending on the thickness and type o plate is the expected one.
From the presented graph in figure 5.27 can be noticed that the larger displacemnet are obtained by the sandwich plates with 5 layers and thicknesses of 0,2mm/ layer. But the biggest damages appear on the plates with 3 layers and thickness of 0,3mm/ layer. Almost the higher energy absorption appear also to this type of sandwich plates.

5.9.7 Conclusions

The importance of performed researches is connected to some measures taken for decreasing the crack risks appearance within the thin coatings of sandwich plates.
Some remarks can be drown-up:
- the results of the tests made with free drop are more closed to reality because the energy required to plates deformation is not influenced by the losses through friction, on the route of impactor drop.
- the stiffness of the plates with the core manufactured from polyurethane foam is higher than the one of the plates with the core manufactured from polypropylene honeycombs .
- The energy absorbed by the plates with polystyrene core is lower than the one of the plates with polypropylene honeycombs core.

5.10 Impact tests made by means of dynamic tests pneumatic system

5.10.1 Dynamic experimental modelling of composite sandwich plates

The materials velocity deformation effect on mechanical properties is very important to the kind of stress to which is exposed during exploitation. This addiction was noticed during quasi-static tests, which displayed that the materials strength increases at the same time with velocity deformation. This phenomenon appears much ore when material is “softer”. In order to analyse in detail this phenomenon, was made a determination system for the materials characteristics in dynamic conditions, based on the force developed on the expansion of a compressed gas.

The impact test was performed in Advanced Materials Resistance Laboratory from Mechanical Engineering Department of Dunărea de Jos University from Galați, using the stand for impact tests that uses the force developed by a pneumatic system.
The dynamic tests stand consists of (Fig. 5.28):
- force system development;
- support system of the composite plate;
- measurement system of test parameters;
- compressed gas cylinder;

Figure 5.28 Dynamic tests pneumatic stand

The velocity measurement is made by means of a tensometric sensor installed on the launching cylinder; (Fig. 5.29).
The time is measured with two tensometric mark, stick to one elastic lamella 1 and 2, fastened on rigid supports 3 and 4, all of them representing the tensometric sensor. To the gas expansion in the cylinder no 7, the impact bar no 5 will move together with arm 6. During his travelling, arm 6 will hit in series, at the moments t1 and t2, the end of lamella 1 and 2, producing elastic deformations, ε1 respectively ε2 (Fig. 5.30 și 5.34). Because the acquisition plate received data in real time, the time difference when the impulses appear in marks is $\Delta t=t2-t1$.

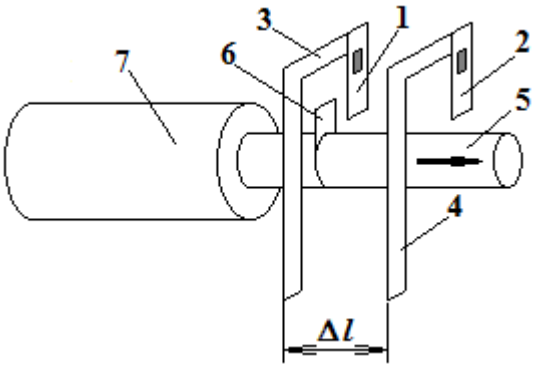

Figure 5.29 Electro resistance sensor

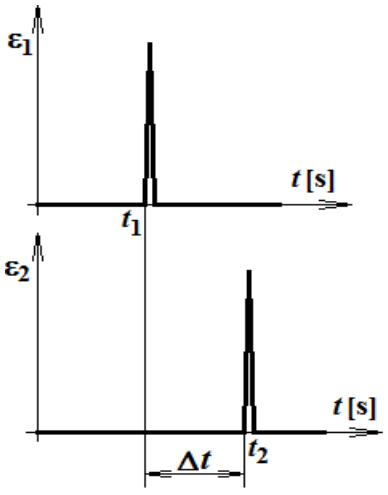

Figure 5.30 Time determination

Considering that the two sensors are placed to a distance Δl one from another, the velocity hit can be determined

$$v = \frac{\Delta l}{\Delta t} \tag{5.4}$$

Ehen the impactor hits the plate, his kinetic energy is transformed into plates deformation energy.

The force development system is composed of: compressed gas cylinder, pressure controlling device, trigger, the gas expansion cylinder, core-bar impactor piston.

The gas cylinder is a standard one, which contains compressed gas to a certain pressure la p1. The gas is nitrogen because has the property of maintaining the components on the move to a low temperature, in order not to have energy losses by parts heating during travelling due to friction.

Pressure controlling device is a system that adjusts the pressure to the value from cylinder, p1, to a value required to gas expansion in work cylinder (impact force development), p2. This adjuster has two air-pressure gauges, by means of which can be known at any moment the pressure in both connecting pipes (cylinder - adjuster and adjuster –trigger).

The trigger introduces the gas immediately (pressure p2) in driving cylinder. It is supposed that the expansion is adiabatic, so that to have the relation:

$$p2 \cdot V2 = p3 \cdot V3 \tag{5.5}$$

where:

- V2 is the pipe volume on the route adjuster-trigger;
- V3 is the cylinder volume;
- p3 is the pressure from the driving cylinder. Is the pressure that reacts on the piston developing the impact force, F.

Hydraulic cylinders the space where the gas gets expanded to create the impact force. The cylinder was built-up to provide the required pressure to develop the impact force.

The piston with driving core bar is manufactured to be able to hit the test structure. Between the piston and cylinder cover were installed sealing rings to allow the transfer of gas pressure p3 on the piston surface.

The entire system is designed to be able to develop a certain force fi with a certain velocity. To calibrate the system there were made measurements which are presented in the table 5.11.

Table 5.11 Force variation based on the pressure developed inside the cylinder

P [MPa]	F1 [kN]	F2 [kN]	F3 [kN]	F4 [kN]	F5 [kN]	Fmed [kN]
1.5	0.2361	0.1933	0.1984	0.1498	0.1962	0.1948
2.0	0.2808	0.2716	0.2671	0.2623	0.2431	0.2650
2.5	0.2225	0.2855	0.3896	0.3678	0.3339	0.3199
3.0	0.3498	0.3375	0.3425	0.3715	0.3482	0.3499

In the table 5.11 are shown the values of the five 5 tests to 4 different pressures. The values depend also on the pressure regulation step from the piston (it is used the average forces value).

After calibrating the system (table 5.11), it resulted the diagram from 5. 31, and it represents the variation of the average force based on the pressure developed in the cylinder.

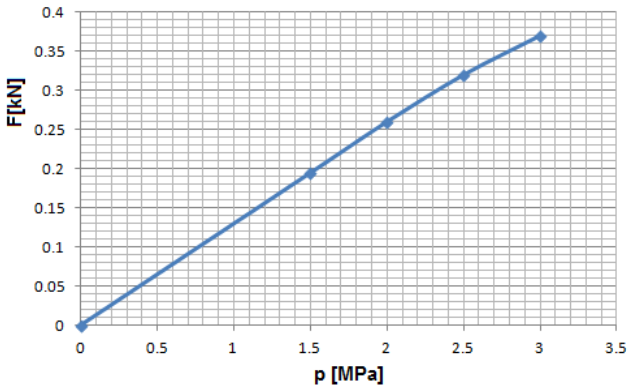

Figure 5.31 Impact force variation based on the pressure developed in the cylinder

The pressure gauge has the scree divided in [bar]. The table 5.11 and the figure 5.31 were analysed for the pressure transformed into [MPa] (1 bar=0.1MPa).

5.10.2 Impact tests

Maximum values of composite plates deformation were measured by the travelling transducer LVDT, being presented in the table 5.12.

Table 5.12 Maximum displacement results measured by travelling transducer

No	Cases	Mark1	Mark2	Traduccerl displacemnet LVDT [mm]
1	SP10/0,2x5	0.1479	0.01731	0.3966
2	SP10/0,33x3	0.05995	0.035	0.2772
3	SP15/0,2x5	0.01840	0.02328	0.1625
4	SP15/0,33x3	0.03184	0.02827	0.1976
5	SP20/0,2x5	0.02677	0.02473	0.2838
6	SP20/0,33x3	0.04572	0.04233	0.2880
7	SP28/0,2x5	0.06017	0.08414	0.1542
8	SP28/0,33x3	0.8720	0.01692	0.1866
9	SF20/0,2x5	0.1114	0.1655	0.5307
10	SF20/0,33x3	0.02607	0.06843	0.2509

Figure 5.32 Measurement of the plate maximum deformation

Table 5.13 Results of the energy absorbed by the plate

Specimen	dt [ms]	Maximum impact deformation [mm]	Impact velocity 1 [m/s]	Recovery deformation [mm]	Recovery velocity 1 [m/s]	Energy absorbed [J]
SP10/0,2x5	4.00	3.22	0.81	0.97	0.24	0.59
SP10/0,33x3	4.00	3.44	0.86	1.25	0.31	0.64
SP15/0,2x5	4.00	2.41	0.60	1.03	0.26	0.30
SP15/0,33x3	4.00	2.96	0.74	0.74	0.19	0.51
SP20/0,2x5	4.00	2.92	0.73	0.83	0.21	0.49
SP20/0,33x3	4.00	2.9	0.73	1.29	0.32	0.42
SP28/0,2x5	4.00	4	1.00	1.6	0.40	0.84
SP28/0,33x3	4.00	2.31	0.58	0.38	0.10	0.32
SF20/0,2x5	4.00	3.45	0.86	1.38	0.35	0.62
SF20/0,33x3	4.00	2.76	0.69	1.03	0.26	0.41

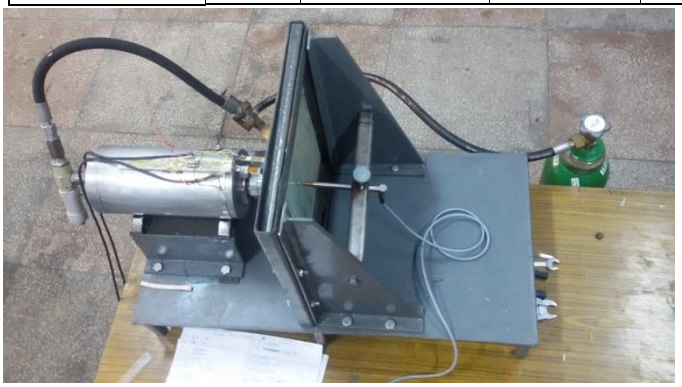

Figure 5.33 Measurement of the plate travelling – top view

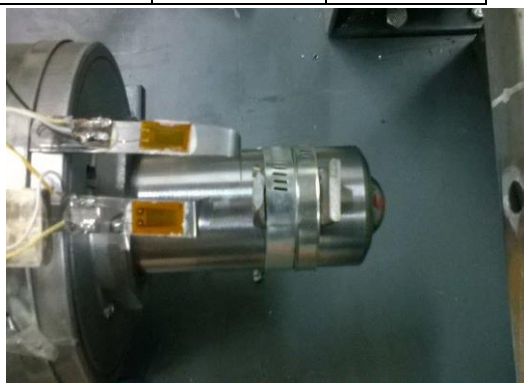

Figure 5.34 Tensometric system to determine the impact velocity impact

During the dynamic test, the hit point travelling was measured by means of the travelling transducer. Also the entire impactor route was recorded by high velocity camera (1000 frames/ s).

In the figure 5.35 recording equipment are presented, used during dynamic test.

Figure 5.35 Dynamic test – used equipment

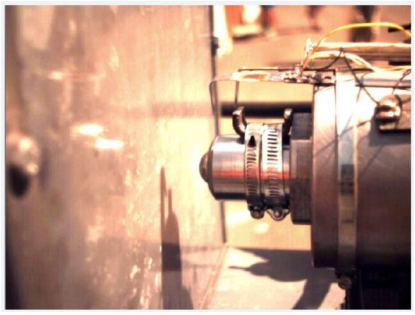

a)

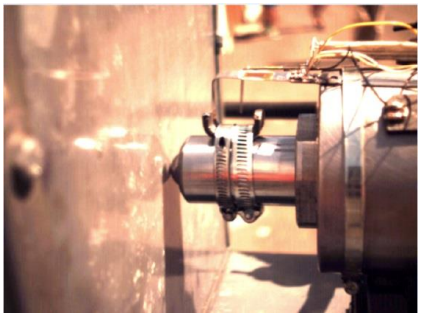

b)

Figure 5.36 a) The dynamic test at moment t=0 (image taken by high velocity camera) b) The dynamic test at moment t=0.022s – the moment when the plate surface is hit (image taken by high velocity camera)

5.10.3 Pneumatic impactor tests results

In figure 5.37 is presented the variation in time of the signals obtained from those two tensometric marks for the plate SF20/0,33x3. The time distance between the two heads represents the time difference when the arm from impactor core bar hit each of those two lamella. Knowing the distance between the two lamella, it was determined the travelling velocity of impactor.

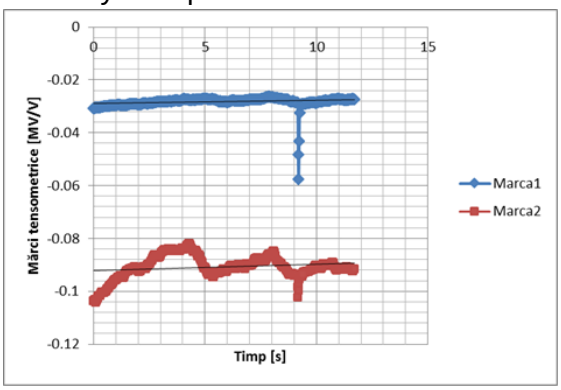

a)

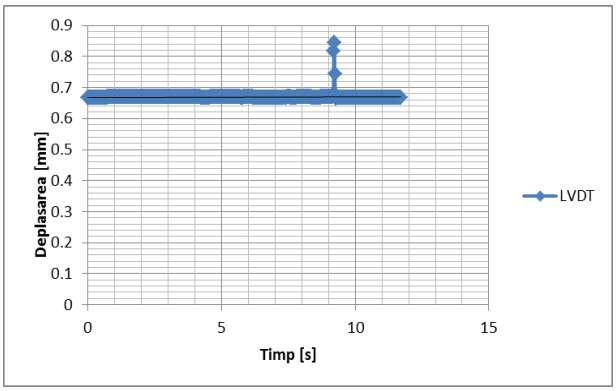

b)

b) Figure 5.37 a) The deformation variation given by tensometric valves of the electro-resistance sensor, depending on time, for case SF20/0,33x3; b) travelling variation in time for the case SF20/0,33x3

In figure 5.37 is presented the time variation of the plate maximum travelling SF20/0,33x3 during impact.

5.10.4 Conclusions

The energy absorbed by the plate material is the characteristic that can give us the information regarding its impact behaviour.

After performing the tests the following remarks can be drawn-up:

- the difference between suspension manner (embedding) considered theoretically in FEM calculation and the realistic manner of plates suspension during experiments, may be considered as errors that can influence the measurements;
- errors may appear due to improper pressure adjustment;
- other errors that may affect the measurement results may be connected to plate manufacturing (imperfections, inclusions, delamination etc.).

The behaviour requirements, to which the composite sandwich structure has to react, are related to the good strength and stiffness, dynamic stability, stability to different types of damages.

CHAPTER 6 COMPARATIVE ANALYSIS OF RESULTS

6.1 Comparative analysis of the static calculations

This chapter compares the numerical and experimental results shown separately in Chapters 4 and 5. In the table 6.1 the maximum displacement values for the ten kinds of sandwich panel studied are selected, for the case of a static loading with the force F = 53.55 [N], since it is the most representative value, also being the largest of all. (At this force value, errors that could have occurred due to the reading sensitivity of the values from the chart when they were read are smaller).

Table 6.1 The comparative results for the displacements of the sandwich obtained in calculation with Solid-Solid-Solid, Shell-Solid-Shell models and in experiments

No.	Plate	Results with elements of Solid-Solid-Solid (Ansys)	Results with elements Shell Solid-Shell (Ansys)	Experimental results
		F = 53.55 [N]		
1	SP10/0,2x5	0.07765	0.1206	0.0719
2	SP10/0,33x3	0.07841	0.1217	0.0733
3	SP15/0,2x5	0.05432	0.0750	0.0505
4	SP15/0,33x3	0.05475	0.0755	0.0519
5	SP20/0,2x5	0.04128	0.0553	0.0394
6	SP20/0,33x3	0.04153	0.0556	0.0404
7	SP28/0,2x5	0.03137	0.0403	0.0303
8	SP28/0,33x3	0.03152	0.0405	0.0308
9	SF20/0,2x5	0.04942	0.0593	0.0488
10	SF20/0,33x3	0.04971	0.0591	0.0487

Table 6.1 shows the results obtained numerically (with solid-solid-solid and solid-shell-shell models) and experimental

Table 6.2 Calculation of the differences between the numerical and the experimental results for F = 53.55 [N]

No.	Plate	The absolute difference [mm]			The percentage difference (%)		
		Mixed-Solid	Solid -Exp.	Mixed - Exp.	Mixed-Solid	Solid - Exp.	Mixed - Exp.
1	SP10/0,2x5	0.04295	0.00575	.0487	36	8	68
2	SP10/0,33x3	0.04329	0.00511	.0484	36	7	66
3	SP15/0,2x5	0.02068	0.00382	.0245	28	8	49
4	SP15/0,33x3	0.02075	0.00285	.0236	27	5	45
5	SP20/0,2x5	0.01402	0.00188	.0159	25	5	40
6	SP20/0,33x3	0.01407	0.00113	0.0152	25	3	38
7	SP28/0,2x5	0.00893	0.00107	0.01	22	4	33
8	SP28/0,33x3	0.00898	0.00072	.0097	22	2	31
9	SF20/0,2x5	0.00988	0.00062	.0105	17	1	22
10	SF20/0,33x3	0.00939	0.00101	0.0104	16	2	21

Table 6.2 presents the differences between the maximum deformations obtained in numerical models (solid type element model, the mixed model: shell-solid-shell) and the experiment for F = 53.55 [N].
The percentage differences between the two types of numerical models (mixed-solid column) are between 16% and 36%.
The percentage differences between numerical models with the solid-type element type and the experiment (Solid-Exp. column) is between 1% and 8%.
The percentage differences between numerical models with mixed type elements (shell-solid-shell) and the experiment (Mixed-Exp. column) is between 21% and 68%.

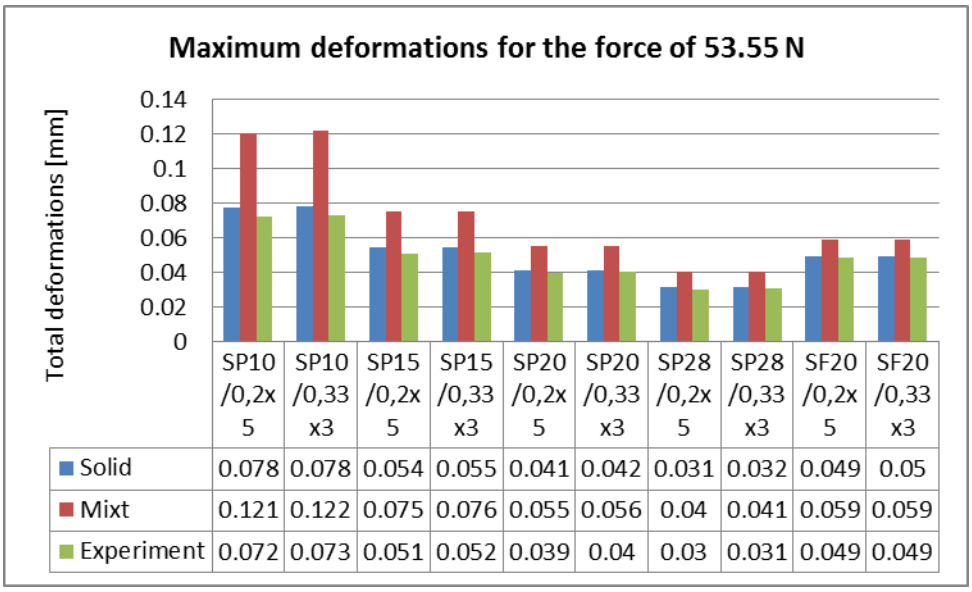

	SP10/0,2x5	SP10/0,33x3	SP15/0,2x5	SP15/0,33x3	SP20/0,2x5	SP20/0,33x3	SP28/0,2x5	SP28/0,33x3	SF20/0,2x5	SF20/0,33x3
Solid	0.078	0.078	0.054	0.055	0.041	0.042	0.031	0.032	0.049	0.05
Mixt	0.121	0.122	0.075	0.076	0.055	0.056	0.04	0.041	0.059	0.059
Experiment	0.072	0.073	0.051	0.052	0.039	0.04	0.03	0.031	0.049	0.049

Figure 6.1 The variations of the deformations obtained in the numerical modelling with Solid-type elements, respectively Mixed and in the experiment

As can be seen in figure 6.1 the closest values to those of the maximum deformations obtained in the experiment are those obtained in the solid element model.
Generally, even though they have the same total thickness, the three-layer coatings have a lower resistance than the five-layer coatings. The rigidity of the plates whose coatings have five layers is less than those with 3 layers.

6.2 Comparative analysis of the dynamic impact calculations

The table 6.3 compares the results obtained experimentally with the results obtained numerically with the ANSYS software (Explicit Dynamics -ANSYS Autodyn PrePost). Significant differences due to several types of errors can be observed. The differences can be attributed to experimental errors. For possible errors in numerical calculation there are a number of possible causes, which can be listed as follows:

- Choosing the type of model, as was done for the static calculation, where the mixed method was also used for the mesh, respectively Shell-Solid-Shell gave large differences, both when reported with the experiment, as well as when reported with the second model. With this method a series of short-comings were met (errors in the software, because of which the calculation could not be finished);
- Meshing problems that were met because of a weak computer processor due to which it was not possible to make a finer mesh;
- Insufficient data for material characteristics.

In the dynamic analyses (impact), the energy used to deform the structures is more important, rather than the maximum displacement values obtained.
Calculations were made for the duration of 2.5ms.
The aim of the calculations was to determine the behaviour of each type of material used for the sandwich plates, so as to determine the best configuration and the most suitable type of material for the impact loading. For technical reasons, the phenomenon analysis was performed in 2.5ms (a part of the total duration of the phenomenon). The trend of each configuration was taken into consideration, so the behaviour of the sandwich plate specimens can be anticipated, to be able to make decision at the end in this regard, resulting a behaviour according to the experimental results. The results of this calculation were compared with those obtained in experiments, yielding for the sample of 2.5ms a good match. Based on this comparison it can be concluded the fact that the anticipation of the behaviour of plates until the end of the impact phenomenon in the numerical calculation is justified. The used methodology can also be applied to design, so it can save calculation time, only in the material choosing stage and the configuration of the sandwich plate.

Table 6.3 The values obtained for the absorbed energy determined experimentally and numerically

No.	Specimens plates	Internal energy [J] (Experimental results for the impactor in free fall) (First Impact)	internal energy [J] (ANSYS) (Only for the first 2.5ms)
1	SP10/0.2x5	31.52	26.324
2	SP10/0.33x3	36.02	26.063
3	SP15/0.2x5	36.13	31.754
4	SP15/0.33x3	37.94	31.514
5	SP20/0.2x5	34.16	20.569
6	SP20/0.33x3	37.11	20.839
7	SP28/0.2x5	32.19	16.746
8	SP28/0.33x3	33.78	16.689
9	SF20/0.2x5	33.93	26.386
10	SF20/0.33x3	38.85	20.865

Tabelul 6.4 Valorile obținute pentru deplasări proiectate pe direcțiile x și y,[mm] determinate numeric și experimental

Specimen plate	The displacement in the x direction Numeric (ANSYS)	Displacement in the y direction Numeric (ANSYS)	Traveling in the x direction -Experiment-	The movement in the y direction -Experiment-	State of decay the final
SP10/0,2x5	1.4	1.6	5.5	5.6	unstick
SP10/0,33x3	1.4	1.6	10	7.3	fissure
SP15/0,2x5	3.4	3.2	7.1	6.4	unstick
SP15/0,33x3	3.4	3.2	6.2	7.6	fissure
SP20/0,2x5	4.5	3.8	5.5	5.1	unstick
SP20/0,33x3	4.5	3.8	4.3	4.9	fissure
SP28/0,2x5	4.6	2.0	4.6	5.9	unstick

SP28/0,33x3	4.6	4.6	6.9	7.1	fissure
SF20/0,2x5	5.5	3.6	6	6.5	unstick
SF20/0,33x3	0.5	0.5	9.6	6	fissure

Table 6.3 presents the values of energy absorbed by the plate for its destruction, after the first-order impact (main impact).

During experiments cracks appeared only in the 3-layer coatings. Meaning that their impact resistance is lower than that of the 5-layer coatings even though the total thickness is the same. It is observed that the numerical variation trend of the absorbed energy is the same, both in calculations and in experiments.

The total impact energy has two components:

- The energy absorbed for elastic deformations;
- The energy absorbed for inelastic deformations (including cracks).

For plates with inelastic deformations the consumed energy was used both for the elastic deformation of the plate, as well as the degradation phenomena of the coating and the core.

Other conclusions:

- The experiments and simulations underlying dynamic responses can be used to design stronger structures and more effective at impact or even explosions at extreme dynamic loads.

For high load intensities, light coatings and the low-density cores, allow the greatest shock attenuation. It is obvious that the high-density cores face fragmentation and tearing at a large scale and are not significantly superior than the low-density structures according to the results shown in table 6.4.

For low load intensities the sandwich structures with high density cores can be used to save space and to provide effective resistance against shocks, since they are much thinner than the sandwich structures with low density (based on weight). Provided that the dimensional constraints are satisfied, on the basis of weight, a combination of thick cores, with lower density and rigid thin faces provides better shock attenuation.

- The experiments are supported by finite element simulations, which reflect the effects of degradation in the form of cracks, breakages, deformations and detachments in coatings, deformation, cracks, core tears. The dynamic response of sandwich panels is investigated using finite element modelling and show that the experiments and the simulations are in agreement.

- In general, although the same total thickness of the coatings, the internal energy of plates whose coatings have five layers is greater than those with 3 layers. The explanation is offered by the existence of additional interlaminar tangential tensions at the 5-layer coatings compared to those with 3 layers, which performs additional mechanical work than those with 3 layers.

- From the conducted research it is shown that a comparison between experimental and numerical results can be completed with some errors that may occur due to multiple parameters and material characteristics to be introduced into the calculation. The software used in this thesis was ANSYS. In the conclusions of the thesis can be seen that one of the causes of errors that occurred in the calculation is the difficulty of considering the mechanical properties of materials natural, for example. In the work an impact study for composite sandwich plates was carried out. At the end, the experimental and the numerical results for the energy absorbed by the plates were compared. In [99] and [100] comparative analyses were performed to layered specimens both experimentally and also in ANSYS, where the results were a bit different and then it was necessary to calculate the percentage of error.

CHAPTER 7 GENERAL CONCLUSIONS, ORIGINAL CONTRIBUTIONS AND PERSPECTIVES

7.1. General conclusions

Due to economic and technological development, particularly advanced materials, reduced energy consumption globally, the crisis of traditional raw materials (wood, steel, other metals, etc.) and increasing policy of environment protection by reducing polluting emissions, it came to the creation of new materials and new nonconformist technologies.

Composite sandwich materials are included in the compound materials group. Given the characteristics and their future developments, a particular importance is given to composite materials, which were originally called reinforced plastics. These have superior properties and are the result of a mixture of at least two components. Component properties complement each other, resulting in a superior material with specific qualities for each material that constitutes it. These materials have been developed to substitute in as high an extent as possible the existing traditional materials (ferrous and non-ferrous), which showed some shortcomings in terms of performance, processes for manufacturing and processing, masses, volumes, geometric complexity, significant costs and areas of application.

Regarding the technical part, the composite material term refers to materials that exhibit the following properties:

- are a combination of at least two materials which are chemically different aspect between these there is a clear separation surface;
- they are made artificially, by combining different components;
- they have properties that aren't present in any of the components of the material taken alone.

Development of the manufacturing technologies for composite materials has imposed the creation of characteristics determination tests for structures made from these materials and especially those of impact type.

Experimental impact tests are done with different stands for testing and control of their quality, with a proper structure, by having, firstly, a measurement system with data acquisition on the time evolution of the values of the dynamic parameters and that allows specific testing procedures to be carried out. The most flexible stands use pneumatic / hydraulic components which are part of the system of the dynamic force's action and development.

In the thesis, a series of activities for achieving the main objective have been realised:

- Manufacturing of composite sandwich plates;
- The processing of the composite plate;
- Calibration of the stand (determination of the impact force based on the pressure of the gas in the cylinder, the determination of the impactor speed based on the gas pressure in the cylinder, using resistive electrical tensometry);
- Bonding the tensometric marks on the surface of the plates and inserting them into the strain gauge circuit;
- Static load test of composite sandwich panels;
- Impact loading tests of composite sandwich plates with the gravity stand;
- Impact loading tests of composite sandwich plates with the pneumatic stand.

The impact tests were conducted in the Laboratory of Advanced Strength of Materials from the Department of Mechanical Engineering of the University "Dunarea de Jos", using two stands:

- an impact test stand using the force developed by a pneumatic system;
- an impact test stand using gravitational force developed by the free fall of a rigid ball from a certain height.

The numerical and experimental analyses, the results that were obtained, the conclusions and the discussions that were made represent original contributions which, in summary, can be formulated as follows:

1. The design, the development and the implementation of methods and technology for the manufacture of stratified composites for coatings with the complete use of all the obtained results, the foundation, theoretically, of the bases of the physical and mathematical model of the stratified composites for obtaining a sandwich plate with a good strength;
2. The realization of a numerical and experimental database on the materials used, allowing the development of experimental research and highlighting aspects of scientific interest;
3. After the macromecanic analysis of each layer and of the stratified composite coating as a whole, it was observed that for the same thickness of the stratified composite, the rigidity and strength depend on the number of layers, the properties of each layer and the orientation of the layers in the stratified composite coatings;
4. In the experimental tests, by using equipment based on resistive electric tensometria, the main mechanical characteristics of the composite materials used in the construction of the plates were determined. The tensile test results were compared with the data provided by the manufacturer of the fiberglass fabrics and with the characteristics found in the specialty literature, noting the fact that the elasticity modules E correlate very well. Also, for the values that were obtained for the tensile stresses σ_r, for the specimens made of the bi-directional fabric, differences of 10% were obtained, compared to those indicated by the manufacturer of the glass fibre fabrics and the characteristics found in the specialty literature;
5. Processing the results of the traction tests to determine the characteristics of the materials;
6. Designing sandwich plate structures with two epoxy resin impregnated glass fiber webs;
7. Design and realization of the technological process of manufacturing sandwich plates;
8. The structural model of the plates was developed (the coating and the core of the material were modeled from composite matrials). Following the static and impact simulations with the plate structure, the stiffness and strength of the plates were checked under a static loading. The results of the multiple experimental simulations were validated by the results obtained with the numerical tests;
9. The strength of the plates at impact has been checked according to the following criteria: the maximum tensions and deformations, Tsai-Wu, Tsai-Hill;
10. The degradation mode of the plates by the experimental impact was observed, yielding concluding that: the three-layered coatings have a lesser resistance than the five-layer coatings, although the total thickness of the stratified composite is the same.

7.2. Original contributions

The overall objective of the thesis is to investigate the impact resistance mechanisms that influence the degradation phenomena of composite sandwich plates. To achieve this overall objective, three key objectives are identified, each of which being addressed in the numerical impact analysis chapter and in the experimental analysis chapter.

Following the numerical analyses, the following general conclusions can be drawn regarding:

- The identification of a numerical model able to capture the phenomena that appear at the impact of the composite sandwich plates.

The numerical model developed in ANSYS, calibrated and validated based on experimental analyses consists of the following modelling elements:
- the representation of the material behaviour of the sandwich plate, by using volumetric finite elements.
- the adaptation of the explicit-dynamic procedure to be able to study static and quasi-static phenomena.
- the numerical validation analyses performed in ANSYS/Explicit indicate a good capacity of the numerical model of representing the structural response both in determining the strength characteristics of the volume elements, and also of the plate elements.

The main elements of originality of the thesis are:
1. Following the theoretical analysis of the impact phenomenon, I realized an original modelling of the phenomenon that appeared in the sandwich plates.
2. The creation of an original experimental stand, used for studying the gravitational impact of free fall.
3. The ability of the stand to perform reproducible impact experiments, due to a sufficiently precise calibration.
4. The tensometric measurement of the impact force by means of the force transducer and the impact velocity of the impactor on the plates fixed in the experimental stand.
5. The experiments that were performed, which have shown that the impact loading produces irreproducible degradation phenomena, depending on the type of material.
6. The highlighting of the mechanical characteristics of the material, which determines decisively their behavior to the impact loading.
7. The performance of the measurement of traces of degradation left of the impact surfaces by the impactor.
8. The determination of the relative dimensions of the impact traces, on their basis being able to perform a comparison between different materials subjected to impact.
As part of the doctoral training program, I have done, in colaboration, a series of 6 scientific papers, in which I have shown the progress of my impact studies.
This paper contains an elaborated study on the behavior of composite sandwich plates, which have been analyzed mechanically under static and dynamic loadings. It began with the analysis of the geometry of different cell types: circular, hexagonal and square. This study was conducted to observe their behavior at static loadings, and then to be able to choose the shape of the core for the entire plate.

Cell analysis results have, however, been unsatisfactory because it sometimes contained uncertainties and questions about how the entire plate will behave in response to loadings. Under these conditions , the whole sandwich plates had to be statically analyzed.
9. The geometrical shape of the polypropylene cores was analysed: circular, hexagonal and square cells. In the case of circular and square ones, the unstructured form was also analysed. The results were compared using graphs showing inflections and jumps, but also using tables to highlight the values obtained. For these models, the faces had a thickness of 1 mm and the composite material was a unidirectional glass fibre reinforced epoxy resin. The thicknesses of the statically analysed core were 20 mm. After these models were made using the ANSYS Software with the finite element method, the hexagonal cell sandwich core was chosen to study more thoroughly into the experimental analysis step.

This material was chosen for the good properties and characteristics revealed by the finite element analysis. A lot of decision-making was done on the basis of the cost of purchasing the material.

10. The experiments were performed both statically and dynamically on polypropylene hexagonal honeycomb sandwich panels of different thicknesses, namely: 10, 15, 20, 28 [mm].

The same was done for the foams: they were analysed with the finite element method in the ANSYS software, both statically and dynamically, different foams: SAN Foam 81 Kg/m^3 (SAN styrene acrylonitrile), SAN Foam 103kg/m^3, PVC Foam 60 kg/m^3, PVC Foam 80 kg/m^3 with thicknesses of 20 mm, and then for more detailed study the extruded polystyrene with a density of 30Kg/m^3 was chosen, with a thickness of 20mm for the core. This choice was strictly in terms of a much lower price compared to other materials, but also because it has a very low density which helps global structures to be much lighter, given this is a search trend in all areas but especially in naval and aerospace industry.

11. Different types of sandwich faces were analysed, namely: faces with unidirectional and bidirectional layers, however, the materials were always the same: epoxy resin reinforced with glass fibre. Plain fabrics with a thickness of 0.33 mm and a satin fabric with a thickness of 0.2 mm were used. For cores, the materials used were: polypropylene and a foam category.

12. After the static analysis and after the new parameters had beed discussed, the composite sandwiches were analyzed at shock with two different systems, namely gravitational impact and pneumatic impact. The pneumatic impact is a modern method and a relatively new concept, because the pneumatic impactor system has been developed in the Strength of Advanced Materials Laboratory of the Faculty of Engineering, "Dunarea de Jos" University, and improved by me with the help of a professor and my PhD supervisor.

13. Improvements consisted of applying a new argon cylinder and a pressure reducer to the system, as well as improvements for the mounting bracket of plates of different thicknesses. I added the fastening system of the metal frame, twelve butterfly screws for successfully fixing the plates. These improvements have helped to eliminate some errors in the piston friction in the cylinder due to the new acquisitions.

14. I also made improvements and contributions to the gravity stand. At the gravity stand many errors appeared due to friction occurring in the guides and I had to give up that system to conceive another where the only frictions are with the air.

15. The composite sandwich plates were handmade by me. I designed and made two sets of ten different types of sandwich plates as follows:

1) SP10/0,2x5; 2) SP10/0,33x3; 3) SP15/0,2x5; 4) SP15/0,33x3; 5) SP20/0,2x5;
6) SP20/0,33x3; 7) SP28/0,2x5; 8) SP28/0,33x3; 9) SF20/0,2x5; 10) SF20 0,33x3.

SP stands for polypropylene core sandwich followed by the thickness in mm of the core plate, which may be 10, 15, 20, 28. After the thickness of the core, the thicknesses of the faces are added, denoted 0,2x5 or 0,33x3 (the thickness of the fabric may be 0.2 mm or 0,33mm, followed by the number of forming layers, 5 layers or 3 layers respectively).

16. Regarding the characteristics of the materials used in this work, some of them were taken from various sources such as: the Ansys library, which contains many of the characteristics used in this study, from research papers and the experimental tests of some authors. Thus, some material characteristics were determined for: the extruded polystyrene and for the polymer matrix reinforced with glass fibre fabrics.

This research is based on the analysis of a large number of scientific papers done in this direction, works that have inspired this thesis and some methods used by other researchers have been improved or compared.

7.3. Proposals for future studies

For future studies on the impact behaviour of composite plates, the stands that I've used for my tests can be improved for a better value accuracy and the complete disappearance of errors.

Use of other stands or other impact measuring devices. For example, the ballistic impact, or impact with the CEAST Fractovis Plus 9350 Testing Machine, professional impact testing devices, could be a more effective solution.

Experimental research on the behaviour of sandwich plates can be extended to other types of load: three or four point bending, fatigue, shear, delamination, impact bending, impact compression, vibration, interlaminar rupture could yield remarkable results of advanced development of sandwich plate analyses.

Residual resistance studies of sandwich composite slabs after impact.

The design and execution of other types of sandwich plates with other types of materials used for the faces and the cores, such as: for the faces carbon fibres, kevlar fibres, aramid fibres may be used and the matrix could be from unsaturated polyester, vinyl ester, phenolic resin (thermosetting). The cores may be made of other types of materials (eg CORREMAT, balsa wood, other foams of other densities than those used in this sentence, aluminium cores).

The finite element methodology discussed in this thesis was developed on the basis of ANSYS calculations, using the Explicit Dynamic module for Impact Calculation. Other software such as ABAQUS and LS-DYNA or extensions such as VUMAT, AUTODYN can also be used in this idea.

Bibliography

[1] N. Manafi, *Bazele Mecanicii Aplicate, Partea V-a Dinamica solidului rigid conținut, (*http://cat.mec.pub.ro/archive/Bazele%20Mecanicii%20Aplicate%20(6)%20-%20DINAMICA%20SOLIDULUI%20RIGID.pdf).

[2] R. Voinea, D. Voiculescu și V. Ceaușu, *Mecanica,* București, 1975.

[3] L. Tong, A. P. Mouritz și M. K. Bannister, *3D Fibre Reinforced Polymer Composites,* Elsevier Science Ltd, Londra, 2002.

[4] G. Jeronimidis și J. Hou, *Impact and postimpact mechanics of composite laminate circular plates,* ICAM'96, Beijing.

[5] M. Szarvas, *Thesis: Crash of the boat into the pier,* Slovak University of Technology Bratislava, 2011.

[6] S. V. Kilchert, *Nonlinear finite element modelling of degradation and failure in folded core composite sandwich structures,* institute Aircraft Design, University of Stuttgart, 2013.

[7] M. Bunea Schițanu, *Contribuții la studiul solicitărilor la impact ale compozitelor cu matrice epoxidică armate cu țesături,* Universitatea "Dunarea de Jos ", Galați, 2015.

[8] T. Anderson și E. Madenci, „*Experimental investigation of low-velocity impact characteristics of sandwich composites*," Composite Structures*,* vol. 50, nr. 3, p. 239–247, 2000.

[9] J. P. Dear, H. Lee și S. A. Brown, „*Impact damage processes in composite sheet and sandwich honeycomb materials*," International Journal of Impact Engineering*,* vol. 32, nr. 1-4, p. 130–154, 2005.

[10] J. H. Park, S. K. Ha, K. W. Kang, C. W. Kim și H. S. Kim, „*Impact damage resistance of sandwich structure subjected to low velocity impact*," Journal of Materials Processing Technology, vol. 201, nr. 1-3, p. 425–430, 2008.

[11] K. B. Shin, J. Y. Lee și S. H. Cho, „*An experimental study of low-velocity impact responses of sandwich panels for Korean low floor bus*," Composite Structures*,* vol. 84, nr. 3, p. 228–240, 2008.

[12] A. D. Borîtu, *Contribuţii privind evaluarea integrităţii materialelor şi structurilor compozite prin inspecţie nedistructivă,* Bucureşti, 2011.

[13] S. Abrate, *Impact on composite structures,* Southern Illinois University at Carbondale, First published 1998, This digitally printed first paperback version 2005 ISBN 0-521-47389-6.

[14] I. Chirică, *Elasticitate - Fundamente. Exemple. Aplicații,* Editura Tehnică, București, ISBN 973-31-1129-5, 1997.

[15] D. Alcalay. [Interactiv]. Available: http://www.carmel-lab.com/sites/deven.cometousa.co.il/files/Drop%20Shock%20Theory.pdf.

[16] M. Aktas, H. E. Balcioglu, A. Aktas, E. Turker și M. Deniz, *Impact and post impact behaviour of layer fabric composites,* vol. 94, Composite structures, vol. 94, p. 2809-2818, 2012, p. 2809–2818.

[17] S. Heimbs, J. Cichosz, S. Kilchert și M. Klaus, *Sandwich panels with cellular cores made of folded composite material: mechanical behaviour and impact performance,* ICCM17, Germany, 2009.

[18] N. A. Apetre, *Thesis: Sandwich panels with functionally graded core,* University of

Florida, 2005.

[19] C. Akin și M. Șenel, *An Experimental Study of Low Velocity Impact Response for Composite Laminated Plates,* DPU Fen Bilimleri Enstitusu Dergisi , Sayi 21, Nisan, 2010.

[20] M. A. Hassan, S. Naderi și A. R. Bushroa, *Low-velocity impact damage of woven fabric composites: Finite element simulation and experimental verification,* Materials and Design 53, p. 706–718, 2014, p. 706–718.

[21] N. Tarim, F. Findik și H. Uzun, „*Ballistic impact performance of composite structures*," Compos Struct*,* vol. 56, nr. 1, p. 13–20, 2002.

[22] F. Findik și N. Tarim, „*Ballistic impact efficiency of polymer composites*," Compos Struct*,* vol. 61, nr. 3, p. 187–92, 2003.

[23] F. Findik, M. Misirlioglu și U. Soy, *„The structural features of glass fibre reinforced polyester matrix composites*," Sci Eng Compos Mater*,* vol. 10, nr. 4, p. 287–295, 2002.

[24] *Standard Test Method for Measuring the Damage Resistance of a Fiber-Reinforced Polymer Matrix Composite to a Drop-Weight Impact Event1 D7136/D7136M – 12.*

[25] S. V. Lefter, *Teza: Contribuţii la Calculul Structurilor Navale confecţionate din Plăci Armate cu Fibre de Sticlă, la solicitări dinamice de impact,* Universitatea „Dunărea de Jos" Galați, 2011.

[26] M. Altenaiji, G. K. G.K.Schleyer și Y. Y. Zhao, „*Characterisation of Aluminium Matrix Syntactic Foams Under Static and Dynamic Loading, Capitolul 19, Materials Science, Composite Materials*," în *"*Composites and Their Properties*", book edited by Ning Hu*, ISBN 978-953-51-0711-8, 22. August, 2012.

[27] W. Cantwell și J. Morton, „*Impact perforation of carbon fibre reinforced plastic*," Composites science and technology*,* vol. 38, p. 119–141, 1990.

[28] A. Ahmed și L. Wei, *The low-velocity impact damage resistance of the composite structures (a review),* Rev.Adv.Mater.Sci., vol. 40 (2015), p. 127-145, 07 iulie 2014, p. 127–145.

[29] C. Naslund și O. O. UYANIK, *Parametric Study of Joint Design in a HSLC Composite Vessel – Load-carrying Characteristics of Foam Core and Joint Geometry in Sandwich Structures,* Sweden: Department of Shipping and Marine Technology, Gothenburg, Sweden, 2011.

[30] L. Aktay, *Thesis: Improved Simulation Techniques for Modelling Impact and Crash Behaviour of Composite Structures,* Turcia: University Stuttgart, Ankara, Turcia, January 2010.

[31] E. Green și Associates, *Marine Composites,* Annapolis Maryland, ISBN 0-9673692-0-7, 1999.

[32] A. Shenoi, R. Beck, D. Boote, P. Davies, A. Hage, D. Hudson, K. Kageyama, J. A. Keuning, P. Miller și L. Sutherland, *Sailing Yacht Design,* vol. 2, Korea: 17th International ship and offshore structures congress, 16-21 august, Volume2, Seoul, Korea, 2009.

[33] I. Chirică, E. F. Beznea și I. Gavrilescu, *Metode moderne de calcul al structurilor compozite,* Ed. Cermi, Iasi, ISBN 978-973-667-283-5, 2007.

[34] E. F. Beznea și I. Chirica, *Structuri compozite,* Editura Galați University Press, ISBN 978-606-8008-86-8, 2010.

[35] G. Vasile, *Teza: Structuri cu rigiditate ridicată, din material compozite, utilizate în*

construcția de autovehicule, Nr. 5981 din iulie 2013, Brașov, Romania.

[36] A. Zinno, *Thesis: Multiscale Approach for the Design of Composite Sandwich Elements,* University of Napoli FEDERICO II, 30 November 2010.

[37] Z. Voyiadjis G. și P. I. Kattan, *Mechanics of Composite Materials with MATLAB,* ISBN-10 3-540-24353-4 Springer Berlin Heidelberg New York, ISBN-13 978-3-540-24353-3 Springer Berlin Heidelberg New York, 2005.

[38] R. Murugan, K. Padmanabhan și R. Ramesh, „*Study of vibration characteristics and interaction of cyclic fatigue loading on vibration responses of thin walled woven fabric glass-carbon epoxy composites for structural applications",* 13.ian.2016.

[39] P. K. Mallick, „*Fiber Reinforced composites, Materials, Manufacturing and Design",* U. of Michigan-Dearborn și F. a. T. E. C. R. C. P. Group, Ed., University of Michigan-Dearborn, Editura CRC Press Taylor and Francis Group , Boca Raton London New York, International Standard Book Number-13: 978-0-8493-4205-9, 2008.

[40] K. K. Autar, „*Mechanics of Composite Materials second edition",* F. a. T. E. Group, Ed., Editura Tailor and Francis Group, International Standard Book Number-13: 978-0-8493-1343-1, 2006.

[41] B. Okutan, „*Stress and failure analysis of laminated composite pinned joints",* Dokuz Eylül University, Thesis of PhD, 2001.

[42] Y. Chen, „*Finite Element Micromechanical Modeling of Glass Fibedepoxy Crossply Laminates",* University of Alberta, Thesis of MS, 2000.

[43] F. E. Sezgin, „*Mechanical Behaviour and Modeling of Honeycomb Cored Laminated Fiber/Polymer Sandwich Structures".* Thesis (Master), Izmir Inst. of Technol., 2008 (library.iyte.edu.tr/tezler/master/makinamuh/T000703.pdf), p. 2008.

[44] J. Araboui, Y. Schmitt, J. L. Pierrot și F. X. Royer, „*Experimental bending behaviour of multy-layer sandwich structures",* Archives of Metallurgy and Materials, Volume 54, 2009.

[45] L. Zhuang și J. Crocker M., *A study of the damping in sandwich structures,* Sweden: 7-10 july 2003, Stockholm, Sweden, Tenth International Congress, p. 227.

[46] *Sandwich concept, DIAB sandwich handbook, Available from www.diabgroup.com.*

[47] P. T. Sarafin, *Spacecraft Structures and Mechanisms: From Concept to Launch,* Microcosm Press, Kluwer Academic Publishers, 2011.

[48] G. Bianchi, *Thesis: Structural Performance of Spacecraft Honeycomb Panels,* University of Southampton, April 2011.

[49] D. Zenkert, „*An Introduction to Sandwich Construction",* Chameleon Press LTD, London, 1995.

[50] [Interactiv]. Available: http://www.scritub.com/tehnica-mecanica/Materiale-de-armare-anvelope85125.php.

[51] H. Lei, *Theses: „Composite sandwich structures with honeycomb core subjected to impact",* Clemerson University, 2012.

[52] R. Roy, J. H. Choi și S. J. Park, „*Characterization of Nomex honeycomb core constituent material mechanical properties",* Impact Factor: 3.12, DOI: 10.1016/j. comp struct, 2014.06.033, Composite Structures, November 2014.

[53] A. Petras și M. Sutcliffe, „*Failure mode maps for honeycomb sandwich panels,"* vol. 44, Composite structure 44, p. 237-252, 1999, p. 237–252.

[54] S. Heimbs, J. Cichosz, M. Klaus, S. Kilchert și A. F. Johnson, „*Sandwich structures with*

textile-reinforced composite foldcores under impact loads," Elsevier, Composite Structures*,* vol. 92, p. 1485–1497, 2010.

[55] I. Chirică, E. F. Beznea și R. Chirica, *Placi compozite,* Editura Fundatiei Universitare Dunarea de Jos, Galati, ISBN (10) 973-627-337-7; ISBN (13) 978-973-627-337-7, 2006, p. 978–973, 2015.

[56] H. Tuwair, M. Hopkins, J. Volz, M. ElGawady, M. Mohaned, K. Chandrashekhara și V. Birman, „*Evaluation of sandwich panels with various polyurethane foam-cores and ribs",* Composites Part B 79, p. 262-276, 2015.

[57] F. Amir, R. Othman A. și H. M. Akil, „*Damage Characterization of Polypropylene Honeycomb Sandwich Panels Subjected to Low-Velocity Impact",* vol. 2013, Hindawi Publishing, Volume 2013, Article ID 129864, 10 pages , 2 October 2013, p. 10.

[58] *ANSYS Mechanical APDL Element Reference,* 2013.

[59] L. J. Gibson și M. F. Ashby, „*Cellular solids, Structure and properties, Second edition",* Editura Cambridge University Press, First paperback edition (with corrections), 1999 version on line 2016.

[60] J. a. A. M. F. Zhang, „*Buckling of Honeycombs under In-plane Biaxial Stresses*," International Journal of Mechanical Sciences*,* vol. 34, nr. 6, p. 491–509, 6 June 1992.

[61] F. Rotaru Paraschiv, I. Chirică și E. F. Beznea, „*Influence of the Honeycomb Geometry on the Sandwich Composite Plate Behavior",* Advanced Materials Research, ISSN: 1662-8985, Vol. 1143, pp 139-144, Trans Tech Publications, Switzerland 2017.

[62] D. Zeleniakienė, P. Griškevičius, V. Leišis și D. Milašienė, „*Numerical investigation of impact behaviour of sandwich fiber reinforced plastic composites",* Article in mechanika Impact Factor: 0.29· JANUARY 2010.

[63] *ANSYS, Contact Technology Guide,* 2009.

[64] *ANSYS, Introduction to Contact, ANSYS Mechanical Structural Nonlinearities, ANSYS, Inc. Proprietary 2010,* 2010.

[65] A. İlke, *Thesis: Investigation of design and analyses principles of honeycomb structures,* Department of Aerospace Engineering, noiembrie 2007.

[66] C. Naresh, A. Gopi, K. Chand, S. R. Kumar și P. Chowdary, *Numerical Investigation into Effect of Cell Shape on the Behavior of Honeycomb Sandwich Panel,* vol. 2, ISSN: 2319-8753, India, Vol. 2, Issue 12, December 2013.

[67] Z. Xue și W. Hutchinson, „*Crush dynamics of square honeycomb sandwich cores*," *Int. J. Numer. Meth. Engng 2006,* vol. 65, p. 2221–2245, 10 online 26 October 2005.

[68] F. Wu, R. Spong și G. Wang, „*Using Numerical Simulation to Analyze Ship Collision",* ICCGS 2004, Izu, Japan, October 25-27, 2004.

[69] A. Vaziri, Z. Xue și J. W. Hutchinson, „*Performance and failure of metal sandwich plates subjected to shock loading*," *Journal of Mechanics of Materials and Structures,* vol. 2, nr. 10, 2007.

[70] F. Rotaru, I. Chirica și E. F. Beznea, „*Static behavior of the sandwich composite plates",* la conferința Advanced Composite Materials Engineering COMAT 2014 Brașov.

[71] F. Rotaru, I. Chirica și E. F. Beznea, „*Strength Analysis of a Composite Joint Used in Ship Structure",* Conferinta CSUD-ului din 4-5 Iunie 2015 The Annals of "Dunărea de Jos" University of Galați . Fascicle IX Metallurgy and materials science.

[72] L. Albertario, „*Development and rapid prototyping of new numerical models oriented to the honeycomb sandwich panels modelling",* 2009 - 2010.

[73] M. Dirk, „*Multi-scale finite-strain plasticity model for stable metallic honeycombs incorporating microstructural evolution*," International Journal of Plasticity, vol. 22, p. 1899–1923, 10 October 2006.

[74] S. Debruyne, D. Vandepitte, E. Debrabandere și M. Hongerloot, „*Influence of design parameter variation on the dynamic behaviour of thermoplastic honeycomb panel",* 10th International Conference RASD 2010, Southampton, july 2010.

[75] S. Debruyne, L. Mehrez, D. Vandepitte, E. Debrabandere și M. Hongerloot, „*Influence of design parameter variability on the dynamic behaviour of honeycomb sandwich panels",* vol. 2010, ISMA2010 0644, Belgium, p. 0644.

[76] F. Rotaru și B. E. F. Chirica I., „*Impact rate evaluation of composite sandwich plates used in shipbuilding",* la conferința "Computational mechanics and virtual engineering" COMEC 2015 Brașov.

[77] S. Tickoo și C. Technologies, ANSYS Workbench 14.0: A Tutorial Approach, CADCIM Technologies, 2012.

[78] B. Gama, S. Chowdhury și J. J. Gillespie, „*Finite element analysis of low velocity impact and compression after impact of sandwich composite structures",* 18th International Conference on Composite materials, 2011.

[79] P. G. Golanó, *Thesis: „Design of a carbon fibre rim for a fuel efficient competition vehicle",* University of Gavle, 2014.

[80] F. Rotaru Paraschiv, R. Roșculeț, I. Chirică și E. F. Beznea, „*Experimental analysis of the sandwich composites loaded to mechanical impact",* de la conferința Internațională The 40th International Conference on Mechanics of Solids, Acoustics and Vibrations &The 6th International Conference on "Advanced Composite Materials Engineering" ICMSAV2016& COMAT2016, Brașov, ROMANIA, 24-25 November 2016.

[81] F. Rotaru Paraschiv, I. Chirică, F. Beznea E. și I. Iacob, „*Numerical simulation and experimental bending composite sandwich plates",* de la conferinta Internațională The 40th International Conference on Mechanics of Solids, Acoustics and Vibrations &The 6th International Conference on "Advanced Composite Materials Engineering" ICMSAV2016& COMAT2016, Brașov, ROMANIA, 24-25 November 2016.

[82] C. Menna, D. Asprone, G. Caprino, V. Lopresto și A. Prota, „*Numerical Simulation Of Impact Tests On GFRP Composite Laminates",* International Journal of Impact Engineering, <10.1016/j.ijimpeng.2011.03.003>. <hal-00829115> Elsevier, 2011.

[83] C. Albertini, E. Cadoni și G. Solomos, „*Advances in the Hopkinson bar testing of irradiated/non-irradiated nuclear materials and large specimens",* Phil. Trans. R. Soc, 2014.

[84] N. Poharel, *Thesis: „Behaviour and design of sandwich panels subject to buckling and flexural wrinkling effects",* School of Civil Engineering, Queensland University of Technology, November 2003.

[85] F. Elragi A., „*Selected Engineering Properties and Applications of EPS Geofoam",* Softoria, 2006.

[86] *ASTM D 3039/D 3039M Standard Test Method for Tensile Properties of Polymer Matrix Composite Materials, in,* 2002.

[87] *AMTS STANDARD Workshop practice for wet lay-ups, AMTS_SWP_0014_2008,* 2008.

[88] [Interactiv]. Available: http://nptel.ac.in/courses/112107085/module5/lecture4/lecture4.pdf.

[89] A. Brent Strong, *Fundamentals of Composites Manufacturing: Materials, Methods, 2nd*

edition, 2nd edition ed., Society of Manufacturing Engineers, 2008.

[90] W. J. Callister, „*Materials Science and Engineering An Introduction."* Seventh Edition, 2007.

[91] *SME video on 'Manual Composite Layup and Spray Up' Product ID: DV05PUB5 from* www.SME.org.

[92] [Interactiv]. Available: http://www.zentyss.ro/products/termosistemul-agrementat-zentyss-term-e/polistiren-extrudat/polistiren-extrudat-xpan/docs_ro/fisa-tehnica/Fisa%20tehnica%20XPS%20Zentyss.pdf.

[93] G. Vineela, G. Tadepalli și A. Krishnaiah, „*Impact behaviour of Fibre Reinforced composites with change in Fibre Orientation",* vol. 6, International Journal of Current Engineering and Technology E-ISSN 2277 – 4106, P-ISSN 2347 – 5161, Vol.6, No.1, 03 Feb 2016.

[94] V. Crupi, G. Epasto și E. Guglielmino, „*Computed Tomography analysis of damage in composites subjected to impact loading*," Frattura ed Integrità Strutturale*,* vol. 17, p. 32–41, 2011.

[95] T. Brown și E. Sevkat, „*Ultrasound Studies of Drop-Weight Impact responses of Woven Hybrid Glass-Graphite/Toughened Epoxy Composites",* Step Ultrasound Composites Final Report, april 2006.

[96] R. Mirityunjay, Doddamani și M. K. Satyabodh, „*Flexural Behaviour of Functionally Graded Sandwich Composite", Chapter 6,* Mechanical Engineering, National Institute of Technology Karnataka, Surathkal, India, 2012.

[97] R. Cormos, H. Petrescu, A. Hadar, M. Adir G. și H. Gheorghiu, „*Finite Element Analysis of the Multilayered Honeycomb,*" Materiale Plastice*,* vol. 54, nr. 1, 2017.

[98] S. Mohiyuddin C., R. Jayalakshmi și H. Manjunath, „*A Study On Behavior of Sandwich Panels under Impact Loads",* SSRG International Journal of Civil Engineering (SSRG-IJCE) – EFES April 2015.

[99] B. Berek, R. Karakuzu, M. Icten B., V. Arikan, Y. Arman, C. Atas și A. Goren, „An experimental and numerical investigation on low velocity impact behaviour of composite plates," *Journal of composite materials,* vol. 50, nr. 25, p. 3551–3559, 2016.

List of papers published

[1]. F. **Rotaru**, I. Chirică, E.F. Beznea *Impact rate evaluation of composite sandwich plates used in shipbuilding***,** la conferința ”Computational mechanics and virtual engineering” COMEC 2015, Brașov; BDI.

[2]. F. **Rotaru**, I. Chirică, E.F. Beznea *Static behavior of the sandwich composite plates,* la conferința Advanced Composite Materials Engineering COMAT 2014, Brașov; BDI.

[3]. F. **Rotaru**, I. Chirică, E.F. Beznea *Strength Analysis of a Composite Joint Used in Ship Structure,* Conferinta CSUD-ului din 4-5 Iunie 2015 The Annals of ”Dunărea de Jos” University of Galați . Fascicle IX Metallurgy and materials science. BDI.

[4]. F. **Rotaru** Paraschiv, I.Chirică E.F. Beznea, *Influence of the Honeycomb Geometry on the Sandwich Composite Plate Behavior,* Advanced Materials Research, ISSN: 1662-8985, Vol. 1143, pp 139-144, Trans Tech Publications, Switzerland 2017*;* ISI (fără factor de impact).

[5]. F. **Rotaru** Paraschiv, I Chirică, E. F. Beznea, I. Iacob, *Numerical simulation and experimental bending composite sandwich plates,* de la conferinta Internațională The 40th International Conference on Mechanics of Solids, Acoustics and Vibrations &The 6th International Conference on “Advanced Composite Materials Engineering” ICMSAV2016& COMAT2016 Brașov, ROMANIA, 24-25 November 2016; BDI.

[6]. F. **Rotaru** Paraschiv, R. Roșculeț, I. Chirică, E.F. Beznea, *Experimental analysis of the sandwich composites loaded to mechanical impact*, de la conferința Internațională The 40th International Conference on Mechanics of Solids, Acoustics and Vibrations &The 6th International Conference on “Advanced Composite Materials Engineering” ICMSAV2016& COMAT2016 Brașov, ROMANIA, 24-25 November 2016. BDI.